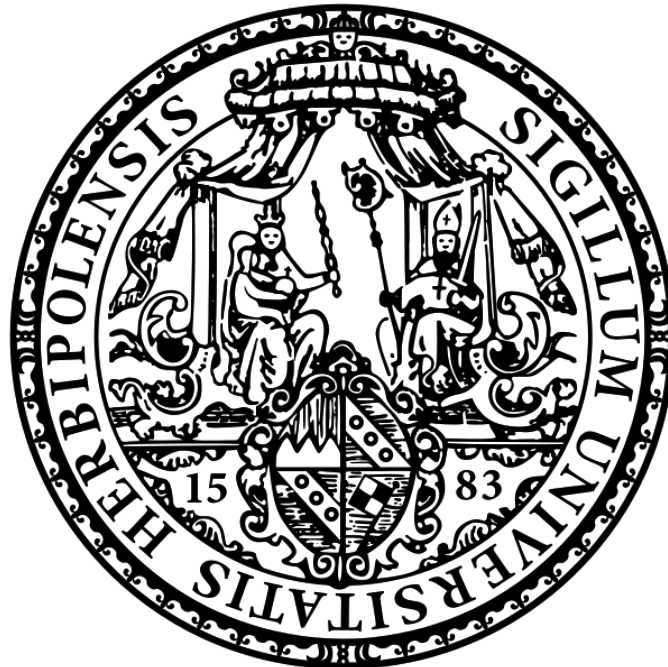


Role of CNTF-STAT3 signaling for microtubule dynamics in axon growth and maintenance: Implications in motoneuron diseases

Dissertation zur Erlangung des naturwissenschaftlichen Doktorgrades der Bayerischen Julius-Maximilians- Universität Würzburg



Vorgelegt von

Bhuvaneish Thangaraj Selvaraj

aus Chennai, India

Würzburg, 2013

Eingereicht am:

Mitglieder der Promotionskommission:

Vorsitzender: Prof. Dr. Wolfgang Rössler

Gutachter: Prof. Dr. Michael Sendtner

Gutachter: Prof. Erich Buchner

Tag des Promotionskolloquiums:

Doktorurkunde ausgehändigt am:

For Amma, Appa, Deepz and Abi

TABLE OF CONTENTS

1. SUMMARY	1
2. ZUSAMMENFASSUNG	3
3. INTRODUCTION	5
3.1 MOTONEURON DISEASE: DEFINITION AND PATHOMECHANISM	5
3.1.1 Etiology of motoneuron disease.....	6
3.1.2 Increased oxidative stress	7
3.1.3 Impaired axonal transport in motoneuron disease.....	8
3.1.4 Dysregulated RNA metabolism in SMA and ALS.....	9
3.2 MOUSE MODELS OF MOTONEURON DISEASES	12
3.2.1 Progressive motor neuronopathy (pmn) mouse.....	12
3.3 CILIARY NEUROTROPHIC FACTOR : EFFECTS IN THE PMN MODEL OF MOTONEURON DISEASE	14
3.3.1 CNTF signalling components.....	15
3.3.2 Signal Transducer and Activation of Transcription (STAT3).....	16
3.3.3 Transcriptional independent activity of STAT3	18
3.4 MICROTUBULE BIOGENESIS: ROLE IN MOTOR AXON GROWTH AND MAINTENANCE	21
3.4.1 Chaperonin mediated folding of Tubulin.....	21
3.4.2 Post-translational modifications of Tubulin.....	23
3.4.3 Stathmin, a microtubule destabilizing protein.....	24
3.5 ROLE OF TBCE IN SYNAPSES	26
3.6 GOAL OF THE THESIS	28
4. MATERIALS AND METHODS	29
4.1 MATERIALS.....	29
4.1.1 Animals	29
4.1.2 Cell Lines	30
4.1.3 Buffers and Reagents	31
4.1.4 Media for cell culture	35
4.1.5 Chemicals	35
4.1.6 List of Antibodies	37
4.1.7 List of Plasmids.....	38
4.1.8 List of Oligonucleotides.....	38
4.1.8 List of Commercial Kits.....	39
4.1.9 Software	39
4.2 METHODS	40
4.2.1 DNA isolation (Phenol-Chloroform)	40
4.2.2 RNA isolation	40
4.2.3 Genotyping of mouse lines	41
4.2.4 Reverse transcriptase PCR.....	45
4.2.5 Real time quantitative PCR analysis	45
4.2.6 Isolation of mouse embryonic motoneurons	46
4.2.7 Immunocytochemistry	47
4.2.8 Nuclear fractionation.....	47

4.2.9 Immunoprecipitation (IP)	48
4.2.10 Transient transfection of HEK 293T or N2A cells	49
4.2.11 Fluorescent in-situ hybridization	50
4.2.12 Microtubule regrowth assay	50
4.2.13 Cortical precursor cell culture	51
4.2.14 Dephosphorylation assay	52
4.2.15 Drug treatment	52
4.2.16 Site-Directed mutagenesis of STAT3 ^{Y705F} EYFP	53
5.RESULTS	55
5.1 CNTF RESCUES AXONAL PATHOLOGY IN PMN MUTANT MOUSE	55
5.2 CNTF INDUCES PHOSPHORYLATION OF STAT3	58
5.2.1 Cytoplasmic localization of activated STAT3 in primary motoneurons	58
5.2.2 Specificity of p-STAT3 ^{Y705} antibody	60
5.2.3 Axonal fractionation of primary motoneurons using Xona microfluidic chambers	61
5.3 TRANSCRIPTIONAL INDEPENDENT ACTIVITY OF STAT3 NECESSITATES RESCUE OF AXON PATHOLOGY IN PMN MUTANT MOTONEURONS	63
5.3.1 Generation of STAT3 DNA binding and phosphorylation mutants	63
5.3.2 STAT3 ^{EE434-435AA} mutant does not induce transcription	64
5.3.3 STAT3 phosphorylation but not its transcriptional activity is necessary for CNTF dependent axon growth in pmn mutant motoneurons	66
5.4 STAT3 INTERACTS WITH STATHMIN, A MICROTUBULE DESTABILIZING PROTEIN	68
5.4.1 Colocalization of Stathmin and STAT3	68
5.4.2 Co-immunoprecipitation of Stathmin and STAT3	69
5.4.3 CNTF application enhances STAT3-Stathmin interaction in primary motoneurons	71
5.4.4 STAT3 phosphorylation at Y705 is required for its interaction with Stathmin	72
5.5 STATHMIN KNOCKDOWN RESCUES AXONAL PATHOLOGY IN PMN MUTANT MOTONEURONS	74
5.5.1 Lentiviral knockdown of Stathmin in primary motoneurons	74
5.5.2 Stathmin knockdown rescues axon growth defect in pmn mutant motoneurons	76
5.5.3 Stathmin levels are not altered in pmn mutant motoneurons	77
5.6 CNTF ALTERS THE MICROTUBULE DYNAMICS IN PMN MUTANT MOTONEURONS	78
5.6.1 Post-translation modifications in α -tubulin represent microtubule dynamics	78
5.6.2 Microtubule fractionation	81
5.6.3 Microtubule stabilization promotes axon growth in pmn mutant motoneurons	83
5.7 CNTF ENHANCES MICROTUBULE POLYMERIZATION IN PRIMARY CULTURED MOTONEURONS ...	85
5.8 STABILITY OF TBCE PROTEIN	89
5.8.1 Tyryptophan to Glycine mutation in TBCE renders it unstable	89
5.8.2 CNTF does not alter the stability of TBCE protein	92
5.8.3 CNTF does not regulate the expression of <i>Tbce</i> gene	93
5.9 STAT3 ACTIVATION IN SCIATIC NERVE OF PMN MOUSE	96
5.10 CHARACTERIZATION OF SYNAPSE ASSOCIATED PROTEIN 1 (SYAP1) AND INTERACTION WITH TBCE	98
5.10.1 Characterization of antibodies against SYAP1	98
5.10.2 Lentiviral knock down of SYAP1 in primary motoneurons	100

5.10.3 Colocalization of <i>Tbce</i> and <i>SYAP1</i>	101
5.10.4 <i>SYAP1</i> interaction with <i>TBCE</i>	102
6. DISCUSSION	104
6.1 CNTF HAS A SPECIFIC ROLE IN AXON MAINTENANCE	104
6.2 LOCAL FUNCTION OF STAT3 IS NECESSARY FOR CNTF MEDIATED AXON OUTGROWTH IN <i>PMN</i> MOTONEURONS	106
6.3 STATHMIN - A DOWNSTREAM TARGET OF STAT3	107
6.4 ROLE OF STATHMIN IN NEURONAL DIFFERENTIATION	109
6.5 MICROTUBULE DYNAMICS IN NEURODEGENERATIVE DISEASES	110
6.6 MICROTUBULE DYNAMICS OBSERVED IN <i>PMN</i> MUTANT MOTONEURONS	111
6.7 <i>TBCE</i> ^{W524G} PROTEIN IS FUNCTIONAL BUT HIGHLY UNSTABLE	113
6.8 POSSIBLE ROLE OF <i>TBCE</i> IN SYNAPSE MAINTENANCE	114
7. REFERENCE	116
8. APPENDIX	133
8.1 LIST OF FIGURES	133
8.2 LIST OF TABLES	135
8.3 LIST OF ABBREVIATIONS	136
9. DECLARATION	139
10. ACKNOWLEDGEMENTS	140
11. CURRICULUM VITAE	142

1. SUMMARY

Neurotrophic factor signaling modulates differentiation, axon growth and maintenance, synaptic plasticity and regeneration of neurons after injury. Ciliary neurotrophic factor (CNTF), a Schwann cell derived neurotrophic factor, has an exclusive role in axon maintenance, sprouting and synaptic preservation. CNTF, but not GDNF, has been shown to alleviate motoneuron degeneration in *pmn* mutant mice carrying a missense mutation in *Tbce* gene, a model for Amyotrophic Lateral Sclerosis (ALS). This current study elucidates the distinct signaling mechanism by which CNTF rescues the axonal degeneration in *pmn* mutant mice.

Cultured primary motoneurons from *pmn* mutant embryos show reduced axon elongation and increased number of axonal swellings with mitochondrial accumulation, a characteristic feature of many neurodegenerative diseases. In resemblance to the previous *in-vivo* finding, application of CNTF, but not GDNF or BDNF, rescued axon elongation deficits in *pmn* mutant motoneurons. CNTF mediates its cellular functions through a tripartite receptor complex involving gp130, LIFR β and CNTFR α . Binding of CNTF to this receptor complex activates cytoplasmic STAT3 through phosphorylation at tyrosine 705 and induces transcription of responsive target genes. In primary motoneurons, CNTF was observed to phosphorylate STAT3^{Y705}, however, most of the p-STAT3^{Y705} remained in the cytoplasm. Cytoplasmic activation of STAT3 was necessary for CNTF induced axon elongation in *pmn* mutant motoneurons. Over-expression of wildtype and DNA binding mutant but not tyrosine phosphorylation mutant of STAT3 completely rescued axon growth defects in *pmn* mutant motoneurons upon CNTF application, confirming that a transcription- independent activity of STAT3 is sufficient for CNTF mediated rescue of axonal pathology. Further studies showed that activated STAT3 interacts with the cytosolic protein Stathmin and inhibits its microtubule destabilizing activity. Microtubule stability was altered in *pmn* mutant motoneurons with increased level of tyrosinated tubulin, a marker for highly unstable microtubules. Inhibition of Stathmin activity by lentiviral knockdown or by application of CNTF in *pmn* mutant motoneurons significantly reduced the level of tyrosinated tubulin, indicating that CNTF influences microtubule

dynamics and stabilizes them. CNTF was also observed to enhance microtubule polymerization in primary motoneurons by suppressing Stathmin activity. These findings indicate that STAT3, apart from its canonical transcriptional activity plays a vital role in axon maintenance by altering axonal cytoskeleton through Stathmin and Stathmin inhibition, This effect could be a target for therapy in neurodegenerative disorders such as motoneuron disease.

2. Zusammenfassung

Neurotrophe Faktoren beeinflussen die neuronale Differenzierung, das Wachstum und die Stabilisierung von Axonen sowie Synaptische Plastizität und die Regeneration von Neuronen nach Verletzung. Der von Schwannzellen synthetisierte neurotrophe Faktor Ciliary neurotrophic factor (CNTF) spielt eine wichtige Rolle bei der axonalen Erhaltung sowie bei der Induktion und Reduktion von axonalen Verzweigungen. Die Behandlung der *pnn* Mausmutante mit CNTF, aber nicht mit GDNF führt zu einem späteren Krankheitsbeginn und verminderten Fortschreiten der Motoneuronendegeneration. Diese Mausmutante, die eine Punktmutation im *Tbce* Gen trägt, dient als Modell für die Amyotrophe Lateralsklerose. Ziel der vorliegenden Arbeit war es, die zugrunde liegenden Signalkaskaden aufzudecken, die den CNTF-vermittelten Effekt auf den Krankheitsverlauf bei der *pnn* Maus verursachen.

Isolierte Motoneurone aus *pnn*-mutierten Embryonen zeigen ein verringertes axonales Auswachsen und eine erhöhte Zahl an axonalen Schwellungen mit mitochondrialen Akkumulationen, einer charakteristischen Veränderung bei vielen neurodegenerativen Erkrankungen. Die Gabe von CNTF, aber nicht von GDNF oder BDNF, kann diese axonalen Wachstumsdefekte bei *pnn*-mutierten Motoneuronen verhindern, ähnlich wie schon zuvor *in vivo* gezeigt. Von CNTF ist bekannt, dass es seine Funktion durch einen dreiteiligen Rezeptorkomplex, bestehend aus gp130, LIFR β und CNTFR α , vermittelt. Die Bindung von CNTF an diesen Rezeptorkomplex aktiviert cytoplasmatisches STAT3 durch die Phosphorylierung an Tyrosin 705 und induziert so die Transkription von Zielgenen. In primären Motoneuronen wurde beobachtet, dass CNTF Gabe zur Phosphorylierung von STAT3^{Y705} führt, jedoch, ein Großteil des p-STAT3^{Y705} verbleibt im Cytoplasma. Die cytoplasmatische Aktivierung von STAT3 ist erforderlich für die CNTF-vermittelte Axonelongation in den *pnn*-mutierten Motoneuronen, da die Überexpression sowohl von wildtypischem, als auch der DNA-Bindemutante, aber nicht der Tyrosin-Phosphorylierungs-defizienten Mutante von STAT3 den CNTF-Effekt auf die Axonelongation vermittelt und dadurch die Transkriptionsunabhängigkeit dieses Effektes unterstreicht. Aktiviertes

STAT3 interagiert zytosolisch mit Stathmin und inhibiert dadurch die destabilisierende Wirkung auf Mikrotubuli. In *pmn*-mutierten Motoneuronen ist die Mikrotubulistabilität verändert, da eine erhöhte Menge von tyrosiniertem Tubulin, einem Marker für instabile Mikrotubuli, detektiert werden konnte. Die Reduktion der Stathmin Aktivität durch einen lentiviralen siRNA Ansatz oder durch die Applikation von CNTF in *pmn*-mutierten Motoneuronen, reduziert die Menge an tyrosiniertem Tubulin und zeigt daher einen CNTF-vermittelten Einfluss auf die Mikrotubulidynamik in Richtung einer Stabilisierung. Weiterhin verstärkt CNTF die Polymerisierung der Mikrotubuli durch Unterdrücken der Stathmin Aktivität. Diese Ergebnisse zeigen, dass STAT3, neben der bereits bekannten transkriptionalen Aktivität, eine wichtige Rolle auf die Axonerhaltung durch die modulierenden Effekte auf das axonale Cytoskelett über die Interaktion mit Stathmin ausübt. Diese Stathmin Inhibition durch CNTF könnte ein Target für neue Therapien bei neurodegenerativen Erkrankungen wie der Amyotrophen Lateralsklerose darstellen.

3. INTRODUCTION

Neurodegenerative diseases are characterized by neuronal dysfunction due to pathological loss of synapses and neurons in the central or peripheral nervous system. These include Alzheimer's disease, Amyotrophic lateral sclerosis, Parkinson's disease, Huntington's disease, but also neuroinflammatory diseases such as Multiple sclerosis in which synapse, axon and neuronal losses correlate with disease progression. Vast amounts of research in these disorders have revealed some parallels in molecular and cellular disease mechanisms, such as formation of protein aggregates and, disruption of long distance axonal transport. Identification of such similarities provides a sense of hope for finding therapeutic targets to alleviate these diseases concomitantly.

3.1 Motoneuron disease: Defenition and Pathomechanism

Motoneuron diseases represent a clinically and genetically heterogeneous group of progressive neurological disorders that destroy cells for controlling muscle activity for body functions such as speaking, walking, breathing and swallowing etc. Common pathological feature of this diseases are progressive degeneration and cell death of upper (cortex and brain stem) and/or lower motoneurons (brain stem motor nuclei and spinal cord). Upper motoneurons are those motoneurons present in the motor cortex and brain stem that signal to brain stem motor nuclei and spinal cord. Lower motoneurons in brainstem and spinal cord project to muscle fibers. Glutamatergic upper motoneurons triggers depolarization of lower motoneurons present in the ventral horn of the spinal cord, either directly or indirectly via interneurons, which in turn causes action potential to propagate along axons that innervating the muscle, thereby causing it to contract (movement). Injury or cell death of upper motoneurons leads to spasticity, stiffness of limb muscles, hyperactivity of tendon reflexes. The degeneration of lower motoneurons causes progressive weakening and wasting of muscles and rapid twitching of muscles (fasciculation).

Motoneuron diseases are classified depending on the cell types that are affected (Donaghy, 1999). First, combined upper and lower motoneurons disorders as observed in amyotrophic lateral sclerosis (Christensen et al., 1990), second, pure lower motoneuron disorder such as spinal muscular atrophy (SMA) and third, pure upper motoneuron disorder such as hereditary spastic paraplegia (HSP) where loss of upper motoneurons in pyramidal tract leads to loss of control of lower motoneurons and thereby results in spasticity in limbs (Fink et al., 1996). Several pathological mechanisms are thought to cause motoneuron diseases and have propagated research to identify therapeutic strategies. Some of them are reported in the following section.

3.1.1 Etiology of motoneuron disease

Amyotrophic lateral sclerosis

Amyotrophic Lateral Sclerosis is the most common form of motoneuron disease with a prevalence of 2 per 100,000 people. The mean age of onset is 55-60 years, although rare juvenile form of ALS is also observed. The disease progression varies among individuals with mean survival of 3 years after onset of symptoms, however some individuals are observed to have extended life span. Over 90-95% cases of ALS are sporadic. Several sporadic and familial inherited mutations in various genes have been found in ALS patients. Understanding the functions of these proteins is essential for identifying the pathomechanism of motoneuron diseases. First breakthrough in finding a causative gene for ALS was the identification of 11 different missense mutations in Cu/Zn-binding superoxide dismutase gene from 13 different ALS families (Rosen, 1993). Mutation in the *SOD1* gene is observed in 20% of familial ALS patients. Several other genes that are associated with fALS are C9ORF72 (Renton et al., 2011), Senataxin (Chen et al., 2004), Fused in sarcoma (Vance et al., 2009), TAR DNA binding protein (Sreedharan et al., 2008), Valosin containing protein (Johnson et al., 2010).

Spinal muscular atrophy (SMA)

Spinal muscular atrophy is characterized by degeneration of anterior horn cells of the spinal cord leading to limb. This is an autosomal recessive disorder caused by mutation observed in survival motor neuron gene *SMN1* (Bussaglia et al., 1995; Lefebvre et al., 1995). The incidence of this disease is 1 in 6000. Humans have 2 nearly identical SMN genes, namely telomeric *SMN1* and centromeric *SMN2*. *SMN1* codes for full-length protein of molecular weight 32 kDa, whereas the C-T nucleotide exchange at +6 position of exon7 in the *SMN2* gene leads to altered splicing pattern (exclusion of exon 7) and produces SMN Δ 7 protein that eventually gets degraded in the cell. *SMN2* could still code for full-length SMN protein but almost 80-90% of transcripts are alternatively spliced and thus lack exon 7. Due to deletions or mutations leading to conversion of *SMN1* to *SMN2*, SMA patients show absence of *SMN1* exon 7, and therefore reduced amount of SMN full-length protein (Wirth et al., 2006). The severity of the disease depends on the amount of SMN full-length protein produced *SMN2* gene.

Studies so far suggest that in motoneuron diseases there might be a complex interplay between genetic factors, oxidative stress, protein aggregation, impaired axonal transport, dysregulated RNA processing and signaling (Ferraiuolo et al., 2011).

3.1.2 Increased oxidative stress

Oxidative stress is caused by an imbalance between generation of reactive oxygen species and the ability of the cell to detoxify them. Resulting accumulation of free radicals damages all components of the cell, such as proteins, lipids and DNA. Accumulation of reactive oxygen species during ageing in post mitotic neurons reduces its ability to cope with toxic mutation, further exacerbates the symptoms in many neurodegenerative disorders. Higher levels of 4-

hydroxynonenal, a marker of lipid peroxidation caused by free radicals, was observed in cerebrospinal spinal fluid (Smith et al., 1998) and serum (Simpson et al., 2004) of sALS patients. SOD1 is an enzyme that catalyzes the conversion of superoxide (free radical) to oxygen and hydrogen peroxide. Mutation in SOD1 gene in fALS cases led to the study of role of oxidative stress in ALS. Increased level of 3-nitrotyrosine, an indicator for peroxynitrite damage, was observed in spinal cord motoneurons of both fALS and sALS (Beal et al., 1997). Transgenic mice carrying the mutations in SOD1 develop clinical and pathological phenotypes that closely resemble human motoneuron disease; therefore, the mutations in SOD1 functions as a toxic gain of function mutation. The mutations extensively studied are SOD1^{G93A} (Gurney et al., 1994), SOD1^{G37R} (Wong et al., 1995) and SOD1^{G85R} (Bruijn et al., 1997). These mice differ in the onset and severity of disease progression. Increased levels of oxidative damage in DNA, RNA, proteins, lipids have been observed both in patients and all the mouse model of transgenic SOD1 mice (Andrus et al., 1998; Ferrante et al., 1997). However, mutant SOD1 that is enzymatically inactive did not modify the onset and progression of motoneuron disease in SOD1 mutant mice (Subramaniam et al., 2002), suggesting that oxidative damage is not the major cause for motoneuron disease in ALS.

3.1.3 Impaired axonal transport in motoneuron disease

Motoneurons are highly polarized cells with very long axons and therefore, transport of mitochondria (energy source), proteins, RNA for protein synthesis, synaptic components to the distal part of neurons are vital for maintenance of the motoneuron itself. Impaired transport along the axon (both anterograde and retrograde) is a hallmark feature of many motoneuron diseases. For instance, mutant SOD1 disrupts both anterograde and retrograde mitochondrial transport (Marinkovic et al., 2012; Williamson and Cleveland, 1999). Similarly, other mouse models of motoneuron disease such as *pnn-* caused by mutation in the *Tbce* gene that alters a microtubule assembly (Sagot et al., 1998), SMN Δ 7 (Dale et al., 2011), *wobbler-* caused by

mutation in vesicle sorting protein (vps54) (Schmitt-John et al., 2005) also exhibit axonal transport defects. Microtubule based fast axonal transport is dependent on motor proteins such as kinesins (anterograde) and dyneins (retrograde). Mutations observed in the components facilitating the axonal transport are prime targets to understand the disease mechanism in motoneuron degeneration. Mice carrying missense mutation in dynein heavy chain results in progressive motoneuron degeneration (*Loa* mice). Using fluorescent-tagged tetanus toxin, it was identified that the retrograde transport was perturbed in *Loa* mice (Hafezparast et al., 2003). A mutation in the p150 subunit of dynactin has also been found in a family with a slowly progressive autosomal dominant form of motoneuron disease with vocal cord paralysis (Puls et al., 2003). Mutations in KIF5A and KIF1B-beta have been associated with early onset of hereditary spastic paraplegy (Reid et al., 2002) and Charcot Marie Tooth-type 2A (Zhao et al., 2001) respectively. Disruption of axonal transport eventually leads to accumulation of cargos such as mitochondria, vesicles, neurofilaments that are characteristic feature of motoneuron disease.

3.1.4 Dysregulated RNA metabolism in SMA and ALS

Recent findings in the field of spinal muscular atrophy (SMA), a pure lower motoneuron disorder, led to intensive studies to understand the role of RNA processing and its transport along the axons. SMN protein plays a pivotal role in assembly of small nuclear ribonucleo protein (snRNP) complexes that functions in pre m-RNA splicing (Burghes and Beattie, 2009). SMN protein is observed both in the nucleus and the cytoplasm. Analysis in spinal cord of mouse models of SMA showed reduced activity of snRNP assembly in the cytoplasm and comparable reduction was also observed in other tissues (Gabanella et al., 2007). Therefore, it is still unclear why motoneurons appear more vulnerable than other types of cells under the specific conditions of SMN reduction. Primary motoneurons from $Smn^{-/-};SMN2^{tg}$, mouse model of the severe form of SMA where human SMN2 is introduced to *Smn* null background (Monani

et al., 2000), exhibit shorter axons and smaller growth cones in-vitro. Ectopic expression of mutant *Smn* that retains the ability to induce snRNP assembly did not rescue the axonal phenotype observed in *Smn*^{-/-};SMN2^{tg} (Carrel et al., 2006) indicating *Smn* function in motoneuron goes beyond its classical snRNP biogenesis and presumably SMN might have a motoneuron specific function. Subsequent studies showed a significant reduction of β -actin mRNA and protein in growth cones of primary motoneurons while overall levels β -actin mRNA were unaltered (Rossoll et al., 2003). This led to the hypothesis that *Smn* protein is also involved in axonal mRNA transport and local translation. Conversely, restoration of β -actin mRNA and protein levels in *Smn*^{-/-};SMN2^{tg} using cAMP treatment (Jablonka et al., 2007) or inhibition of PTEN (Ning et al., 2010) rescues the axonal defects and increased the life span of SMA mice. *Smn* has been observed to interact with mRNA binding proteins hnRNP-R (Glinka et al., 2010), HuD (Atlas et al., 2004), KSRP (Gu et al., 2002). These proteins bind mRNAs, and are found in axons. Suppression of hnRNP R in isolated motoneurons or in zebrafish embryos leads to axonal defects in motoneurons that resemble those identified in *Smn* deficient motoneurons, thus supporting the hypothesis that these proteins act together in maintenance of axons. Moreover, local translation of β -actin mRNA in axonal growth cones is deregulated in primary motoneurons from *Smn*^{-/-};SMN2^{tg} mice (Rathod et al., 2012). These findings indicate that the mechanisms to facilitate mRNA trafficking and local translation are disturbed in *Smn* deficient motoneurons (Fallini et al., 2012).

Recent studies in ALS patients led to identification of some more mutations in RNA/DNA binding proteins. TAR DNA binding protein-43 (TDP-43) has recently been identified as a major component of ubiquitinated inclusion bodies in patients with ALS associated with Frontotemporal lobe dementia (FTLD) (Neumann et al., 2006). Several mutations have been identified in the glycine rich C-terminal domain of TDP-43 that is responsible for protein –protein interactions (Mackenzie et al., 2010). TDP-43 is mainly a nuclear protein with multiple roles in RNA processing, transcriptional regulation, alternative

splicing and micro RNA processing. Like wise, mutations in another DNA/RNA binding protein named Fused in sarcoma (Gouilleux-Gruart et al.) were also observed in ALS-FTLD. These mutations also lead to ubiquitinated inclusions bodies (Drepper et al., 2011; Mackenzie et al., 2010). However, it still remains elusive whether the mutations observed in FUS/TDP-43 causes loss of function or toxic gain of function in motoneurons. Since most of the mutations occur in glycine rich domain of TDP-43 that is involved in protein-protein interactions, it is widely speculated that mutation disrupt the RNA transport complex, thus leading to motoneuron degeneration (Ferraiuolo et al., 2011). Various missense mutations in Senataxin, a DNA/RNA helicase functions in separating RNA/DNA hybrids at transcriptional pause sites (R loops) (Skourti-Stathaki et al., 2011), was observed in a rare form of juvenile ALS (Chen et al., 2004). Most recently, a large hexanucleotide repeat expansion (GGGGCC) in the first intron of C9ORF72 chromosome 9p21 has been identified in both familial and sporadic ALS in a Finnish population (Renton et al., 2011). Function of this protein and how this repeats causes motoneuron diseases are still unknown. The levels of C9orf72 transcript was observed to reduced in ALS patients with repeat expansions linking to haploinsufficiency mechanism (DeJesus-Hernandez et al., 2011). Alternatively, it is also believed that the expansion in RNA editing process might be impaired due to such large repeats (Polymenidou et al., 2012). These observations show that RNA metabolism and its transport plays a major role in pathomechanism of motoneuron disease.

3.2 Mouse models of motoneuron diseases

Mouse models have been used extensively to study disease mechanism in various forms of motoneuron disease.

1. $SOD1^{G93A}$, $SOD1^{G37R}$, $SOD1^{G87R}$: mouse models of familial ALS
2. $Smn^{-/-};SMN2^{tg}$, $Smn^{-/-};SMN2^{tg};SMN\Delta 7^{tg}$: mouse models for SMA
3. *pmn*: motoneuron disease caused by defective microtubule biogenesis
4. *wobbler*: motoneuron disease caused by mutation in vesicle sorting protein (Vps54)
5. *nmd* : mouse model for SMA with respiratory distress-SMARD

3.2.1 Progressive motor neuropathy (*pmn*) mouse

The *pmn* mouse mutant is a spontaneous mutant that was first identified in a stock of Pan:NMRI (Naval Medical Research Institute) mice at the Panum Institute, Copenhagen in 1988. Disease inheritance follows an autosomal recessive pattern. Heterozygote animals are normal and indistinguishable from wildtype mice, where as all homozygous mutants (25 %) developed clinical symptoms. Atrophy in hind limbs becomes first detectable at an age of 3 weeks and affected mice die 4 – 6 weeks after birth due to respiratory failure (Schmalbruch et al., 1991). The hind limb muscle of 4 week old *pmn* mutant mice showed features of neurogenic atrophy (Schmalbruch et al., 1991). The motor endplates in gastrocnemius muscle show distinct post synaptic fold covered with degenerating axons, indicative of dying back neuropathy. Histological analysis of these mice showed loss of myelinated axons in phrenic nerve that innervates the diaphragm. Moreover, 30% loss of motoneurons in facial nucleus was observed in homozygous mutants (Sagot et al., 1996; Sendtner et al., 1992b). These clinical phenotypes resemble amyotrophic lateral sclerosis (ALS) by progressive death of motoneurons in early postnatal period (Schmalbruch et al., 1991).

The underlying mutation in *pmn* mice was genetically mapped to chromosome 13 in the region defined by the markers D13Mit172 and D13Mit207 (Martin et al., 2001). Subsequent analysis using expression sequence tags and 5' rapid amplification of cDNA ends (5'RACE) helped to identify the mutation in the *Tbce* (Tubulin specific binding chaperone E) gene locus. Sequencing of pcr products from brain samples of *pmn* and NMRI mice revealed a T-G transition at nucleotide position 1682 of the *Tbce* gene. This mutation results in a missense mutation exchanging amino acid tryptophan to glycine at position 524 of the TBCE protein. This mutation in the *Tbce* gene co-segregated with the *pmn* phenotype (Bommel et al., 2002; Martin et al., 2002).

The protein encoded by the *Tbce* gene is also known as cofactor E and plays an important role in microtubule assembly. TBCE along with TBCB assists in proper folding of α -tubulin and also formation α/β tubulin heterodimers, the components of which microtubules are assembled (Lewis et al., 1997; Lewis et al., 1996; Tian et al., 1996). TBCE protein comprises of three functional domains, a glycine rich cytoskeleton associated protein (CAP-Glycine) domain, Leucine rich repeat domain (LRR) and a ubiquitin-like domain (Hahnen et al., 2006). The CAP-Glycine domain is the site for interaction with α -tubulin (Bartolini et al., 2005; Grynberg et al., 2003; Parvari et al., 2002). The mutation in *Tbce* gene causing Typ534Gly substitution affects stability of the protein. The mutant protein is more susceptible to trypsin digestion indicating difference in confirmation between the wildtype and mutant TBCE (Martin et al., 2002). Electron microscopic analysis of phrenic nerve of *pmn* mice showed loss of microtubule and increase in neurofilaments (Martin et al., 2002), which was also consistent in cultured primary motoneurons from *pmn* mutant embryos (Bender F.L.P Ph.D thesis). Mutations in other regions of the *Tbce* gene that abolish the enzymatic activity of the corresponding protein (c.155-166del12; p.del 52-55) have been associated with the hypoparathyroidism-retardation-dysmorphism syndrome (Parvari et al., 2002; Rohde et al., 2003) a rare autosomal recessive

disorder characterized by short stature due to GH insufficiency, mental retardation, facial dysplasia and endocrinological defects such as hypocortisolemia.

3.3 Ciliary neurotrophic factor: Effects in the *pnn* model of motoneuron disease

Neurotrophic factors are members of several families of secreted proteins that are involved in growth, survival, and maintenance of neurons. Ciliary neurotrophic factor (CNTF) is a member of neuropoetic cytokine family. CNTF was first identified in chicken eye (hence the name) supporting survival of ciliary ganglionic neurons *in-vitro* (Adler et al., 1979). This factor is also present in high amounts in adult sciatic and other peripheral nerves. Further research has shown that CNTF is involved in survival of embryonic motoneurons *in-vitro* (Arakawa et al., 1990) and *in-vivo* (Masu et al., 1993), sympathetic neurons (Saadat et al., 1989; Sendtner et al., 1991) oligodendrocytes (Lillien and Raff, 1990). Cloning and sequence pattern matching analysis predicted similarities between CNTF and LIF, IL6 (Bazan, 1991). Unlike other neurotrophic factors, CNTF does not possess a leader sequence that facilitates secretion by classical ER-Golgi pathway and so far its unclear how CNTF is exposed to the target neurons (Lin et al., 1989). Expression CNTF is mostly confined to the nervous system, in adult rat, CNTF mRNA was mainly identified at the optic nerve, olfactory bulb (Stockli et al., 1991), spinal cord and peripheral nerves such as sciatic nerve (Sendtner et al., 1992c). In contrast to the other neurotrophic factors such as BDNF and GDNF, CNTF expression is absent in target skeletal muscle (Stockli et al., 1989). Expression of CNTF starts early postnatal and does not peak until 4th postnatal week, which parallels with the differentiation of Schwann cells in the nerve (Jessen and Mirsky, 1992). *In-situ* hybridization and immunocytochemistry analysis have shown CNTF is localised at Schwann cells in the sciatic nerve (Friedman et al., 1992; Simon et al., 2010). CNTF knockout mice showed no signs of developmental defects until early postnatal life. After 3 weeks of birth CNTF^{-/-} mice develops progressive loss of spinal motoneurons (Masu

et al., 1993), which parallels with the expression pattern. These findings indicate that CNTF is important for maintenance of mature neurons but not essential during early development of mice. Neurotrophic property of CNTF led to studies whether it has therapeutic potentials on motoneuron diseases. Subcutaneous injections of CNTF to *wobbler* mice prolonged the disease progression by 1 month, as measured by behavioural and histological analysis (Mitsumoto et al., 1994a; Mitsumoto et al., 1994b). In *pmn* mouse, CNTF treatment was given by intraperitoneal injection of stable D3 cell line transfected with leader sequence / CNTF genomic DNA construct that was expressed under control of CMV promoter. CNTF treatment increased the survival and improved the motor function of *pmn* mice. Moreover the histological manifestations, such as loss of axons in phrenic nerve and degeneration of facial motor nucleus were greatly reduced upon CNTF treatment (Sendtner et al., 1992b). Interestingly, treatment of *pmn* mice with another potent neurotrophic factor GDNF improved the loss of spinal and facial motoneuron cell bodies, but the loss of motor axon in phrenic nerve and the survival of mice were not altered (Sagot et al., 1996). Similarly, over expression anti-apoptotic protein Bcl-2 in *pmn* mice also prevented the loss of facial motoneurons but did not prevent axon degeneration and subsequent death of *pmn* mice (Sagot et al., 1995). These findings highlight the role of unique unknown function of CNTF in axon maintenance of peripheral nervous system. Clinical trials performed by treating ALS patients with subcutaneous injection of CNTF led to side effects such as fever, cough and local reactions at the site of injection (BROOKES et al., 1993b). Some group of patients resisted loss of muscle strength during the time of treatment when compared to placebo treated group.

3.3.1 CNTF signalling components

The receptor that binds to CNTF was identified using ‘tagged ligand panning’ method and named CNTFR α (Davis et al., 1991). Unlike the receptors used by other neurotrophins - Trk, receptor for CNTF was similar to Interleukin-6 (IL6) receptor sharing 30% identity but lacked the cytoplasmic domain. It is anchored to the cell membrane via glycosyl-phosphatidyl-

inositol linkage (GPI) (Davis et al., 1991). Subsequent screening for CNTF receptor complex led to the finding that CNTF induce heterodimerization of Glycoprotein 130 (GP130) and Leukemia Inhibitor Factor Receptor- β (LIFR β), receptors involved in LIF and IL6 signaling (Ip et al., 1992). CNTF activation is observed only when all three receptors (CNTFR, GP130, LIFR β) were overexpressed in COS cells, whereas LIF activates GP130 and LIFR β in absence of CNTFR, moreover, immunoprecipitation studies identified CNTFR to form a tripartite complex with GP130 and LIFR β (Davis et al., 1993). Expression of CNTFR α is largely confined to nervous system and skeletal muscle, with prominent expression in upper and lower motoneurons (Helgren et al., 1994). Unlike mice lacking CNTF, CNTFR α knockout mice die perinatally due to severe loss of facial motor neurons and lumbar spinal motoneurons (DeChiara et al., 1995). CNTF binding to this tripartite receptor leads to the activation of Tyk2, a member of Janus Kinase (BROOKES et al.), which in turn phosphorylates cytoplasmic tail of gp130 and LIFR β (Stahl et al., 1994; Stahl et al., 1993; Stahl and Yancopoulos, 1994). Prior to CNTF activation, JAK kinases are inactively associated with LIFR β and Gp130 and are activated after heterodimerization (Hirano et al., 1997). The phosphorylated receptors become the docking site of Signal Transducer and Activation of Transcription 3 (STAT3) (Stahl et al., 1995). STAT3 upon activation gets phosphorylated at tyrosine 705, dimerizes, translocates to nucleus and activates transcription of target genes.

3.3.2 Signal Transducer and Activation of Transcription (STAT3)

STAT3 was initially identified as a factor involved in IL6 or LIF mediated acute phase response in liver hence named as Acute Phase Response Factor (APRF). In HepG2 cells, phosphorylation of APRF/STAT3 was observed by treatment with LIF or IL6 (Wegenka et al., 1993). The tyrosine phosphorylation of APRF was stimulated with other cytokines (CNTF, OncostatinM) that uses the GP130 receptor as a signaling receptor (Akira et al., 1994; Wegenka et al., 1994). Purification from rat liver and sequencing of APRF revealed a 87 kDa band with

high homology with STAT family of proteins (Akira et al., 1994; Zhong et al., 1994). Upon cytokine stimulus, STAT3 is phosphorylated; activated STAT3 then dimerizes and subsequently translocates to the nucleus, binds to the CTGGGA motif in the DNA and activates transcription of certain target genes (Akira et al., 1994; Darnell et al., 1994). Several genes have been identified as STAT3 targets, namely, cyclin D1, c-myc, Bcl-2, Bcl-xl, SOCS3 (Turkson and Jove, 2000). STAT3 functional motifs include an amino terminus involved in dimerization, coiled coil domain for protein-protein interactions, a central DNA binding domain, a SRC homology domain (SH2) containing the conserved tyrosine phosphorylation site at 705, and a C-terminus which plays a roles in transcription activation (Reich and Liu, 2006). Sequence alignment of STAT3 to STAT1, in which tyrosine 701 is phosphorylated revealed high similarity and that tyrosine (Y) in STAT3 at position 705 could be a putative site of phosphorylation. Site directed mutagenesis of tyrosine (Y) at position 705 to phenylalanine (F) completely abolished IL6 induced phosphorylation and downstream signaling (Kaptein et al., 1996). Moreover, it was also observed that over-expression of mutant STAT3^{Y705F} suppressed the phosphorylation endogenous STAT3 indicating that this mutant form acts in a dominant negative way (Kaptein et al., 1996). Another phosphorylation at serine 727 of STAT3 was also induced by IL6, although the time course was slightly slower than tyrosine phosphorylation (Lutticken et al., 1995; Lutticken et al., 1994). STAT3 dimerization could be homodimer or heterodimer with other STAT molecules especially STAT1. STAT3 homodimerization is favored when serine 727 is also phosphorylated. Phosphorylation at both sites is required for maximum transcriptional activity of STAT3 (Shen et al., 2004; Wen et al., 1995). Embryonic fibroblasts from STAT3^{S727A}/ STAT3^{S727A} mice had 50% loss of transcriptional activity when compared to wildtype cells (Shen et al., 2004). DNA binding domain of STAT3 was characterized and localized to the region of 400-500 aminoacids of STAT3 protein. Mutations at two highly conserved regions within this 400-400 aminoacid stretch of STAT3 completely abolished the DNA binding capacity of STAT3. First, the aminoacids EE at position 434-435 were mutated to

AAA and second, aminoacids VVV at position 461-463 were mutated to AAA. These mutants were phosphorylated and dimerized upon cytokine stimulus, but the DNA binding capacity and further transcriptional activation were abolished (Horvath et al., 1995; Rajan and McKay, 1998) Unlike other STAT molecules, STAT3 translocation to nucleus is phosphorylation independent and mediated by interaction of importin -3 α to coiled-coil domain of STAT3 (Liu et al., 2005) Classical STAT3 knock out mouse in which exons 20, 21 and 22 are excised die at embryonic day 6-7, indicating that STAT3 plays an important role in early embryonic development before implantation (Takeda et al., 1997). Conditional ablation of STAT3 in mature neurons using NFL-Cre as a driver did not reveal any significant difference in survival of motoneurons present in facial nucleus and spinal cord. However, motoneuron survival after axotomy was impaired in conditional STAT3 knockout mice (Schweizer et al., 2002). Activated STAT3 has been observed in various human tumors and tumor cell lines such as breast cancer (Watson and Miller, 1995), leukemia (Gouilleux-Gruart et al., 1996) and lymphoma (Weber-Nordt et al., 1996) and therefore STAT3 is considered as an oncogene.

3.3.3 Transcriptional independent activity of STAT3

Although canonical pathway of STAT3 activation leads to translocation to the nucleus and regulation of its target genes, most of the activated STAT3 remains localized in cytoplasm and recent studies have identified alternative cytoplasmic targets of STAT3 in various biological process (Figure 3.1).

First, STAT3 is involved in regulation of microtubule dynamics by antagonizing the depolymerization activity of Stathmin. Yeast two-hybrid screen of mouse brain library using the C-terminus of STAT3 (amino acids 395-770) as bait lead to the identification of its interaction with SCLIP and Stathmin. Stathmin is widely characterized as a microtubule destabilizing protein and thereby aids in depolymerizing the microtubule network. The interaction of STAT3 with Stathmin attenuates microtubule depolymerization induced by Stathmin in mouse

embryonic fibroblasts. STAT3 deficient fibroblasts also showed impaired microtubule network, indicating that it plays an important role in microtubule dynamics (Ng et al., 2006). This interaction has also been shown to play a role in microtubule dynamics for T-cell migration (Verma et al., 2009).

Second, STAT3 is involved in cellular respiration by regulating the activity of mitochondrial complexes I and II of electron transport chain. STAT3 was observed to localize in mitochondria and interact with complex I components and GRIM 19. Conditional ablation of STAT3 in heart cells of mice, showed significant reduction in activities of complex I and II of electron transport chain. Moreover, the mitochondrial activity of STAT3 was confined to serine phosphorylation at position 727, as overexpression of STAT3^{S727A} in STAT3^{-/-} cells did not restore the mitochondrial complex I activity. Surprisingly, STAT3^{Y705F} and STAT3^{EE434-435AA} mutants completely restored mitochondrial activity in STAT3 deficient cells, indicating that transcriptional activity is not required for this effect (Wegrzyn et al., 2009).

Third, synaptic plasticity was induced by STAT3 independent of its transcriptional activity. JAK2 inhibition using pharmacological or genetic approaches inhibited NMDA receptor dependent long-term depression (LTD). The downstream signaling molecule STAT3 was also involved in JAK2 mediated LTD. Interestingly, LTD was not impaired by blocking the transcriptional activity of STAT3 using Gallielalactone (Nicolas et al., 2012). The mechanism by which STAT3 regulates LTD still remains unknown.

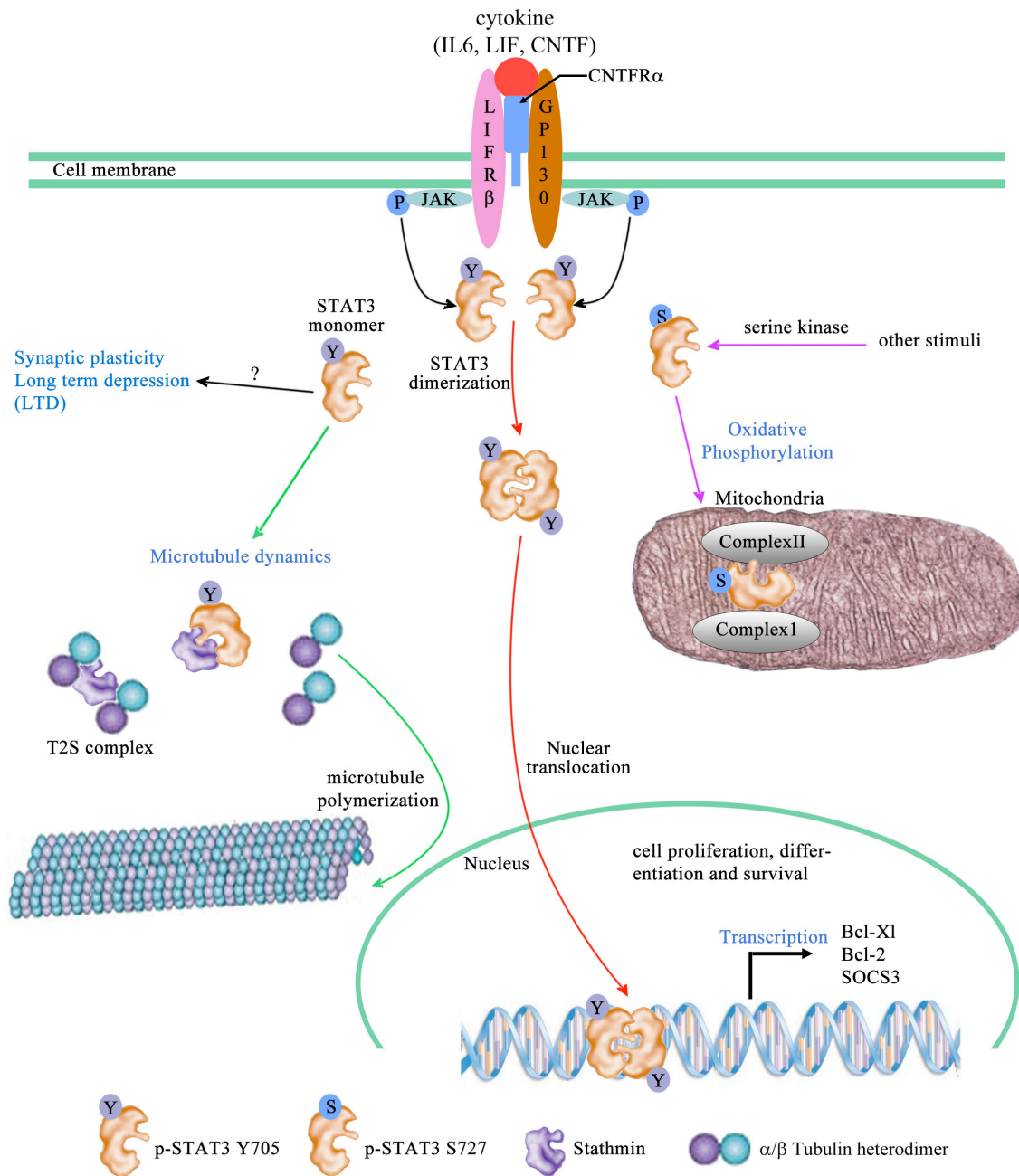


Figure 3.1 Various role of STAT3 in the cell

Schematic representation of various signaling pathways stimulated by STAT3 after cell stimulation by cytokines.

1. p-STAT3^{Y705} upon cytokine stimulus translocates to the nucleus and activates transcription of genes required for survival and differentiation (follow red arrows).
2. p-STAT3^{Y705} in cytosol alters microtubule dynamics by sequestering Stathmin from α/β tubulin heterodimers and also potentiates LTD via an unknown mechanism (follow green arrows).
3. p-STAT3^{S727} localizes to mitochondria and regulates cellular respiration (follow magenta arrows).

3.4 Microtubule biogenesis: Role in motor axon growth and maintenance

Microtubules are important component of the cytoskeleton, which helps in maintenance of shape and integrity of cells. Moreover, microtubules acts as rails along which cytosolic components are transported within the neuron (fast axonal transport). Microtubules are long hollow cylinders made up of polymerized α/β tubulin heterodimers. α -tubulin and β -tubulin heterodimers form a protofilament and 13 such protofilaments yield a helical arrangement (Figure 3.2A) The head to tail orientation of microtubules renders as polarized structures. The polarity of the microtubule depends on the orientation of α and β tubulin, with β -tubulin exposed at the faster growing 'plus' end and α -tubulin exposed at slower growing 'minus' end. In axons, the microtubules are oriented with their 'plus' ends directed towards the axon terminals whereas in dendrites both orientations are observed. Dynamic instability during polymerization is based on the effect that α and β tubulin of the heterodimers are bound to GTP that could be hydrolyzed to GDP. GTP bound to α -tubulin in α and β tubulin heterodimers gives rise to stable microtubules; whereas GDP bound α -tubulin are prone to microtubule to depolymerization.

3.4.1 Chaperonin mediated folding of Tubulin

Tubulins monomers (α and β) interact after translation with prefoldin, a heterohexameric protein which functions as a chaperone transferring the tubulin monomer to cytosolic chaperone (CCT) (Vainberg et al., 1998). Chaperonins facilitate the proper folding and formation of α and β tubulin subunits utilizing GTP as energy source (Gao et al., 1993). The tubulin subunits then bind to series of tubulin binding cofactors (TBCA-TBCE). α -tubulin binds to TBCB and TBCE whereas β -tubulin binds to TBCA and TBCD. The tubulin monomers are dimerized by a complex formation of monomers attached to their respective chaperone (TBCE- α -tubulin and TBCD- β -tubulin), finally, the α/β tubulin heterodimer are released in presence of TBCC (Lewis et al., 1997) (Figure 3.2B)

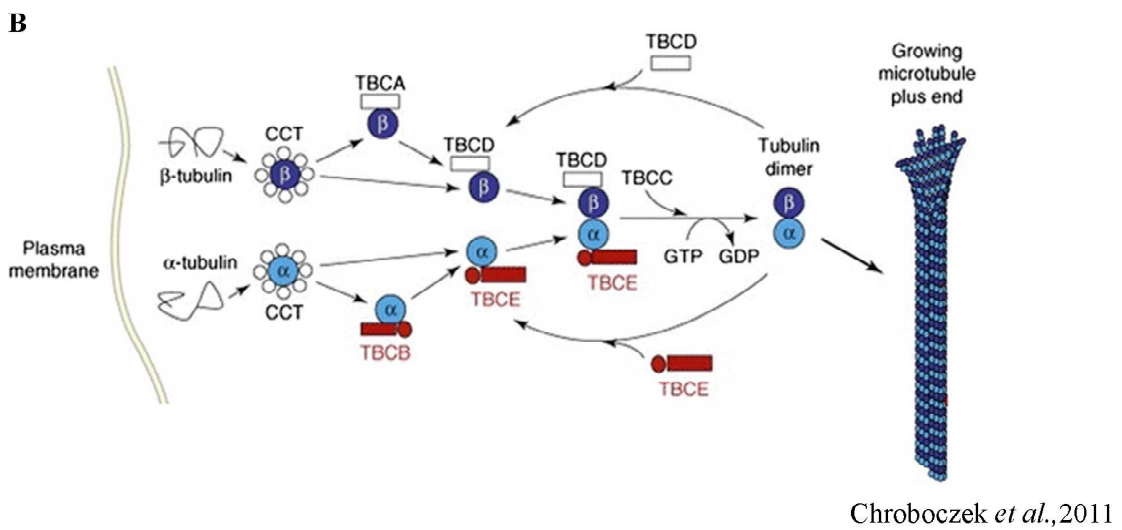
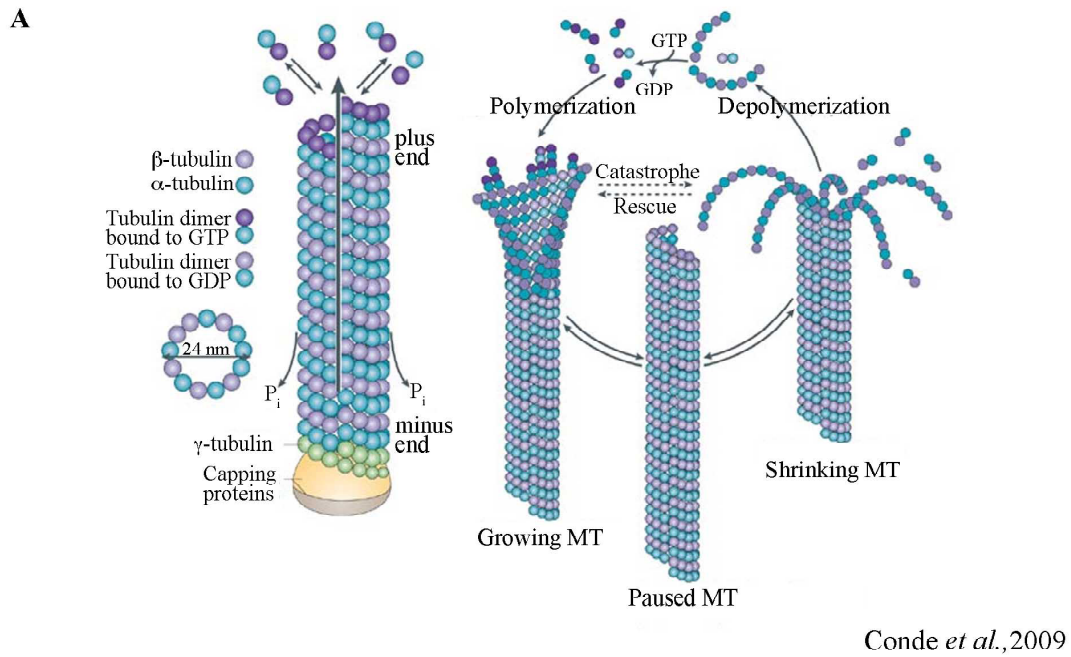


Figure 3.2: Microtubule biogenesis

(A) Schematic diagram showing microtubule polymerization / depolymerization cycle (Conde and Caceres, 2009)

(B) Scheme of chaperone mediated formation of α/β tubulin heterodimers (Szolajska and Chroboczek, 2011)

3.4.2 Post-translational modifications of Tubulin

In neurons, microtubules are greatly involved in neuronal polarization, trafficking of components across the axon, remodeling of dendritic spines etc. Although the structure and components of microtubules are highly conserved, different posttranslational modifications in tubulins make them highly dynamic and versatile. Nascent α -tubulin after translation has a C-terminal tyrosine aminoacid (Tyr-Tubulin), and this is found in most of the α -tubulin genes across different species. Newly assembled α/β tubulin heterodimers exhibit this C-terminal tyrosine thus marking highly dynamic and readily available subunits for polymerization into microtubules. Removal of tyrosination from α -tubulin was initially observed in 1973, this process is mediated by at least one unknown carboxypeptidase (Barra et al., 1973). The process is reversed by the enzyme Tubulin tyrosine ligase (Raybin and Flavin, 1977). Tyrosinated tubulin was observed to be crucial for kinesin-1 to distinguish axon and dendritic compartment. The tyrosinated tubulin which is abundant in dendrite prevents binding of kinesin-1 to microtubules, thereby navigating it and its associated cargo to axons (Konishi and Setou, 2009). Furthermore, CLIP170, a +TIP end binding protein, interacts with tyrosinated tubulin and its activity is thus concentrated in growth cone (Robson and Burgoyne, 1989). Detyrosinated tubulin can be further modified by removal of a penultimate glutamate residue resulting in $\Delta 2$ -tubulin that cannot be reversed to detyrosinated state. Once the glutamate residue is removed it cannot be reversed, this makes microtubules more stable and less vulnerable for depolymerization. Another important tubulin posttranslational modification observed is acetylation at lysine 40 of α -tubulin (L'Hernault and Rosenbaum, 1985). Several acetyltransferases such as ARD1-NAT1 (Ohkawa et al., 2008) and Elongator protein complex (ELP complex) (Creppe et al., 2009) have been shown to increase the acetylation of tubulin. This reaction is reversible involving deacetylases such as Histone deacetylase 6 (Hubbert et al., 2002) and Sirtuin2 (North et al., 2003). Acetylation occurs in the microtubule polymer state and is widely considered to mark a stable form of tubulin. Overexpression of HDAC6 led to reduced

levels of acetylated tubulin and increased its propensity to microtubule depolymerization (Tran et al., 2007). Microtubule acetylation is often associated with neuronal differentiation (Falconer et al., 1989). Microtubule dynamics is critical for neuronal polarization; recent evidence from cultured hippocampal neurons *in-vitro* showed increased microtubule stability in the axonal shaft of single neurites, which then develops into the future axon. The neurites where the microtubules are highly unstable (high tyrosinated tubulin) develops into dendrites (Witte and Bradke, 2008; Witte et al., 2008). Alteration of tubulin dynamics towards stabilization by treatment with taxol has been shown to reduce tissue scarring after spinal cord injury and to support axon regeneration (Hellal et al., 2011). These findings suggest that the post-translational modifications of tubulin are important in providing the basis for regulatory mechanisms of neuronal differentiation, transport and axon guidance (Janke and Bulinski, 2011).

3.4.3 Stathmin, a microtubule destabilizing protein

Various proteins other than α and β tubulin and its own posttranslational modifications regulate microtubule dynamics. They fall into two categories, the first category represents microtubule associated proteins (MAPs) that induce microtubule polymerization by either promoting microtubule polymerization or by arresting their depolymerization. Tau and MAP1B were observed to associate with microtubules near the growth cone region and promote axon length. The second category includes microtubule-destabilizing proteins such as Stathmin family members. This protein family includes Stathmin1, SCG10, SCLIP and RB3. Stathmin1 is a 19 kDa oncoprotein that was identified as a regulatory phosphoprotein in signal transduction controlling cell proliferation and differentiation. Sequence analysis of Stathmin showed the regulatory domain with phosphorylation sites to be present in the amino terminal and carboxy domain contains α helices, presumably for interaction with coiled coil domain proteins (Beretta et al., 1993; Maucuer et al., 1993). Search for interacting proteins to carboxy terminal of Stathmin revealed tubulin as a binding partner (Curmi et al., 1997). Characterization of this

interaction helped to understand the function of Stathmin protein in microtubule dynamics, Stathmin interacts with two molecules of soluble α/β tubulin heterodimers in phosphorylation dependent manner to form a tight ternary T2S complex. The α/β tubulin heterodimers bound to Stathmin T2S complex cannot polymerize to microtubules, and thereby Stathmin acts as a tubulin sequestering factor that arrests microtubule polymerization. Stathmin1 does not bind to the microtubules to promote microtubule catastrophe (Jourdain et al., 1997). There are 4 serine phosphorylation sites in Stathmin at positions 16, 25, 38, 63 that negatively regulates the sequestering of tubulin by Stathmin (Di Paolo et al., 1997). Other members of the Stathmin family have similar domain pattern such as Stathmin. The amino terminal regulatory domain and carboxy terminal interaction domain are highly conserved, and variations occur in length of amino terminal presumably for specific targeting. Stathmin1 is ubiquitously expressed unlike other members that are exclusively present in the nervous system. The function of SCG10, SCLIP and RB3 are very similar to Stathmin1 in sequestering α/β tubulin heterodimers, although they vary in the kinetics and the strength of T2S complex formation. Surface plasmon resonance analysis on different members of the Stathmin family for binding to α/β tubulin heterodimers showed higher stability and slow kinetics for RB3 and medium stability and kinetics for SCLIP, SCG10 and Stathmin1 (Charbaut et al., 2001).

High expression of Stathmin family members in nervous system prompted functional studies on the role of these molecules in neuronal differentiation. Stathmin knock out mice did not show any obvious developmental phenotype, but aging mice developed axonopathy both in the central and peripheral nervous system. Stathmin^{-/-} mice showed degenerating axons, demyelination, reduced motor nerve conduction velocity (Liedtke et al., 2002), deficits in long-term potentiation and decreased learning in amygdala fear conditioning (Shumyatsky et al., 2005). SCG10 is found to be phosphorylated by c-Jun N-terminal Kinase, this phosphorylation regulates microtubule dynamics and leads to increased neurite outgrowth in cortical neurons (Tararuk et al., 2006). Another study showed that activation of voltage gated calcium channels

leads to CaMKII dependent phosphorylation of Stathmin at serine 16, and subsequent microtubule stabilization and formation of dendritic arborization (Ohkawa et al., 2007). Thus, the functional correlation between Stathmin and neurite outgrowth by altering microtubule dynamics in various models provides evidence that Stathmin might play a vital role in axonal maintenance and possible therapeutic target to treat neurodegenerative diseases.

3.5 Role of TBCE in synapses

Microtubule and microfilament dynamics in the neuronal growth cone are critical for reaching the target tissue and for forming mature synapse. The dynamic growth cone responds to the external stimuli such as ephrins, laminin by locally altering microtubule and microfilament dynamics.

Recent studies in *Drosophila melanogaster* have opened a new perspective on the function of microtubules in synapses. Futsch, the *Drosophila* homologue for MAP1B, was observed to regulate the formation and stabilization of microtubule loops in synaptic boutons. Formation of these microtubule loops in which Futsch was present correlated with bouton division. Futsch null mutants that are unable to maintain microtubule loops and had reduced number of boutons (Roos et al., 2000). Another intriguing finding is the localization of TBCE in NMJ's of *Drosophila melanogaster* in-vivo (Jin et al., 2009) and the enrichment in growth cones of mouse primary motoneurons in-vitro (Bender FLP Ph.D thesis) suggesting that TBCE might have a novel function at synapse. Tissue specific knockdown of TBCE in neurons and target muscle lead to locomotion defects in *Drosophila melanogaster* (Jin et al., 2009). Closer look at the NMJ revealed increased bouton number and decreased bouton size demonstrating that TBCE is required for normal development of NMJ. Increased neurotransmission, reflected by higher excitatory junction potential, was observed upon pre-synaptic alteration of TBCE, presumably because of increased synaptic vesicle size. Interestingly, overexpression and knockdown of TBCE in the pre-synaptic compartment resulted in similar phenotype both in number of boutons

and synaptic transmission suggesting that TBCE expression is involved in the precise control of microtubule dynamics required for normal NMJ function (Jin et al., 2009).

A recent study from Dr. N Funk identified TBCE-like protein, a homologue of TBCE in *Drosophila* and Human, as an interaction partner in yeast-two-hybrid screen using Synapse Associated Protein 47 (SAP47) as a bait (unpublished results). SAP47 was identified from a screen using a hybridoma antibody library of *Drosophila* brain extracts (Hofbauer et al., 2009). Selective staining of synaptic terminals in immunohistochemical preparations was used as a parameter to screen the antibodies. Western blot analysis of *Drosophila* brain homogenates with MAB nc-46 recognized a protein of 47 kDa size (Hofbauer et al., 2009; Reichmuth et al., 1995). Ultrastructural analysis showed that SAP47 was localized within 30 nm of a synaptic vesicle. Functional analysis of SAP47 was carried out using *Sap47*^{l56} null allele, SAP47 null flies are viable and fertile, they exhibit normal motor performance and neurotransmission at NMJ. However, these flies showed 50% loss of associative learning in odorant conditioning (Saumweber et al., 2011). The mouse homologue of SAP47 is Synapse associated protein 1 (SYAP1). The function of this protein is still unknown. The *Syap1* gene maps to the X-chromosome in mouse and codes for a transcript length of 2087 bp and translated to a protein of 365 aminoacids. Expected molecular weight of this SYAP1 protein is around 42 kDa. In hindsight, with the existing knowledge of SAP47 interaction with TBCE-like protein, functional characterization of SYAP1 might be helpful for understanding the role of TBCE in synapses.

3.6 Goal of the thesis

Neurotrophic factors produced by the target tissues promote survival, regeneration of injured axons and axonal maintenance. Treatment with CNTF prevents axonal degeneration of motoneurons and death in *pmn* mutant mice (Sendtner et al., 1992b) which carries a point mutation in *Tbce* gene leading to a unstable mutant protein TBCE^{W524G} (Bommel et al., 2002; Martin et al., 2002). On the contrary, GDNF, another potent neurotrophic factor only rescued the loss of motoneurons but did not prevent axon degeneration and disease progression in *pmn* mice (Sagot et al., 1996). Similarly, over expression of Bcl-2 in motoneurons in *pmn* mutant mice prevented the death of cell bodies, but did not influence the disease onset or progression (Sagot et al., 1995) Taken together these findings indicate CNTF has a distinct role in axonal maintenance. The work presented in this thesis aimed to characterize the molecular mechanism by which CNTF in contrast to other neurotrophic factors prevents axon degeneration in *pmn* mutant motoneurons *in-vitro*. Additionally, regulation of the mutant form of TBCE that is responsible for motoneuron degeneration in *pmn* mice was analyzed with respect to its stability. We also checked whether CNTF could regulate TBCE at the transcriptional and translational level.

Since TBCE has been observed to play a role in maintenance of the neuromuscular junction and the regulation of neurotransmission in *Drosophila* (Jin et al., 2009) and its homologue E-like protein was identified in yeast-two-hybrid screen to interact with *Drosophila* Synapse Associated Protein 47 (SAP47), this present study by utilizing various molecular techniques addressed whether TBCE interacts with mouse synapse associated protein 1 (SYAP1), a homologue of SAP47. Moreover, this work also characterized the mouse SYAP1 protein, with the goal to understand the function of TBCE in synapse.

4. MATERIALS AND METHODS

4.1 MATERIALS

4.1.1 Animals

All laboratory animals were bred in the animal husbandry of Institute of clinical neurobiology, University of Würzburg. They were maintained in 12h/12h day night cycle with proper access to food and water. Following animals were used in this present study.

4.1.1.1 CD-1

CD-1 mice were used as a wildtype mouse in this study. These were maintained as an outbred line obtained from Charles River animal facility.

4.1.1.2 *pnn*

pnn mouse was identified as spontaneous mutant in a colony of Pan: NMRI mice at the animal department of the Panum Institute in Copenhagen (Schmalbruch et al., 1991). These mice were maintained as an outbred strain (NMRI background) as the litter size was larger than inbred strain (C57 BL/6).

4.1.1.3 NFL-Cre^{tg}

NFL-Cre^{tg} mouse line was generated and characterized by Ulrich Schweizer (Schweizer et al., 2002). The Cre recombinase was cloned under human NF-L promoter. The transgenic mice expressed Cre recombinase in brain and spinal cord, but not in other organs such as kidney, liver and spleen. This mouse line was cross bred to STAT3^{KO} to generate STAT3^{KO};NFL-Cre^{tg/tg}, and subsequently used to generate conditional ablation of STAT3 in primary motoneurons (Schweizer et al., 2002).

4.1.1.4 STAT3^{KO} and STAT3^{FL}

STAT3^{KO} and STAT3^{FL} mouse were generated in Shizuo Akira's laboratory. The Mouse STAT3 gene consists of 24 exons spanning a region greater than 37 kb and located in chromosome 11. The gene structure is similar to human STAT2 (Shi et al., 1996). STAT3^{KO}

mice was generated by targeting genomic fragment containing exons 20, 21 and 22 of STAT3. Mice heterozygous for STAT3^{KO} were phenotypically normal and viable. The homozygous mice dies at embryonic day 7.5 (Takeda et al., 1997). The STAT3^{FL} mouse was generated so that the STAT3 tyrosine phosphorylation could be removed by tissue specific expression of Cre recombinase. The mouse carries loxP sites flanking exon 22 (Takeda et al., 1998), which codes for region containing tyrosine 705 aminoacid.

Conditional STAT3 knockout (KO) was achieved by crossing a mouse line homozygous for NFL-Cre^{tg} and carrying a STAT3 null allele (STAT3^{wt/KO};NFL-Cre^{tg/tg}) with mice homozygous for loxP flanked STAT3 (STAT3^{fl/fl}), as previously described (Schweizer et al., 2002). To obtain STAT3 deficient *pmn* mutant (*pmn*^{mut/mut};STAT3^{fl/KO};NFL-Cre^{tg}) embryos, STAT3^{KO/wt};NFL-Cre^{tg/tg} and STAT3^{fl/fl} mice were crossed with *pmn*^{wt/mut} mice to generate STAT3^{wt/KO};NFL-Cre^{tg}; *pmn*^{wt/mut} and STAT3^{fl/fl}; *pmn*^{wt/mut} animals. These 2 lines served as parental generation for litters that contain STAT3 deficient *pmn* mutant embryos.

4.1.2 Cell Lines

4.1.2.1 HEK 293T cell line:

Human Embryonic Kidney 293 cells were used to generate lentiviruses and protein expression studies. HEK 293T cells are a highly transfectable derivative where simian virus 40 (SV 40) large T antigen was inserted (DuBridge et al., 1987). This allows episomal replication of transfected plasmids containing the SV40 origin of replication.

4.1.2.2 Neuro2A cell line

Mouse neuroblastoma cell line was used for protein expression studies.

4.1.2.3 NSC 34 cell line

NSC 34 cells are mouse-mouse hybrid cell lines generated by fusion of neuroblastoma and motoneuron isolated from embryonic day 12-14 spinal cord. These cells possess motoneuron like properties such as generating action potentials, acetylcholine synthesis, storage and release

(Cashman et al., 1992). These cells are also used for studies in neurotrophin receptor trafficking (Matusica et al., 2008).

4.1.3 Buffers and Reagents

4.1.3.1 SDS-PAGE and Western Blot

Resolving gel:

Reagents	Percentage of the Gel			
	6	8	10	12
30% Acrylamide bis-acrylamide (29:1)	3 ml	4 ml	5 ml	6 ml
1.5 M Tris-HCl pH 8.8	3.75 ml	3.75 ml	3.75 ml	3.75 ml
10% SDS	150 μ l	150 μ l	150 μ l	150 μ l
10% Ammonium persulfate	150 μ l	150 μ l	150 μ l	150 μ l
T.E.M.E.D	10 μ l	10 μ l	6 μ l	6 μ l
Water (Millipore grade)	7.95 ml	6.95 ml	5.95 ml	4.95 ml

Stacking gel:

Reagents	4%
30% Acrylamide bis-acrylamide (29:1)	1.7 ml
1 M Tris-HCl pH:6.8	1.25 ml
10% S.D.S	100 μ l
10% Ammonium persulfate	100 μ l
T.E.M.E.D	10 μ l
Water (Millipore grade)	6.8 ml

Table 4.1: Composition of SDS polyacrylamide gel

SDS running buffer (10 X) 1L	30.3 g Tris Base 144 g Glycine 10 g SDS
Laemmli buffer (5X)	4% SDS 125 mM Tris-HCl pH 6.8 10% mercaptoethanol 20% glycerol 0.004% bromophenol blue
TBS pH:7.4 (10X) 1L	0.2 M Tris Base 1.5 M NaCl
TBST pH:7.4	100 ml 10X TBS 0.5% Tween 20 Made up to 1L with millipore water
Blocking buffer and diluent for antibody:	5% Non fat milk diluted in TBST, boiled for 10 minutes at 99°C
Diluent for antibodies raised against phosphorylated proteins	5% Bovine serum albumin diluted in TBST
Stripping buffer pH:2.2 1L	15 g glycine 1 g SDS 10 mL Tween 20
4.1.3.2 Buffers for protein extraction	
RIPA buffer (Total protein)	50 mM Tris HCl pH: 7.6 150 mM NaCl 1% NP 40 1% Sodium deoxycholate 0.1% SDS 2 mM EDTA

Protease inhibitor 1X (Soto et al.)
1 mM Sodium fluoride
10 mM Sodium pyro phosphate
1 mM okadoic acid
2 mM Sodium orthovanadate

Nuclear fractionation buffer
(Also used for immunoprecipitation)

50 mM Tris HCl
150 mM NaCl
1% NP 40 or 1% TritonX 100
Protease inhibitor 1X
2 mM EDTA
1 mM Sodium fluoride
10 mM Sodium pyro phosphate
1 mM okadoic acid
2 mM Sodium orthovanadate

Microtubule fractionation buffer
(Also called PHEM Buffer)

60 mM PIPES
25 mM HEPES
10 mM EGTA
2mM MgCl₂

4.1.3.3 Buffers for DNA extraction and Agarose gel electrophoresis:

DNA extraction buffer

10 mM Tris pH: 7.5
200 mM NaCl
0.2% SDS
5 mM EDTA

TAE buffer (50X) 1L

2M Tris Base
50 mM EDTA pH:8.0
57.2 ml Glacial acetic acid

4.1.4 Media for cell culture

4.1.4.1 Motoneuron cell culture

Neurobasal with 1X Glutamax
2% horse serum
1X B27 supplement
BDNF 5 ng/ml, CNTF 10ng/ml

4.1.4.2 HEK 293T, NSC 34, N2A cell lines

DMEM with 1X Glutamax
10% fetal bovine serum
1X non essential amino acids
1X penstrep

4.1.4.3 Neural stem cells

Neurobasal with 1X Glutamax
1X B27 supplement
1X Penstrep
bFGF 20 ng/ml, EGF 20 ng/ml, LIF 10 ng/ml

4.1.5 Chemicals

30% Acrylamide bis acrylamide (29:1)	Applichem
Acetic acid	Merck
Agarose	Applichem
Ammonium persulfate	Sigma
B-27 supplement	GIBCO-Invitrogen
Basic FGF	Cell concepts
BDNF	Home made
Bromophenol blue	Merck
Bovine serum albumin	Applichem
Boric acid	Applichem
CNTF	Institute of Clinical Neurobiology
Di-Sodium hydrogen phosphate	Merck
DMEM	GIBCO-Invitrogen
EDTA	Merck
EGTA	Sigma

EGF	Cell concepts
Ethanol	Sigma
Glutamax	GIBCO-Invitrogen
Glycine	Merck
Goat serum	Liniaris
HBSS	PAA
HEPES	Sigma
Horse serum	Liniaris
Laminin	Invitrogen
LIF ESGRO [®]	Millipore
Magnesium chloride	Sigma
Mercaptoethanol	Merck
Methanol	Sigma
Milk powder	Applichem
Non essential amino acids	Invitrogen
Neurobasal	GIBCO-Invitrogen
Okadoic acid	Calbiochem
Page ruler pre stained protein ladder	Fermentas
Penstrep	Invitrogen
PIPES	Sigma
Poly D-L-Ornithine	GIBCO
Protease inhibitor complete mini	Roche
Proteinase k	Roche
Sodium chloride	Merck
Sodium di-hydrogen phosphate	Merck
Sodium pyrophosphate	Merck
Sodium Fluoride	Merck
STAT3 inhibitor VI, S3I-201	Santa Cruz Biotechnology, inc.
TEMED	Merck
Tris Base	Merck
TritonX 100	Sigma
Tween 20	Sigma
Trypsin	Worthington
Trypsin inhibitor	Sigma

4.1.6 List of Antibodies

Antibody	Species	Dilution	Company
α -tubulin	Mouse	WB-1:5000 IF-1:2000	Sigma
Acetylated tubulin	Mouse	WB-1:5000 IF-1:2000	Sigma
GAPDH	Mouse	WB-1:5000	Calbiochem
γ -tubulin	Rabbit	IF-1:1000	Abcam
GFAP	Mouse	WB-1:5000	Abcam
β -tubulin	Mouse	WB-1:2500 IF-1:1000	Sigma
Histone3	Rabbit	WB-1:20000	Abcam
Stathmin	Rabbit	WB-1:2000	Abcam
Stathmin	Rabbit	WB-1:2000 IP-1:100	Abcam
STAT3	Mouse	WB-1:5000 IF-1:1000	Cell signaling
pSTAT3 ^{Y705}	Rabbit	WB-1:2000	Cell signaling
pSTAT3 ^{S727}	Rabbit	WB-1:2000	Cell signaling
p75 ^{NTR}	Mouse	Panning: 15 ng/ml	Prof. Rush lab
TBCE	Rabbit	WB-1:2000 IF-1:1000	Prof. Sendtner lab
Tyrosinated tubulin	Rat	WB-1:2000 IF-1:2000	Abcam
SYAP1	Rabbit	WB: 1:1000, IF:1:1000	Sigma

Table 4.2: List of Antibodies

4.1.7 List of Plasmids

Vector	Source
pLL3.7 sh-Stathmin	Cloned by Dr. Florian Bender
pLL3.7 sh-Stathmin mismatch	Cloned by Dr. Florian Bender
pMDG VSVG	Institute of Virology, Würzburg
pRSV-REV	Institute of Virology, Würzburg
pMDLg/pRRE	Institute of Virology, Würzburg
FuGW-STAT3-EYFP	Cloned by Nicolas Frank
FuGW-STAT3Y705F-EYFP	Cloned in this work/ Nicolas Frank
FuGW-STAT3EE434-435AA-EYFP	Cloned by Nicolas Frank
pGJ3-HA-TBCE	Cloned by Dr. Florian Bender/Dr. N.Funk
pGJ3-HA-TBCE ^{W524G}	Cloned by Dr. Florian Bender/ Dr.N.Funk
pGJ3-FLAG-SYAP1	Cloned by Dr. Natalja Funk
pcDNA3-FLAG-SYAP1	Cloned by Dr. Natalja Funk

Table 4.3: List of plasmids

4.1.8 List of Oligonucleotides

pmn fw	:	5'-TGA CCA ACC AAA TCA CTG TAG TG-3'
pmn rev	:	5'-TAG CAT GCA CCA TCA GAT CG-3'
ST3 KO a	:	5'-AGC AGC TGA CAA CGC TGG CTG AGA AGC T-3'
ST3 KO b	:	5'-TTG CTG CTC TCG CTG AAG CGC AGT AGG-3'
ST3 KO c	:	5'-ATC GCC TTC TAT CGC CTT CTT GAC CAG-3'
STAT3 FL fw	:	5'-CCT GAA GAC CAA GTT CAT CTG TGT GAC-3'
STAT3 FL rev	:	5'-CAC ACA AGC CAT CAA ACT CTG GTC TCC-3'
Tbce fw	:	5'-TCA TTA TCG CCA AGA TTG CTC-3'
Tbce rev	:	5'-GCC TGT TTT TGT CTG GAT CTG-3'
beta_actin_fw	:	5'-AGA TTA CTG CTC TGG CTC CT-3'
beta_actin_rev	:	5'-GGA CTC ATC GTA CTC CTG CT-3'
ST3 Y705F fw	:	5'-GTA GTG CTG CCC CGT TCC GAA GAC CAA G-3'
ST3 Y705F rev	:	5'-CTT GGT CTT CAG GAA CGG GGC AGC ACT AC-3'

4.1.8 List of Commercial Kits

1. Superscript First strand synthesis system for RT PCR - Roche
2. Endofree Plasmid maxi kit - Qiagen
3. LightCycler Fast Start DNA Master SYBR Green1- Roche
4. RNeasy® mini kit – Qiagen
5. Quick Change Lightning multi site-directed mutagenesis kit

4.1.9 Software

1. Adobe Photoshop CS3
2. ImageJ
3. Leica LAS-AF lite (Leica SP2, SP5 software)
4. GraphPad prism 4.0

4.2 METHODS

4.2.1 DNA isolation (Phenol-Chloroform)

Mouse DNA was isolated from tail or head biopsy of day 14 embryos. DNA extraction buffer (500 µl) with proteinase K (20 µl) was added and mixed at 55°C overnight until the tail was dissolved. Next day, equal volume of buffered phenol was added, mixed vigorously and centrifuged at 12,000 x g for 5 minutes. Aqueous layer was removed and mixed with equal volume of phenol:chloroform:isoamyl alcohol at a ratio of 25:24:1 and centrifuged again at 12,000 x g for 5 minutes. The aqueous layer was again removed and DNA was precipitated by adding 1 ml of 2-propanol to the aqueous phase and centrifuged at 20,000 x g for 10 minutes. Pellet was washed with 500 µl of 70% ethanol and centrifuged again at 20,000 x g for 10 minutes. The pellet obtained was then air dried and dissolved in 200 µl of TE buffer. This DNA is used for genotyping the embryos by PCR analysis.

4.2.2 RNA isolation

RNA isolation was performed on cultured primary motoneurons using RNeasy® mini kit. Cells (approx. 200,000 cells) were washed 3 times with DEPC treated PBS (RNase free). Cells were lysed using 350 µl RLT buffer with 4 µl β-mecaptoethanol, scraped off and pipetted 10 strokes to mix. 350 µl of 70% ethanol was added to the homogenised lysate. This mixture was then added to RNeasy spin column and centrifuged at 8000 x g for 15 seconds. This allows the RNA to bind to the column. The flow through was discarded and 700 µl of buffer RW1 was added to the column. The column was centrifuged again at 8000 x g for 15 seconds. RNA bound to the column was then washed 2 times with buffer RPE containing ethanol and centrifuged at 8000 x g for 2 minutes. The RNA was then eluted with 30 µl of RNase free water (provided in the kit) by centrifuging 8000 x g for 1 minute. The quantity and of RNA was analyzed by measuring it in nanodrop and the quality was also assessed by ratio of absorption at 260nm and 280nm. Ratio of 260/280 should be close to 2 for RNA.

4.2.3 Genotyping of mouse lines

4.2.3.1 *p_{mn}* mouse line

P_{mn} genotyping is performed using restriction fragment length polymorphism (RFLP) analysis. RFLP analysis can be used to identify a change in nucleotide sequence (mutation in the case of *p_{mn}* mouse line) that results change in restriction digestion pattern. The transition of T-G at position 1682 in *Tbce* gene lead to additional M_nII restriction site and unique for mutant allele. The strategy for *p_{mn}* genotyping is depicted in Figure 4.1. Briefly, a region (441 bp) of *Tbce* gene was amplified from genomic DNA isolated from tail biopsies (either by phenol chloroform isolation or boiling (99°C) tail biopsies in 100 µl water for 10 min) using polymerase chain reaction (PCR) with *p_{mn}* fw and *p_{mn}* rev primers. The pcr amplicon was then digested with M_nII restriction enzyme and digestion pattern was observed in 3% agarose gel electrophoresis performed with SB buffer. PCR amplicon from WT allele has 1 M_nII restriction site, therefore 2 products of size 226 bp and 215 bp were observed. Mutant allele has an additional M_nII site thereby generating 3 products of size 226 bp, 136 bp and 79 bp. Following table shows the expected product size for different genotypes. PCR conditions and M_nII restriction digestion composition are listed as follows.

Reagents	Volume	PCR cycle conditions	Duration
Tbce Fw (50 pmol/µl)	0.2 µl	94°C	2 min
Tbce Rev (50 pmol/µl)	0.2 µl		
dNTP's (10 mM)	1 µl	94°C	30 cycles
5' Taq polymerase	0.3 µl	53°C	
5' Taq buffer	2 µl	72°C	
DNA	1 µl of purified DNA or 3 µl of supernatant	72°C	7 min
Water	Made up to 20 µl	4°C	hold

Table 4.4: PCR components and cycling conditions for genotyping *p_{mn}* mutant mice

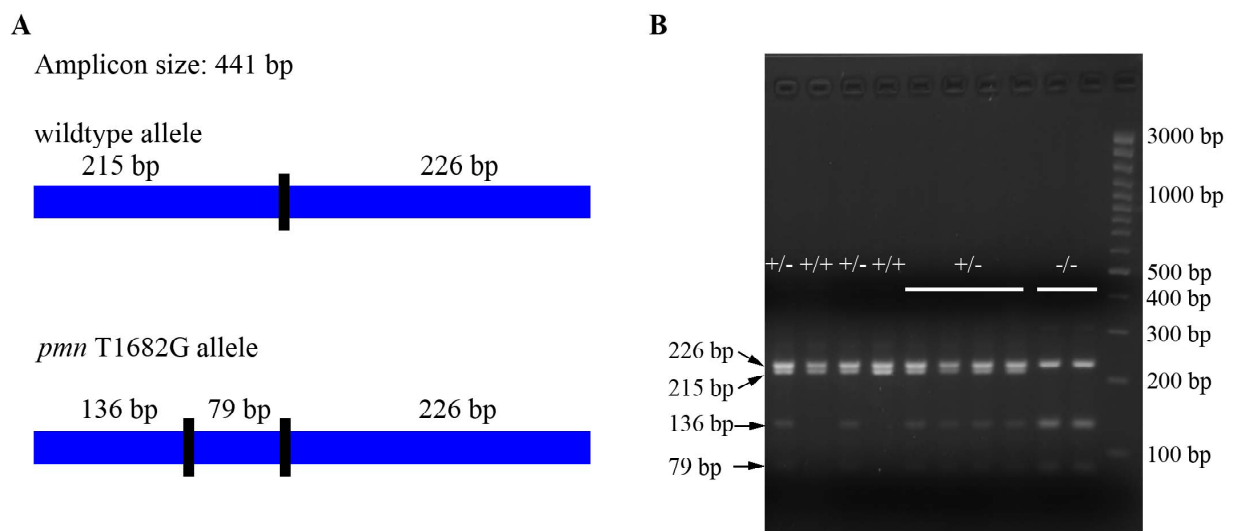
MnII restriction digestion:

PCR product	: 20 μ l
Buffer Green	: 2.5 μ l
MnII enzyme	: 0.2 μ l
Water	: 2.3 μ l

Following table 4.5 shows the expected product size for different genotypes.

Genotype	Product size observed (bp)
Wildtype (+/+)	226 and 215
Heterozygous (+/-)	226, 215, 136 and 79
<i>Pmn</i> homozygous (-/-)	226, 136 and 79

Table 4.5: Expected product sizes for different genotypes of *pmn* after MnII restriction digestion

**Figure 4.1: Genotyping of *pmn* mouse line**

(A) Scheme of MnII restriction digestion pattern in wildtype and *pmn* allele

(B) Representative agarose gel of *pmn* genotyping from mouse tail biopsies, showing different MnII digestion pattern for wildtype, heterozygous and homozygous *pmn* mutants.

4.2.3.2 STAT3 floxed mouse line

Genotyping of STAT3 floxed mouse line was performed using standard PCR analysis. The primers are located outside loxP sites flanking exon 22 of STAT3, thereby the wildtype allele produces PCR amplicon of size 250 bp whereas the floxed allele generates amplicon of size 400 bp. Following table (Table 4.6) shows the PCR reagents and the cycling conditions required for genotyping STAT3 floxed mouse line. Figure 4.2 shows representative gel electrophoresis image for genotyping of STAT3 floxed mouse line.

Reagents	Volume	PCR cycle conditions	Duration
St3 fl Fw (50 pmol/ μ l)	0.2 μ l	94°C	2 min
St3 fl Rev (50 pmol/ μ l)	0.2 μ l	94°C	30 s
dNTP's (10 mM)	1 μ l	56°C	30 s
5' Taq polymerase	0.3 μ l	72°C	1 min
5' Taq buffer	3 μ l	72°C	15 min
Betaine 5M	6 μ l	4°C	hold
DNA	1 μ l of purified DNA		
Water	18.3 μ l		

Table 4.6: PCR components and cycling conditions for genotyping STAT3^{FL} mice

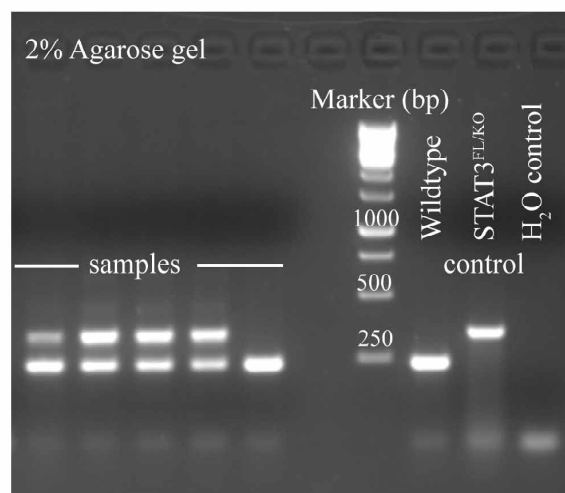


Figure 4.2: Genotyping of STAT3^{FL} mouse line
Representative agarose gel picture of STAT3^{FL} genotyping from mouse tail biopsies.

4.2.3.2 STAT3 knock out mouse line

Genotyping of STAT3 knockout mouse line was performed using standard PCR analysis. Two different PCR's (wildtype and knockout allele) were performed to determine the genotype. Wildtype allele was detected using primer pair St3 ko a + St3 ko b, whereas the knock out allele was detected using primer pair St3 ko a + St3 ko c. Both the PCRs generated an amplicon size of 1 kb. Following table 4.7 shows the PCR reagents and the cycling conditions required for genotyping STAT3 knock out mouse line. Figure 4.3 shows representative gel electrophoresis image for genotyping of STAT3 knock out mouse line.

Reagents	Volume	PCR cycle conditions	Duration
St3 ko a (50 pmol/ μ l)	0.2 μ l	94°C	5 min
St3 ko b or c (50 pmol/ μ l)	0.2 μ l	94°C	30 s
dNTP's (10 mM)	1 μ l	56°C	30 s
5' Taq polymerase	0.3 μ l	72°C	90 s
5' Taq buffer	3 μ l	72°C	35 cycles
Betaine 5M	6 μ l		
DNA	1 μ l of purified DNA		
Water	18.3 μ l	72°C	15 min
		4°C	hold

Table 4.7: PCR components and cycling conditions for genotyping STAT3^{KO} mice

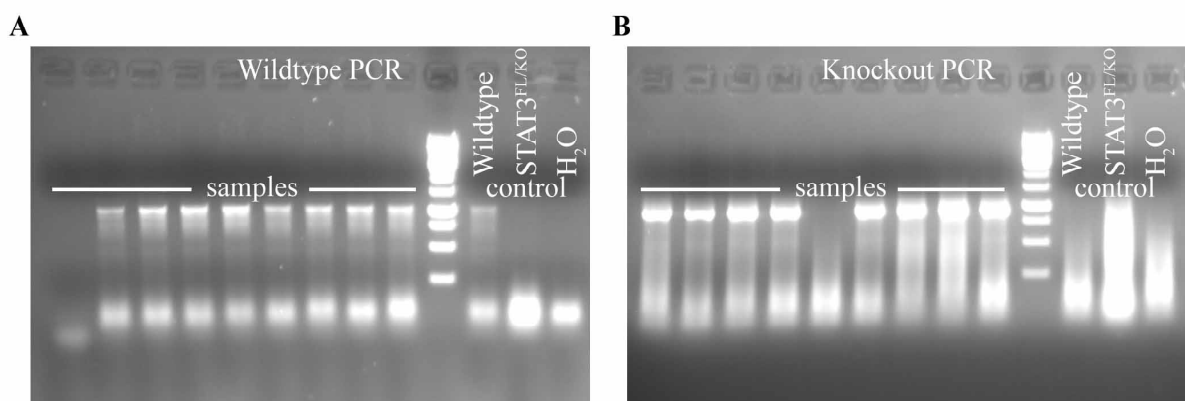


Figure 4.3: Genotyping of STAT3^{KO} mouse line
(A-B) Representative agarose gel pictures of STAT3^{KO} genotyping from mouse tail biopsies.

4.2.4 Reverse transcriptase PCR

Reverse transcriptase PCR was performed using SuperScript™ first strand synthesis system from Invitrogen. The RNA/primer mixture (RNA upto 5 µg, 1 µl of 10 mM dNTP's, 1 µl of 0.5 µg/µl oligo dT primer made upto 10 µl with DEPC water) was incubated at 65 °C for 5 min and kept in ice immediately for 1 min. Then the RT-PCR reaction mix was prepared as follows: 2 µl of 10X RT buffer, 4 µl of 25 mM MgCl₂, 2 µl of 0.1 M DTT, 1 µl RNase out. This RT reaction mix was added to the RNA/Primer mixture and incubated for 2 min at 42 °C. Then, 1 µl of Superscript III reverse transcriptase was added and incubated for 50 min at 42 °C. No-RT control was performed as a negative control. Finally, the RT-PCR reaction was terminated by denaturing the enzyme at 70 °C for 15 min.

4.2.5 Real time quantitative PCR analysis

Quantitative real time polymerase chain reaction is used to amplify and simultaneously quantify the PCR amplicons. This was performed in Lightcycler 1.5 from Roche using lightcycler fast start DNA master SYBR green kit. Following table shows the PCR reagents and cycle conditions performed to analyse the *Tbce* mRNA level.

Reagents	Volume	PCR cycle conditions	Duration
Tbce Fw (5µM)	2 µl	94°C	10min
Tbce Rev (5µM)	2 µl	94°C	0s
SYBR Green	2 µl	55°C	5 s
MgCl ₂ (25 mM)	1.6 µl	72°C	10 s
c-DNA (1:10)	2 µl	83°C	5 s
Water	18.3 µl		

PCR cycle conditions	Duration
94°C	10min
94°C	0s
55°C	5 s
72°C	10 s
83°C	5 s

Table 4.8: PCR components and cycling conditions for real time PCR analysis of *Tbce* mRNA level.

4.2.6 Isolation of mouse embryonic motoneurons

Primary motoneurons from lumbar spinal cord served as a model to understand the molecular mechanism in motoneuron diseases. The culturing of primary motoneurons was performed as described previously (Wiese et al., 2010). Briefly, ventrolateral parts of spinal cord were dissected from E13.5 mouse embryo and stored in 180 μ l HBSS and kept on ice. Tail or head biopsy was taken for genotyping the embryos. In case of wildtype embryos 3-4 spinal cords were pooled in 360 μ l of HBSS. The tissues were then trypsinized with 0.1% trypsin for 15 min at 37°C. Trypsin digestion was arrested by adding 0.1% trypsin inhibitor. The tissues were then triturated mechanically to form single cell suspension. To enrich the motoneurons from mixed population of cells derived from spinal cord, “immuno-panning” method was performed using the p75^{NTR} antibody. Cells were plated on 24-well NunclonTM Δ surface dish (1 embryo per well) precoated with p75^{NTR} antibody (clone: MLR2, 45 ng/ml) for 45 min, for wildtype motoneuron culture the cells were pooled and plated onto a 10 cm NunclonTM Δ surface dish. Cells were then washed three times with NB media to remove unspecific binding to cells to the antibody and eluted with 300 μ l (3 ml for 10 cm dish) depolarization solution. 500 μ l (5 ml for 10 cm dish) of NB media + 2% heat inactivated horse serum + 2% B27 supplement was then added to the dish and cells were eluted. Enriched motoneurons were counted in haemocytometer and plated in poly-DL-ornithine, laminin coated dishes. One hour after seeding, the cells were fed with NB medium containing horse serum, B27 and neurotrophic factors BDNF (5 ng/ml), CNTF (10 ng/ml). Fifty percent of the medium was exchanged on the next day and followed by alternative days.

Number of cells plated for different experiments as listed in the following table 4.9.

Size of Dishes	Number of cells	Application
Coverslip 10 mm or 12 mm	1500 - 2000	Immunocytochemistry
Coverslip 12 mm	5000	Microtubule regrowth assay

Size of Dishes	Number of cells	Application
24 well dish	0.1 - 0.2 x 10 ⁶	Western blot
12 well dish	0.3 - 0.5 x 10 ⁶	Western blot
10 cm dish	1-3 x 10 ⁶	Immunoprecipitation

Table 4.9: Number of motoneurons plated for different experiments

4.2.7 Immunocytochemistry

Immuocytochemistry analysis was performed to analyze the sub-cellular distribution of specific protein and axon length measurements. Motoneurons were cultured either for 5 DIV in the presence of appropriate neurotrophic factors. Cells were washed once with PBS to remove serum components and fixed with 4% paraformaldehyde for 15 min at room temperature. Cells were then washed three times with PBS for 15 minutes at RT. The fixed cells were blocked and permeablised with blocking buffer containing 15% goat serum, 0.3% TritonX-100 in TBS-T for 20 min at RT. The cells were then incubated overnight with primary antibody diluted in blocking buffer at 4 °C. Cells were subsequently washed three times with TBST, each for 15 min, and treated with corresponding secondary antibody for 1 h at RT. Cells were washed 3 times with TBST and mounted on glass slide with poly aqua mount. Imaging was performed with Leica TCS SP2 microscope with 40X oil immersion objective, NA 1.25. Axon length and intensity measurements were performed with LAS-AF lite software (Leica)

4.2.8 Nuclear fractionation

Nuclear translocation of p-STAT3 Y705 after CNTF application was studied by biochemical fractionation of nucleus and cytoplasm from cultured primary motoneurons. Primary motoneurons (approx. 250,000 cells) were cultured for 4 DIV with culture medium containing BDNF (5 ng/ml). Cells were washed 3 times with neurobasal medium to remove serum components and further cultured overnight in serum free medium with BDNF. CNTF (10

ng/ml) was applied for 5 min, 15 min, 30 min. In parallel, CNTF was applied for 5 days continuously to one culture. Cells were washed once with 1X PBS and lysed with the nuclear fractionation buffer, containing 50 mM Tris-HCl pH 7.4, 150 mM NaCl, 1% NP-40; 2 mM EDTA pH 8.0, 1X - protease inhibitor, 10 mM sodium pyrophosphate, 2 mM sodium orthovanadate, 1 mM sodium fluoride, 1 mM okadaic acid, for 10 min at 4 °C. Cells were scrapped off and centrifuged at 1,000g for 15 min at 4 °C. Supernatant was removed and used as cytoplasmic fraction. Pellet was washed once with PBS, and centrifuged again at 20,000g for 10 min at 4 °C. Pellet was used as nuclear fraction. Cytoplasmic and nuclear fractions were controlled using GAPDH (Calbiochem, clone 6C5, CB 1001) and histone 3 (abcam) antibodies as respective markers.

4.2.9 Immunoprecipitation (IP)

Immunoprecipitation is a technique of precipitation a protein of interest from total cell lysate using a specific antibody against the protein. This technique is widely used to enrich low abundance protein, to study protein-protein (Co-IP), protein-RNA (RNA IP) interactions and to identify the DNA binding site for protein (Chromatin IP).

Co-Immunoprecipitation analysis was performed to study whether CNTF activation of STAT3 alters the interaction with Stathmin. Primary motoneurons (approx. 3 million cells) were cultured for 5 DIV. Nuclear and cytoplasmic proteins were extracted as described in nuclear fractionation methods. CNTF was applied for 30 min on day 5 prior to fractionation. Cytoplasmic extracts were used for immunoprecipitation as Stathmin is a cytoplasmic protein. Cell lysates from BDNF (5 ng/ml) and BDNF + CNTF (10 ng/ml) cultured motoneurons were incubated with 5 µl of rabbit anti-Stathmin antibody overnight at 4 °C. IgG control was included by incubating the lysate with irrelevant rabbit anti-TrkB antibody. Protein-G agarose beads were washed with PBS and equilibrated with lysis buffer. Protein lysate with antibody were incubated with equilibrated beads for 1hr under rotary agitation at 4 °C. After incubation, supernatant was

removed by centrifugation at 1000 g and beads were washed 3 times with lysis buffer. Immunoprecipitated proteins were eluted by boiling the beads with 2X Laemmli buffer. Immunoblotting was performed for STAT3, stathmin, tyrosinated tubulin and GFP to confirm co-immunoprecipitation. Densitometry analysis was performed using ImageJ software using the following protocol <http://lukemiller.org/index.php/2010/11/analyzing-gels-and-western-blots-with-image-j/>

4.2.10 Transient transfection of HEK 293T or N2A cells

Transient transfection is used to introduce a foreign DNA into the cells to achieve over-expression of protein of interest. Transient transfections were done using Lipofectamine™ 2000 following the recommended protocol. Briefly, HEK293T or N2A cells were seeded at 70-80% confluent the previous day of transfection so that it becomes 90-95% confluent at the time of transfection. Alternatively, transfection was also done in suspension on the day of transfection, in such cases, the amount of cells used were equivalent to 95% confluent state. The DNA-liposomes mixture was prepared as follows, DNA required for transfection was diluted in OptiMEM® and similarly Lipofectamine™ 2000 was diluted in OptiMEM® for 5 minutes. Later, the diluted DNA mixture was transferred into the lipofectamine mixture and incubated for 20 min at room temperature to form liposomes. This liposome mixture was then added to the cells and mixed gently. Cells were incubated at 37°C for 24 - 48 h until they are ready for assay. Following table lists the amount of cells and lipofectamine used in different experiments.

Experiment	Size of the dish	Number of cells	DNA (µg) and dilution volume (µl)	Lipofectamine™ 2000 (µl) and dilution volume (µl)
Western Blot	24 well (2 cm ²)	0.2 * 10 ⁶	0.8 µg in 50 µl	2 µl in 50 µl
Immunoprecipitation	6 well (10 cm ²)	1.2 * 10 ⁶	4 µg in 250 µl	10 µl in 250 µl

4.2.11 Fluorescent *in-situ* hybridization

Primary motoneurons were cultured for 5 DIV in presence of BDNF (5 ng/ml) and CNTF (10 ng/ml). Cells were fixed with 4% paraformaldehyde for 20 min at room temperature. Cells were then washed 3 times with PBS (DEPC treated) 15 minutes each, permeabilized with 0.3% triton-X 100 for 20 min at room temperature and subsequently washed 3 times with PBS (DEPC treated) 15 minutes each. As a negative control, cells were treated with RNase at a concentration of 0.1 µg/µl diluted in PBS (DEPC treated) for 1 h at 37°C. Cells were then washed 3 times with PBS (DEPC treated) for 15 minutes each. Pre-hybridization was performed with hybridization solution (Sigma) for 1 h at 37°C. Cells were then hybridized overnight with 100 ng/ml antisense Greenstar*TM biotin₁₀ oligonucleotide probe against TBCE mRNA (TGGGCTGAGAAACGCTGCATTTGGCCTGTTTTTGTCTGGATCTGGG). Hybridization with sense probe was used as a negative control. Cells were then washed twice with 1X SSC + 10 mM DTT at 55°C followed by 2 times wash with 0.5X SSC + 10 mM DTT at 55°C and equilibrated with TBST at room temperature. Biotinylated probes were then conjugated with streptavidin-HRP at a dilution of 1:100 (DAKO kit) for 20 min at room temperature and washes 3 times with TBST 5 min each. The signal was amplified by tyramide signal amplification (TSA from DAKO) for 20 min at room temperature and subsequently washed trice with TBST for 5 minutes each. Finally, cells were treated with avidin-rhodamine (1:100) for 15 minutes at room temperature. Cells were then washed 3 times with TBST and proceeded either for immunocytochemistry or mounted on a object carrier with mowiol.

4.2.12 Microtubule regrowth assay

An established MT regrowth assay was performed in cultured motoneurons (Ahmad and Baas, 1995; Schaefer et al., 2007). Briefly, motoneurons were plated on laminin 111 coated coverslips, 1 h after attachment the cells were treated with 10 µM nocodazole and incubated for 6 h at 37 °C to depolymerize the microtubule network. Cells were washed with Neurobasal

medium and treated with CNTF (10 ng/ml) for 5 min. Cells were rinsed with MT stabilizing buffer PHEM (60 mM Pipes, 25 mM Hepes, 10 mM EGTA, 2 mM MgCl₂). Cells were extracted with 0.5% TritonX-100, 10 μM paclitaxel (Sigma Aldrich) in PHEM buffer for 3 min which washes away the soluble tubulin fraction and retains polymerized tubulin. Cultures were fixed with equal volume of PHEM buffer containing 4% PFA. Cells were immunostained for γ-tubulin to label the centrosome and α-tubulin to label polymerized MTs. Images were acquired by confocal microscopy with 63X oil immersion objective, 4X magnification and 1.4 N.A. Images were loaded in one stack using MBF ImageJ (www.macbiophotonics.ca), enhanced by background subtraction radius 50, filter median to reduce noise and a threshold was set to all pictures. Sholl analysis was performed with ImageJ with steps of 0.25 μm.

The total length of MTs formed in each cell was calculated by determining the number of intersections crossed by MTs and multiplying this number with the corresponding distance from the MTOC. This analysis was done starting from the periphery to the centre. Individual MTs were only included once in this analysis when they crossed the most outer circle around the MTOC. Average length was calculated by summing up the length of microtubules obtained and divided by the total number of MTs measured: $\sum ((n_x - n_{x+1}) * \Delta\text{MTOC}_x) / N$, where n is the number of intersection and x is the circle of interest, $x+1$ is the next outer circle, ΔMTOC_x is the distance from MTOC to the circle of interest and N is the total number of MTs.

4.2.13 Cortical precursor cell culture

Cortical precursor cells cultures were prepared as previously described (Gotz et al., 2005). Briefly, embryonic forebrains were dissected at E12, trypsinized and cultured as neurospheres in Neurobasal medium (Invitrogen) containing 500 μM Glutamax, 50 U/ml penicillin G sodium and 50 U/ml streptomycin sulphate (Invitrogen), 2% B27 Supplement (Invitrogen), basic fibroblast growth factor (bFGF) and epidermal growth factor (EGF; Cell Concepts) at final concentrations of 20 ng/ml each. The cells were grown at 37°C in a 5% CO₂

humidified atmosphere. Cells were dissociated cultured on poly-DL-ornithine and Laminin1 coated 12 well cell culture dishes at a density of 100,000 cells per well in culture medium with bFGF and EGF. Appropriate lentiviral infections were done prior to plating of the cells. bFGF and EGF were withdrawn after 48 h and cells were then treated with LIF (10 ng/ml) for 24 h.

4.2.14 Dephosphorylation assay

Dephosphorylation assay was performed to check the specificity of antibody against phosphorylated STAT3 at tyrosine 705 (cell signaling cat. no. 9131). Calf intestine phosphatase (CIP) was used to dephosphorylate the proteins. Protein extracts were isolated from NSC34 cells (approx. 1×10^6 cells) using RIPA buffer without EDTA. Phosphatase inhibitors (okadaic acid, sodium ortho-vanadate, sodium fluoride, sodium pyrophosphate) were added only to the control protein extracts, whereas calf intestine phosphatase (20 units) was added to the sample that had to be dephosphorylated. The sample were incubated at 37 °C for 1 h and subsequently laemmli buffer was added and boiled at 99 °C for 10 min. Western blot analysis was performed with p-STAT3 Y705 antibody (cell signaling cat. no. 9131) and GAPDH served as a loading control.

4.2.15 Drug treatment

4.2.15.1 Proteasome inhibitor

HEK 293T cells and N2A cells were transfected with pcDNA-HA-TBCE (wt and W534G) and empty GFP vector as described in above protocol. One day after the transfection, cells were treated with three different proteasome inhibitors, namely, MG132 (5 μ M), Lactacystin (5 μ M) and PS1 (5 μ M) for additional 24 h. DMSO (0.1%) was added as a vehicle control. Subsequently, cells were lysed and proteins were extracted using 2X laemmli buffer and boiled at 99°C for 10 minutes. Protein samples were subjected to western blot analysis and probed for GFP, HA and GAPDH.

4.2.15.2 STAT3 inhibitor VI, S3I-201

STAT3 inhibitor VI, S3I-201 was used to check the specificity of antibody against phosphorylated STAT3 at tyrosine 705 (cell signaling cat. no. 9131). It inhibits the STAT3 activity by blocking its phosphorylation and subsequent dimerization. Primary motoneurons were cultured for 4 DIV with BDNF. CNTF was applied to activate the phosphorylation of STAT3 at tyrosine 705, this served as a positive control for phosphorylation. In another set, the CNTF along with STAT3 inhibitor VI, S3I-201 (100 μ M) was added. Cells were cultured for further 24 h, proteins were extracted and western blot analysis was performed for p-STAT3 Y705 and GAPDH.

4.2.16 Site-Directed mutagenesis of STAT3^{Y705F} EYFP

STAT3-EYFP-N1 expression vector was kindly provided to us by Prof. F.Horn from University hospital of Leipzig (Kretzschmar et al., 2004). Site directed mutagenesis for dominant negative STAT3 (STAT3 Y705F) was performed using QuickChange lightning multi site-directed mutagenesis kit. It is a PCR based method performed using the vector containing the insert and two oligonucleotide primers with the desired mutation and are complementary to the opposite strand of the vector. PCR was performed with oligonucleotides carrying the mutation and PfuTurbo DNA polymerase, which generates mutated plasmid with nicks. Following the cycle PCR, the product was digested with DpnI endonuclease enzyme that cleaves methylated and hemi-methylated parental DNA. The parental vector DNA produced from *E.Coli* is dam methylated and therefore it is prone to digestion by DpnI. The mutated vector is then transformed to XL-Blue competent cells.

Following table 4.8 shows the PCR reagents and cycling conditions used to generate STAT3Y705F-EYFP

Reagents	Volume	PCR cycle conditions	Duration
ST3 Y705F fw	1 μ l	95°C	2 min
ST3 Y705F rev	1 μ l	95°C	30 s
dNTP's (10 mM)	1 μ l	55°C	30 s
QuickChange lightning multi enzyme blend	1 μ l	65°C	7min
QuickSolution	1.5 μ l	65°C	5 min
ds plasmid DNA (100 ng)	1 μ l	4°C	hold
10X QuickChange lightning multi reaction buffer	2.5 μ l		
Water	16 μ l		

Table 4.10: PCR components and cycling conditions for site directed mutagenesis of STAT3Y705F-EYFP

5. RESULTS

5.1 CNTF rescues axonal pathology in *pnn* mutant mouse

Neurotrophic factors play a major role in survival of motoneurons *in-vivo* and *in-vitro* (Henderson et al., 1994; Sendtner et al., 1996). GDNF prevents cell death of facial motoneurons which were deprived of target muscle by axotomy *in-vivo* and potent survival factor for cultured rat motoneurons *in-vitro* (Henderson et al., 1994). Similarly, CNTF has been shown to influence axon degeneration in variety of mouse models of motoneuron disease, such as *pnn* (Sendtner et al., 1992b) (Haase et al., 1997) *wobbler* (Mitsumoto et al., 1994a). Although, these neurotrophic factors have the same role in preventing motoneuron death, they have distinct mechanisms and targets. CNTF treatment prolong the survival and improves the motor function of *pnn* mice. It also rescues the motor axon loss in phrenic nerves and degeneration of facial motoneurons (Sendtner et al., 1992b). In contrast to CNTF, GDNF application in *pnn* mice significantly rescued the loss of facial motoneurons, but did not have an effect on nerve degeneration and life span of these mice (Sagot et al., 1996). Overexpression of Bcl-2, an anti-apoptotic protein, in *pnn* mutant mice rescued the facial motoneuron loss but not the nerve degeneration, indicating a dichotomy between motoneuron survival and axon maintenance (Sagot et al., 1995). These findings show that CNTF plays a distinct role in axon maintenance of motoneurons in *pnn* mice. To understand the specific role of CNTF in axon maintenance, primary motoneurons from *pnn* mice appeared as a suitable tool. Previous studies have shown that *pnn* mutant motoneurons exhibit shorter axons *in-vitro* (Bommel et al., 2002). We compared the effect of different neurotrophic factors, namely, BDNF, CNTF, GDNF, in cultured *pnn* and wildtype motoneurons. Isolated wildtype and *pnn* mutant motoneurons were cultured with BDNF (5 ng/ml), CNTF (10 ng/ml) and GDNF (5 ng/ml) for 7 days *in-vitro* (DIV), percentage survival of motoneurons of initially plated cells was approximately 60% with all three neurotrophic factors (Figure 5.1.1).

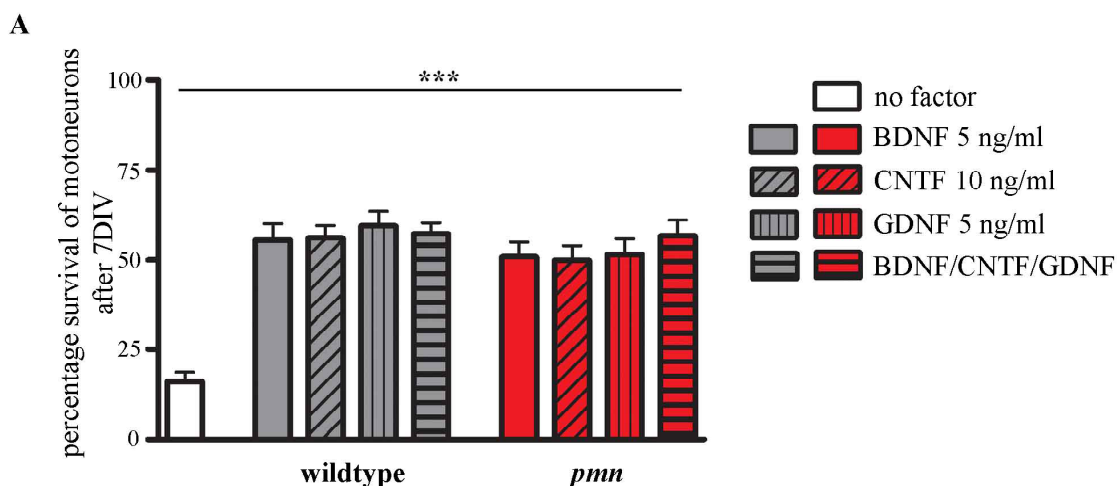


Figure 5.1.1: Survival of motoneurons with various neurotrophic factors

Motoneurons were grown for 7DIV with BDNF (5 ng/ml), CNTF (10 ng/ml), GDNF (5 ng/ml) and combination of these three neurotrophic factors. Survival is shown as percentage relative to originally plated cells. Bars shown represents mean \pm S.E.M from 3 independent experiments. Statistical analysis: *** $P < 0.001$, ANOVA with Bonferroni post-hoc test.

We then analyzed the axon length of *pmn* mutant motoneurons *in-vitro*. According to previous observations, *pmn* mutant motoneurons cultured with BDNF for 5 DIV alone exhibited shorter axon length when compared to wildtype motoneurons (Bommel et al., 2002). Interestingly, addition of CNTF together with BDNF for 5 DIV rescued axon growth deficits in *pmn* mutant motoneurons, resembling previous *in-vivo* studies that CNTF but not other neurotrophic factors (BDNF or GDNF) rescues *pmn* mutant mouse (Figure 5.1.2).

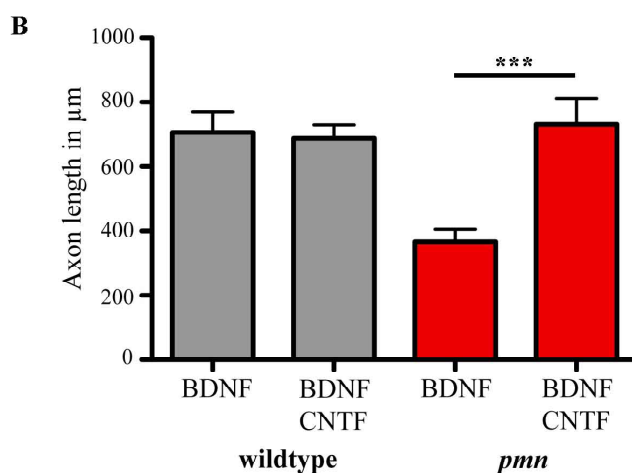


Figure 5.1.2: CNTF rescues axon outgrowth in *pmn* mutant motoneurons

Motoneurons from wildtype and *pmn* mutant embryos were cultured for 7DIV with BDNF (5 ng/ml) or BDNF (5 ng/ml) and CNTF (10 ng/ml). *Pmn* mutant motoneurons cultured with BDNF alone showed shorter axons when compared to wildtype. Application of CNTF rescued the axon length outgrowth in *pmn* mutant motoneurons. Bars shown represents mean +/- S.E.M from 3 independent experiments. Statistical analysis: *** $P < 0.001$, ANOVA with Bonferroni post-hoc test.

CNTF is a member of the IL-6 type cytokine family characterized by a four- α -helix bundle structure (Bazan, 1990). Unlike many other neurotrophic factors, CNTF binds to a tripartite cytokine receptor complex. It binds to CNTFR α , a cell membrane receptor anchored via glycosyl-phosphatidylinositol linkage (GPI) (Davis et al., 1991) to the cell surface, LIFR β and gp130 (Davis et al., 1993). CNTF binding to these receptors results in activation of Tyk2, a member of janus kinase family, which in turn phosphorylates cytoplasmic tail of GP130. The phosphorylated GP130 becomes the docking site of STAT3 (Stahl et al., 1995). STAT3 upon activation gets phosphorylated at tyrosine 705, dimerizes, translocated to nucleus and activates transcription of target genes.

Previous studies have shown that conditional ablation of STAT3 in *pmn* mutant neurons abolished the CNTF effect on axon elongation. In the presence of CNTF, axon length of STAT3^{fl/KO};NFL-Cre^{tg}; *pmn* motoneurons was shorter when compared to wildtype and *pmn* mutant motoneurons cultured with CNTF (Bender F.L.P Ph.D thesis). This result indicated that STAT3 signaling mechanism plays a vital role in CNTF mediated rescue of *pmn* mutant mice.

5.2 CNTF induces phosphorylation of STAT3

5.2.1 Cytoplasmic localization of activated STAT3 in primary motoneurons

Neurotrophic cytokine CNTF has been shown to activate multiple signaling pathways, such as Janus kinase, mitogen activated protein kinase (MAPK), phosphoinositide 3 kinase (PI3K) and mammalian target of rapamycin (mTOR) pathways. CNTF activity leads to phosphorylation of STAT3 at tyrosine 705 and serine 727 although by different kinases. Tyk2 is known to phosphorylate STAT3 at Y705 (Heinrich et al., 1998) and mTOR S6 kinase (Yokogami et al., 2000). Phosphorylation at both the sites is required for maximal transcriptional activity of STAT3 (Wen et al., 1995). With this background study, it became indispensable in current study to identify which phosphorylation plays a role in CNTF mediated rescue of *pnn* axonal pathology and rescue mechanism is transcription dependent. Primary motoneurons were cultured for 5 DIV in the presence of BDNF and CNTF was pulsed for 5, 15, 30 min or continuously applied for 5 days. Cells were then lysed to obtain nuclear and cytoplasmic fractionation. Continuous application or pulse application of CNTF resulted in activation of p-STAT3 Y705 and the amount of phosphorylation increased quantitatively from 5 min to 30 min application of CNTF. Surprisingly, most of the p-STAT3 Y705 was detected in the cytoplasmic fraction and very little STAT3 could be found in nuclear fraction at any point of time in primary motoneurons (Figure 5.2.1).

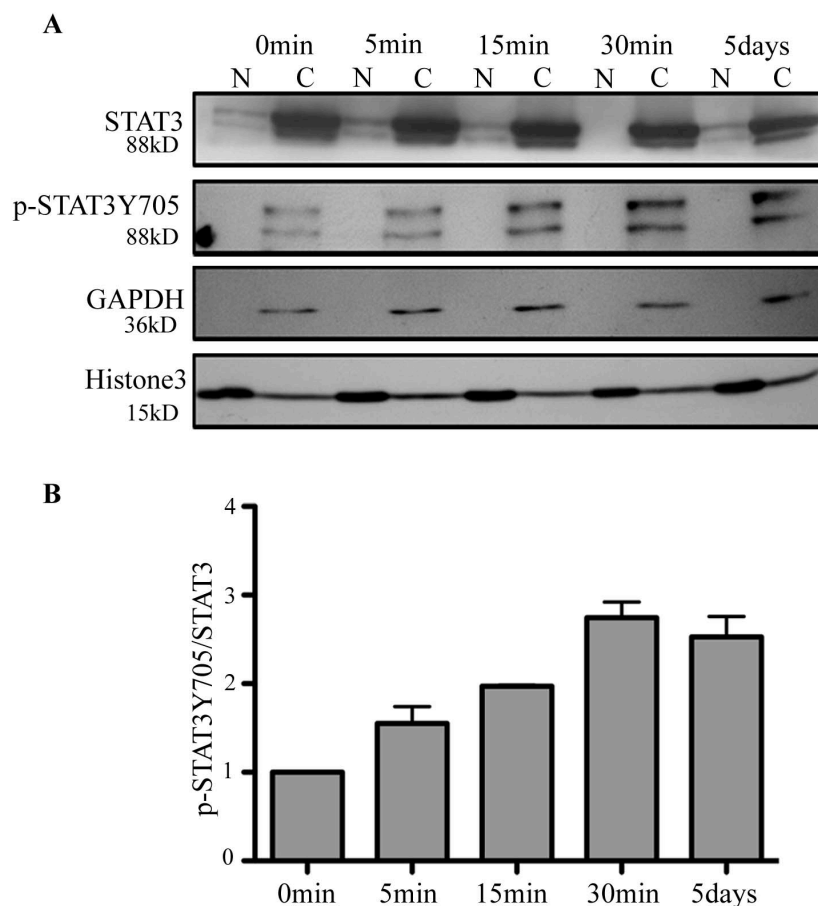


Figure 5.2.1: CNTF activated p-STAT3Y705 localized in cytoplasm of primary motoneurons

(A) Nuclear and cytoplasmic fractionation followed by western blot analysis from primary motoneurons showing activation of p-STAT3 Y705 upon CNTF stimulation. Activated STAT3 is mainly found in the cytoplasm at all time points investigated. Fractionation was controlled with GAPDH (cytosolic) and histone 3 (nuclear) as markers.

(B) Quantification of activated p-STAT3 Y705 in the cytoplasmic fraction of motoneurons after CNTF stimulation, n = 3 independent experiments.

These results indicate that CNTF activates STAT3 at tyrosine phosphorylation in primary motoneurons, and the presence of p-STAT3 Y705 in the cytoplasm indicates that the effects of CNTF activated STAT3 in pmn mutant motoneurons could involve a local effect in the cytoplasm rather than nuclear transcription (Figure 5.2.1).

5.2.2 Specificity of p-STAT3^{Y705} antibody

Dephosphorylation assays and pharmacological blockade of STAT3 activity using S3I-201 was performed to check the specificity of the p-STAT3 Y705 antibody (rabbit polyclonal obtained from cell signaling cat no: 9131). The dephosphorylation assay was carried out with NSC34 cells. Protein lysates treated from NSC34 cells were treated with calf intestine phosphatase for 1 h at 37°C showing reduced phosphorylation of STAT3 Y705 when compared to untreated lysates (Figure 5.2.2A). As an alternative approach, antibody specificity was also tested using a selective chemical probe inhibitor of STAT3 activity, S3I-201. S3I-201 was identified through *in-silico* computational approach to dock to the SH2 domain of STAT3, thereby inhibiting its phosphorylation, dimerization and DNA binding activity (Siddiquee et al., 2007). Western blot analysis with p-STAT3 Y705 antibody showed that the treatment of motoneurons with S3I-201 reduced the levels of phosphorylation of STAT3 Y705 (Figure 5.2.2B). CNTF application for 24 h increased the levels p-STAT3 Y705 when compared to BDNF treated cultures that served as a control.

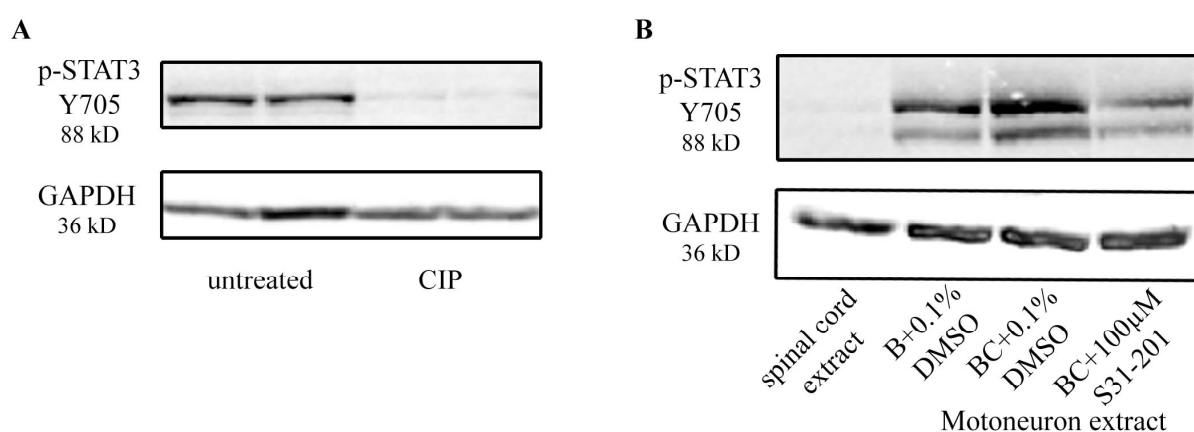


Figure 5.2.2: Specificity of p-STAT3Y705 antibody (cell signaling 9131)

(A) Treatment of protein extracts from NSC34 cells with calf intestine phosphatase (CIP) abolishes phosphorylation of STAT3 at Y705.

(B) Treatment of primary motoneurons with STAT3 inhibitor S3I-201 reduced the levels p-STAT3 Y705. These experiments confirm the specificity of the p-STAT3 Y705 antibody.

These results indicate that detection of STAT3 phosphorylation at tyrosine 705 with rabbit polyclonal antibody (cell signaling 9131) used in this study is indeed specific.

5.2.3 Axonal fractionation of primary motoneurons using Xona microfluidic chambers

STAT3 dynamics after CNTF application in primary motoneurons was investigated using fluorescent recovery after photobleaching (FRAP) technique (Frank.N Ph.D thesis). FRAP analysis in the axons showed no significant retrograde movement of STAT3 towards the nucleus after CNTF treatment.

To understand whether CNTF could activate STAT3 locally in distal compartments of axons, we cultured primary motoneurons in compartmentalized culture system. Xona microfluidic chambers with 150 μm grooves were used to separate cell bodies and dendrites from axons (Taylor et al., 2005). Primary motoneurons were cultured in these chambers for 7 DIV, pulsed with CNTF for 30 min in the axonal compartment and analyzed whether p-STAT3 Y705 remains in axonal compartment or is retrogradely transported to the nuclear compartment. The experimental paradigm of the Xona microfluid chamber is depicted in figure 5.2.3A. Protein lysates of cell body and axonal compartments from 8 chambers were pooled. Immunoblot for total STAT3 and tubulin (abundant protein in axon) was performed to compare the amount of protein obtained from different compartments. (Figure 5.2.3B). Comparison of tubulin in the axonal fraction (100% volume) and the cell body fraction (1.6%-12% of volume) indicated that the amount of protein extracted from axonal compartment is far too less to do quantitative analysis. Amount of tubulin obtained from axonal compartment was less than 1.6% of tubulin obtained from cell body compartment. Amount of STAT3 detected was even less than tubulin, thereby under the current experimental setup this study was inconceivable. Silver staining of these samples and comparing with known standards of bovine serum albumin fraction V also revealed that very low amounts of protein were obtained from axonal compartment. Most of the

proteins observed in axonal compartment were background from medium used for culturing motoneurons. The yield was primarily less because only 10% - 20% of the motoneurons plated close to the boundaries were able to project axons towards the axonal compartment (Figure 5.2.3C).

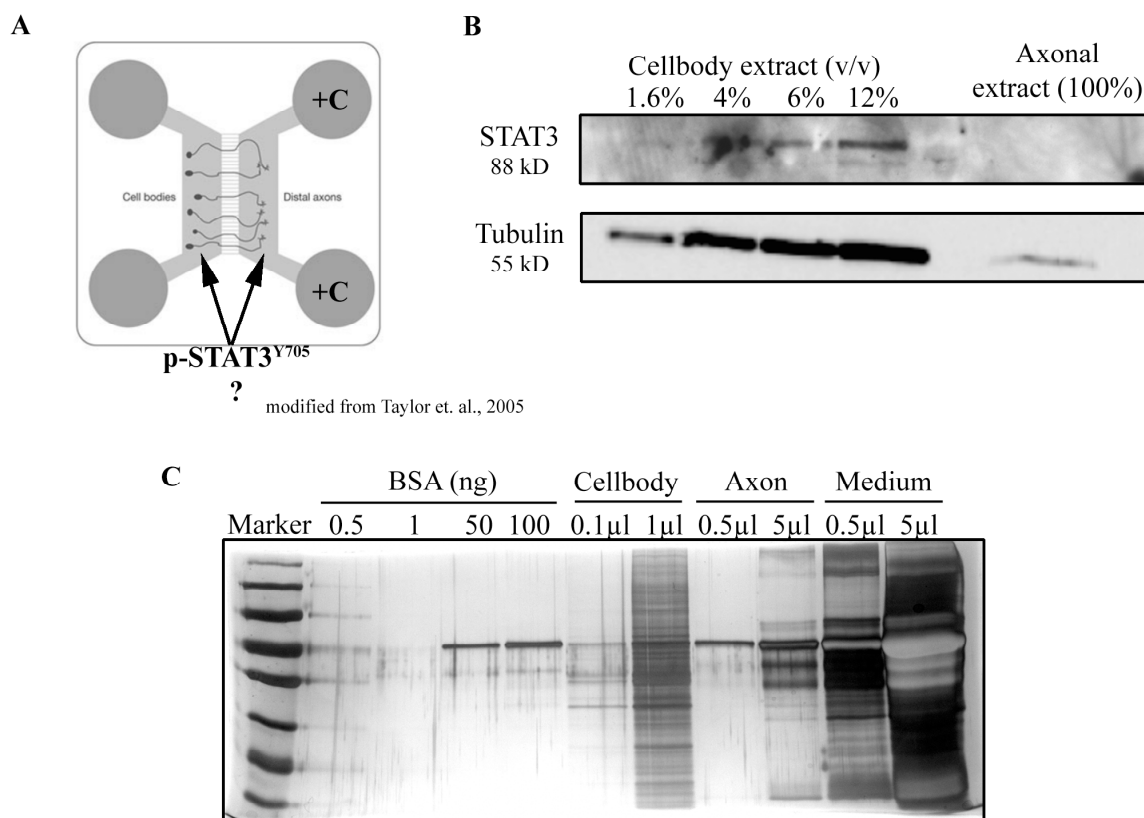


Figure 5.2.3: Compartmentalized cultures to study the localization of activated STAT3

(A) Schematic representation of experimental paradigm with Xona microfluidic chamber. Primary motoneurons were grown for 7 DIV, pulsed with CNTF (C) in the axonal compartments for 30 min and analyzed the localization of p-STAT3 in cell body and axonal compartment.

(B) Westernblot analysis of protein extracts from cell body (1.6% - 12% v/v) and axonal (100%) compartments. Blots probed with STAT3 and Tubulin revealed that amount of proteins obtained from axonal compartment was less to do quantitative analysis.

(C) Silver staining of protein extracts from cell body, axonal compartment and medium components showed that the proteins present in axonal compartment were background from medium components.

5.3 Transcriptional independent activity of STAT3 necessitates rescue of axon pathology in *pnn* mutant motoneurons

STAT3 has been shown in many nerve injury models that it is retrogradely transported and is necessary for regeneration of axons after lesion (Ben-Yaakov et al., 2012; Sun et al., 2011). In the present study with primary motoneurons, CNTF mediated activated STAT3 was found mainly in the cytoplasm and there was no significant retrograde transport observed upon CNTF application. This raised the question whether CNTF-STAT3 mediated rescue of axon growth in *pnn* mutant motoneurons is transcription independent. To address this question, STAT3 DNA binding activity was abolished by genetic approach where in STAT3 was mutated at EE 434-435 AA.

5.3.1 Generation of STAT3 DNA binding and phosphorylation mutants

STAT3 has a central function of signal transduction from the ligand activated receptor kinase complex followed by nuclear translocation and DNA binding to activate transcription (Darnell et al., 1994). Signal transduction is mediated by phosphorylation at tyrosine 705 and the DNA recognition motif comprises of 2 highly conserved regions of STAT3 around 400-500 aminoacid. Mutation at site 434-435 causing aminoacid exchange of EE-AA completely abolishes binding affinity of STAT3 to DNA but retains its tyrosine phosphorylation (Horvath et al., 1995). To understand the role of tyrosine phosphorylation and DNA binding activity of STAT3 in the context of present study, two mutants of STAT3 (phospho negative and DNA binding) were generated by site directed mutagenesis in STAT3^{WT}EYFP-N1 vector (kindly provided by Prof. Friedmann Horn, University hospital of Leipzig, Germany). The phospho-negative mutation was achieved by mutating tyrosine at position 705 to phenylalanine (STAT3^{Y705F}) and DNA binding mutant was achieved by mutating aminoacids glutamate at position 434-435 to alanine (STAT3^{EE434-435AA}). Lentiviral vectors (FUGW) expressing

STAT3^{WT}EYFP, STAT3^{Y705F}EYFP and STAT3^{EE434-435AA}EYFP were cloned and respective lentiviruses were generated.

Primary motoneurons were infected with lentiviruses expressing STAT3^{WT}EYFP, STAT3^{Y705F}EYFP and STAT3^{EE434-435AA}EYFP and cultured for 5 DIV. Immunoblot analysis confirmed the expression of overexpressed STAT3 EYFP protein detected by GFP and STAT3 antibody. As expected both STAT3^{WT}EYFP and STAT3^{EE434-435AA}EYFP but not STAT3^{Y705F}EYFP can be activated and phosphorylated at tyrosine 705 (Figure 5.3.1).

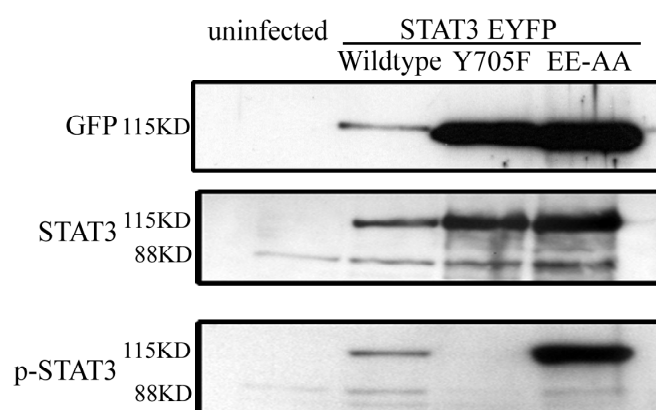


Figure 5.3.1: Expression of STAT3^{WT}EYFP, STAT3^{EE434-435AA}EYFP and STAT3^{Y705F}EYFP mutants in primary motoneurons

Lentiviral overexpression of STAT3^{WT}EYFP, STAT3^{EE434-435AA}EYFP and STAT3^{Y705F}EYFP in primary motoneurons. Wildtype and EE434-435AA mutant STAT3 can be activated at tyrosine 705, but not STAT3^{Y705F} mutant.

5.3.2 STAT3^{EE434-435AA} mutant does not induce transcription

STAT3 phosphorylation and its subsequent transcriptional activity are necessary for LIF induced astrocyte differentiation from neural stem cells (Rajan and McKay, 1998). In this study, it was shown that STAT3^{VVV-AAA} mutant, which cannot bind to DNA, did not induce GFAP expression (marker for astrocytes like cells) from neural stem cells. To test whether STAT3^{EE434-435AA} mutant does not induce transcription of its target genes, LIF induced astrocyte differentiation was used as an assay. Neural stem cells were induced with LIF (10 ng/ml) for 16

h. Phosphorylation of STAT3 and GFAP expression was observed by western blot analysis. As shown in figure 5.3.2 neural stem cells cultured in presence or absence of bFGF and EGF that stimulated proliferation did not induce GFAP expression. LIF treatment for 16 h induced phosphorylation of STAT3 at tyrosine 705, which subsequently induced expression of GFAP. Neural stem cells transduced with STAT3^{WT}EYFP lentiviruses and subsequent LIF induction also stimulated GFAP expression, but neural stem cells transduced with STAT3^{EE434-435AA}EYFP repressed the expression of GFAP, indicating the DNA binding activity of STAT3^{EE434-435AA}EYFP is impaired. As a positive control, a pharmaceutical inhibition of STAT3 DNA binding activity was performed using Galiellalactone (10 μ M). Treatment of Galiellalactone completely abolished LIF induced GFAP expression.

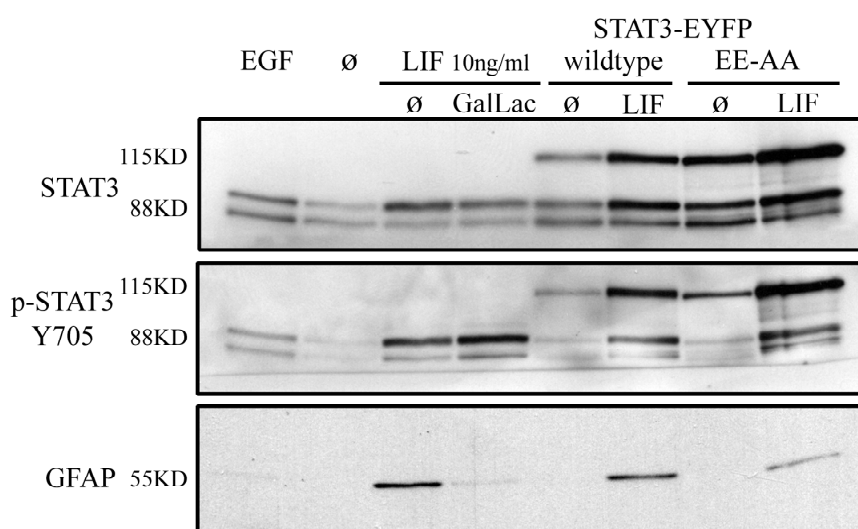


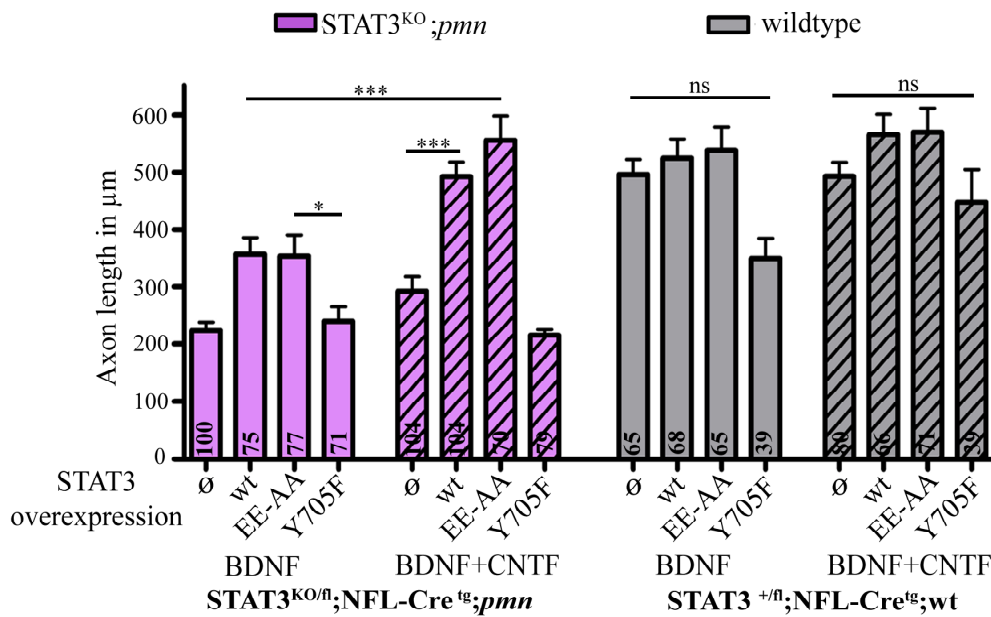
Figure 5.3.2: STAT3^{EE434-435AA}EYFP does not induce GFAP induction in neural stem cells

LIF induced GFAP induction in neural stem cells is dependent on STAT3 transcriptional activity. GFAP induction was reduced by over-expression of STAT3^{EE434-435AA}EYFP or treatment with 10 μ M Galiellalactone (GalLac) indicating that mutant STAT3^{EE434-435AA}EYFP represses transcription of its target genes.

5.3.3 STAT3 phosphorylation but not its transcriptional activity is necessary for CNTF dependent axon growth in *pmn* mutant motoneurons

To understand whether transcriptional activity of STAT3 is required for CNTF dependent axon outgrowth in *pmn* mutant motoneurons, STAT3 deficient *pmn* mutant motoneurons (STAT3^{KO/fl};NFL-Cre^{tg};*pmn*^{-/-}) were transduced with STAT3^{EE434-435AA}EYFP, STAT3^{Y705F}EYFP, STAT3^{WT}EYFP lentiviruses, cultured with either BDNF or BDNF+CNTF and subsequently axon length was measured after 5 DIV. STAT3 deficient *pmn* mutant motoneurons (STAT3^{KO/fl};NFL-Cre^{tg};*pmn*^{-/-}) cultured with BDNF alone showed shorter axons when compared to wildtype littermates. Over-expression of STAT3^{WT}EYFP and STAT3^{EE434-435AA}EYFP in BDNF treated motoneurons marginally increased axon length. Over-expression of STAT3^{WT}EYFP and STAT3^{EE434-435AA}EYFP both completely rescued CNTF dependent axon growth in STAT3^{KO/fl};NFL-Cre^{tg};*pmn*^{-/-} motoneurons, showing that transcriptional activity is not required for this effect. Over-expression of STAT3^{Y705F}EYFP was not capable to rescue CNTF mediated restoration of axon outgrowth, thus providing evidence that STAT3 activation is necessary but not its transcriptional activity for CNTF mediated rescue of axon growth in *pmn* mutant motoneurons. Interestingly, wildtype motoneurons over-expressing STAT3^{Y705F}EYFP also showed shorter axons, presumably because of a STAT3^{Y705F}EYFP dominant negative effect (Figure 5.3.3A-B)

A



B

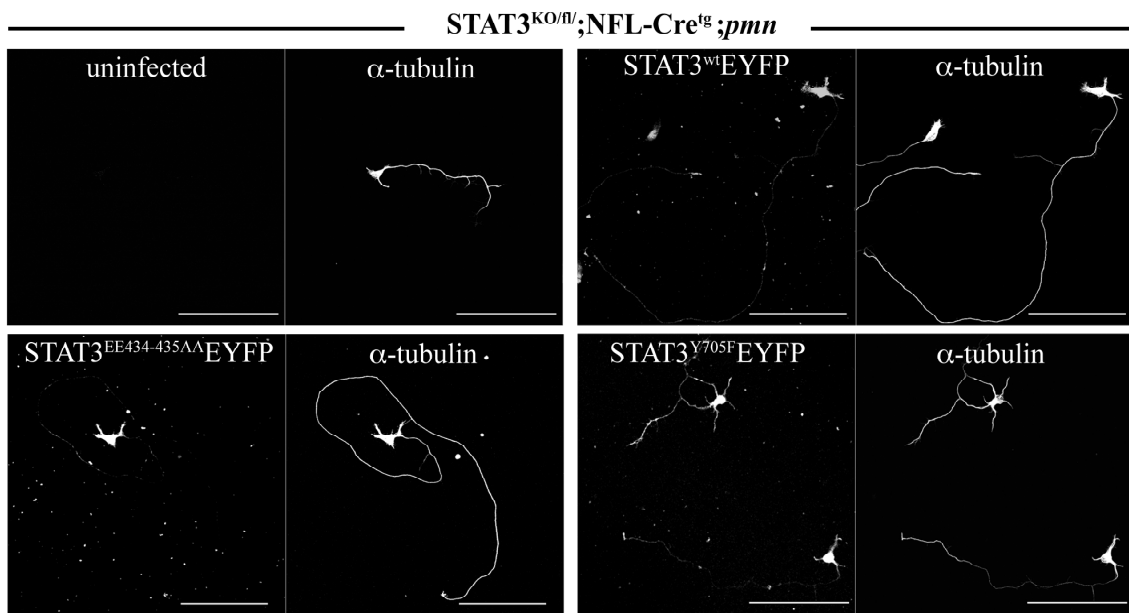


Figure 5.3.3: STAT3 phosphorylation but not its transcriptional activity is required for CNTF mediated axon growth in *pmn* mutant motoneurons

(A) Overexpression mutant STAT3^{EE434-435AA} in STAT3^{KO};*pmn* mutant motoneurons completely rescues axon growth upon CNTF application, in contrast to mutant STAT3^{Y705F}. Numbers in bars indicate numbers of cells analyzed. Data shown represent mean \pm S.E.M., $n = 3$ independent experiments. \emptyset , wt, EE-AA, Y705F represents uninfected, STAT3^{WT}EYFP, STAT3^{EE434-435AA}EYFP and STAT3^{Y705F}EYFP respectively. Statistical analysis: ns (not significant), * $P < 0.05$, ** $P < 0.01$, *** $P < 0.001$; ANOVA with Kruskal-Wallis with Dunn's multiple comparison test.

(B) Representative images of STAT3^{KO};*pmn* mutant motoneurons overexpressing STAT3^{WT}EYFP, STAT3^{EE434-435AA}EYFP and STAT3^{Y705F}EYFP, cultured with BDNF and CNTF. Scale bar: 100 μ m.

Furthermore, inhibition of transcription with actinomycin D did not abolish the CNTF mediated axon length rescue in *pnn* mutant motoneurons (Frank.N Ph.D thesis) thus providing further support that there must be another local function of cytoplasmic STAT3 in CNTF dependent rescue of axon elongation in *pnn* mutant motoneurons.

5.4 STAT3 interacts with Stathmin, a microtubule destabilizing protein

A transcription independent role of STAT3 has been implicated in few recent studies. The study by (Verma et al., 2009) showed that STAT3 regulates microtubule dynamics in migrating T-cells. Further more cytoplasmic STAT3 has been shown to induce NMDA receptor dependent long term depression (LTD) (Nicolas et al., 2012). Earlier yeast-two-hybrid using STAT3 as a bait and co-immunoprecipitation studies in non-neuronal cells have shown that STAT3 interacts with the microtubule destabilizing protein Stathmin (Ng et al., 2006) in phosphorylation dependent manner (Verma et al., 2009). Stathmin binds to α/β tubulin heterodimers in a 1:2 ratio and thereby sequesters them and inhibits tubulin polymerization (Charbaut et al., 2001). Therefore, we studied the role of Stathmin in CNTF-STAT3 mediated rescue of axonal pathology in cultured *pnn* mutant motoneurons.

5.4.1 Colocalization of Stathmin and STAT3

First, the localization of STAT3 and Stathmin was analyzed in cultured primary motoneurons. Primary motoneurons over-expressing STAT3-EYFP were stained for antibodies against Stathmin and tyrosinated tubulin by immunocytochemistry. Stathmin and STAT3 were found to colocalize in cell body, dendrites and axons of motoneurons (Figure 5.4.1A). Interestingly, the colocalization was enriched in growth cone of axons (Figure 5.4.1B).

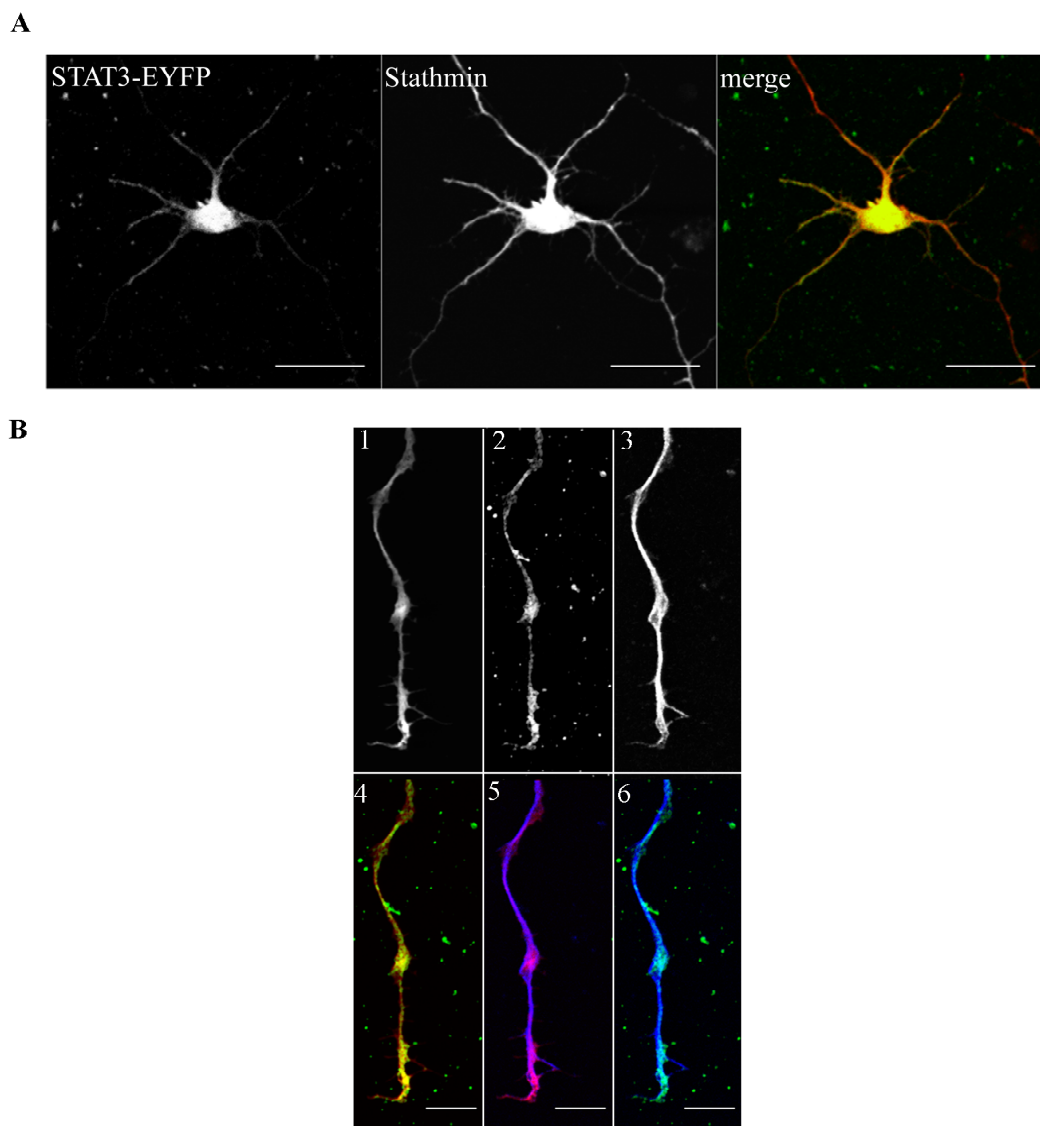


Figure 5.4.1 Co-localization of STAT3-EYFP and Stathmin in cultured motoneurons

(A) Primary motoneurons transduced with STAT3^{WT}EYFP lentiviruses were immunostained with antibodies against Stathmin and tyrosinated tubulin. STAT3^{WT}EYFP and Stathmin were co-localized in cell body and dendrites. Scale bar: 50 μ m.

(B) STAT3^{WT}EYFP and Stathmin were also colocalized in axons of primary motoneurons and specifically enriched at the growth cones. 1-Stathmin (Cy3), 2- STAT3^{WT}EYFP (Cy2), 3 - tyrosinated tubulin (Cy5), 4- merge of STAT3^{WT}EYFP and Stathmin, 5- merge of Stathmin and tyrosinated tubulin, 6- merge of STAT3^{WT}EYFP and tyrosinated tubulin. Scale bar: 10 μ m.

5.4.2 Co-immunoprecipitation of Stathmin and STAT3

Co-localization of two proteins may not necessary mean that the two proteins physically interact. To understand whether STAT3 could sequester Stathmin from α/β tubulin heterodimers,

co-immunoprecipitation studies were performed by using Stathmin antibody. Efficient co-immunoprecipitation is normally achieved when antibody used for pull down is potent enough to immunoprecipitate at least 90% of the protein. In this regard, 2 commercially available Stathmin antibody rabbit polyclonal anti-Stathmin (ab 47468) and rabbit monoclonal anti-Stathmin (ab 52630 clone EP:1573Y) were tested for the efficiency of immunoprecipitation. Approximately 3×10^6 NSC34 cells were lysed with nuclear fractionation buffer. 5 μ l of antibody and 15 μ l of protein A beads were added to the cytoplasmic extracts for immunoprecipitation. Approximately 5% of input and supernatant and 30% of eluate were loaded to the SDS-PAGE to compare the efficiency of pull down. Figure 5.4.2 shows the efficiency of immunoprecipitation of different Stathmin antibody, comparison of input and supernatant exhibited distinct difference between two antibodies, the rabbit monoclonal antibody (ab 52630 clone: EP1573Y) pulled down almost 90% of the Stathmin protein, whereas the rabbit polyclonal antibody (ab 47468) was less efficient. Absence of GAPDH in the eluate shows the pull down was specific for Stathmin. Further experiments were carried out with rabbit monoclonal anti-Stathmin antibody.

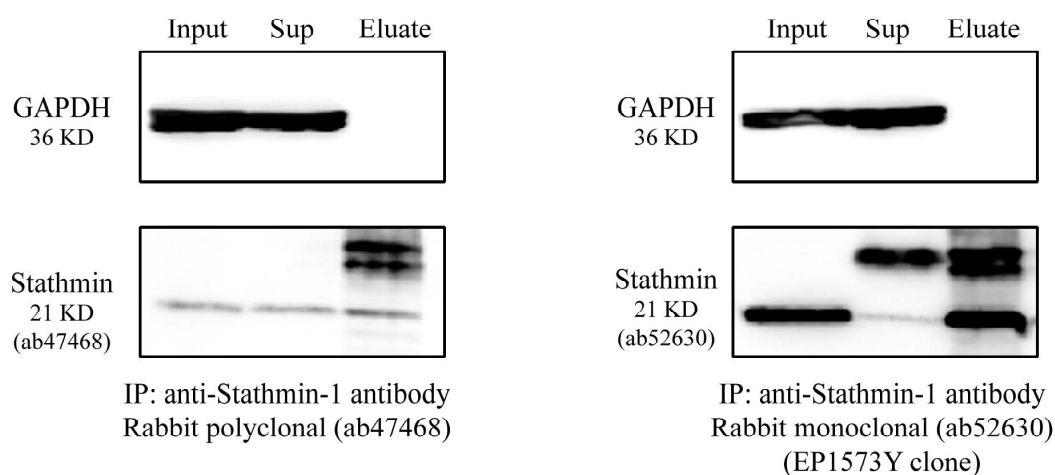


Figure 5.4.2 Testing of Stathmin antibodies for immunoprecipitation

Two commercially available antibodies against Stathmin (from abcam: ab47468 and ab52630) were tested for efficiency immunoprecipitation in NSC 34 cells. Western blot against Stathmin after immunoprecipitation showed that rabbit monoclonal antibody against Stathmin (ab52630) was efficient in immunoprecipitation analysis. Western blot against GAPDH showed that the immunoprecipitation was specific.

3.4.3 CNTF application enhances STAT3-Stathmin interaction in primary motoneurons

To analyze whether STAT3 and Stathmin interaction is dependent on STAT3 phosphorylation, immunoprecipitation analysis was performed on cultured primary motoneurons after application of CNTF. Primary motoneurons were grown for 4DIV with BDNF (10 ng/ml), deprived of serum overnight and stimulated with CNTF (10 ng/ml) the following day. Cells were then harvested with nuclear fractionation buffer. The cytoplasmic fraction was used for immunoprecipitation, Stathmin was immunoprecipitated and levels of STAT3 co-immunoprecipitated was analyzed by immunoblot. Figure 5.4.3 shows the western blot analysis after immunoprecipitation and quantification of amount of STAT3 co-immunoprecipitated by Stathmin after CNTF application. Amount of protein used for immunoprecipitation in both BDNF and BDNF+CNTF treated samples were equal as shown in the input lanes for Stathmin, STAT3 and tyrosinated-tubulin. Intensity of Stathmin in eluate lane shows the pull down efficiency. It was equal in both samples and the signal was specific, as Stathmin was not pulled down by IgG control. Intensity of antibody light chain shows equal amount of antibody was bound to protein-A beads. The amount of STAT3 co-immunoprecipitated by Stathmin was increased in CNTF treated lysates, indicating enhanced interaction between STAT3 and Stathmin upon CNTF application. Interestingly, under the same condition the interaction between Stathmin and tyrosinated tubulin was reduced. Densitometric quantification showed two fold increase of STAT3 interaction to Stathmin and 50% loss of Stathmin interaction with tyrosinated tubulin in cultures treated with CNTF (Figure 5.4.3B). This result indicates increased interaction of STAT3 with Stathmin leads to release of α/β tubulin heterodimers from Stathmin.

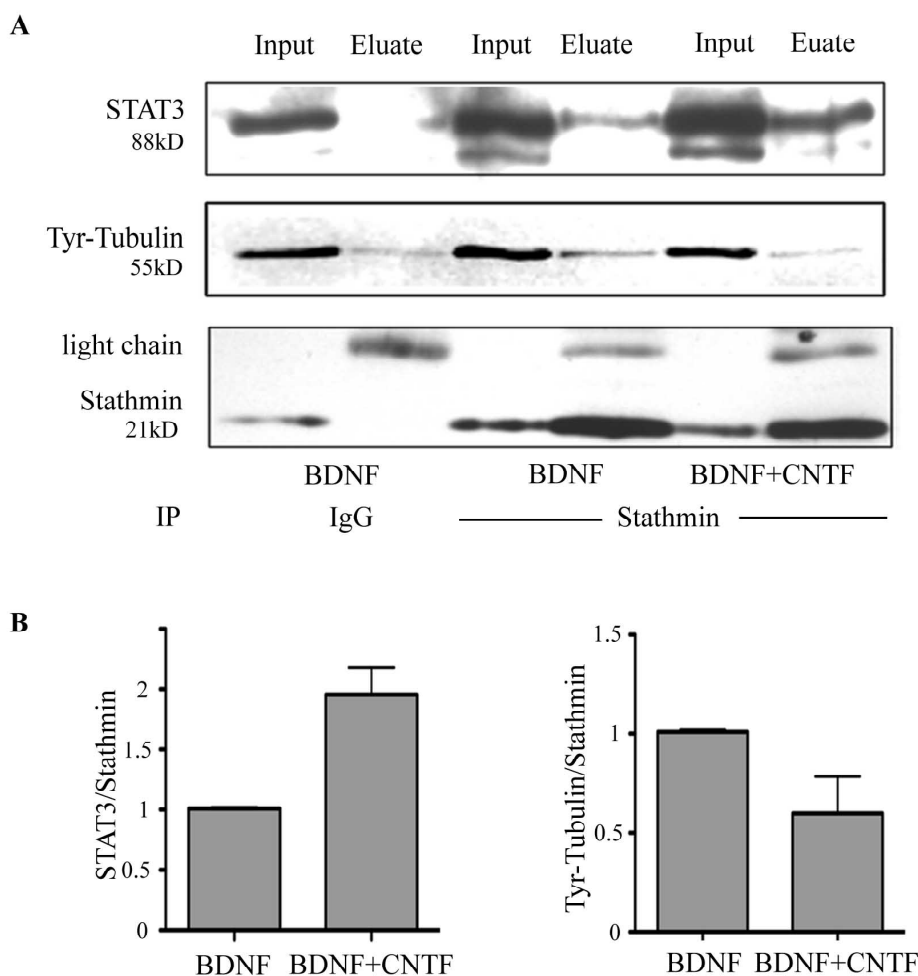


Figure 5.4.3: CNTF enhances STAT3 Stathmin interaction

(A) Immunoprecipitation of Stathmin from motoneurons cultured for 5 DIV. Western blot analysis after immunoprecipitation shows that STAT3 interaction with Stathmin is enhanced after CNTF application. Lane 1-2: Input and eluate from IgG control, lane 3-4: input and eluate from motoneurons cultured with BDNF, lane 5-6: input and eluate from motoneurons cultured with BDNF and pulsed with CNTF for 30 min on day 5.

(B) Quantification of western blot signals shows two-fold increase in STAT3-Stathmin interaction and reduced Stathmin-tyrosinated tubulin interaction after CNTF application, $n = 3$ independent experiments.

5.4.4 STAT3 phosphorylation at Y705 is required for its interaction with Stathmin

Since previous experiment showed that CNTF application enhances the interaction between STAT3 and Stathmin, it was inevitable to check whether tyrosine phosphorylation of STAT3 at position 705 is necessary for observed STAT3-Stathmin interaction. For this experiment, a dominant negative STAT3 mutant (STAT3^{Y705F}EYFP) was used in which the

aminoacid tyrosine (Y) at position 705 of STAT3 was mutated to phenylalanine (F) by site directed mutagenesis, thus inhibiting its phosphorylation. Primary motoneurons were infected with lentiviruses over-expressing STAT3^{WT}EYFP and STAT3^{Y705F}EYFP. Stathmin was immunoprecipitated from motoneurons over-expressing STAT3^{WT}EYFP and STAT3^{Y705F}EYFP and tested for co-immunoprecipitation of over-expressed STAT3 with GFP antibody. Figure 5.4.4 shows western blot analysis for Stathmin and GFP after immunoprecipitation. Western blot analysis of Stathmin showed that the amount of protein used (Input) and the amount of Stathmin immunoprecipitated were equal (Eluate) among all conditions. Western blot analysis with GFP antibody showed the co-precipitation of over-expressed STAT3 (WT or Y705F mutant). The interaction of Stathmin with STAT3^{Y705F}EYFP was reduced when compared to STAT3^{WT}EYFP, indicating that phosphorylation of STAT3 at tyrosine 705 by CNTF is necessary for its cytoplasmic interaction with Stathmin (Figure 5.4.4).

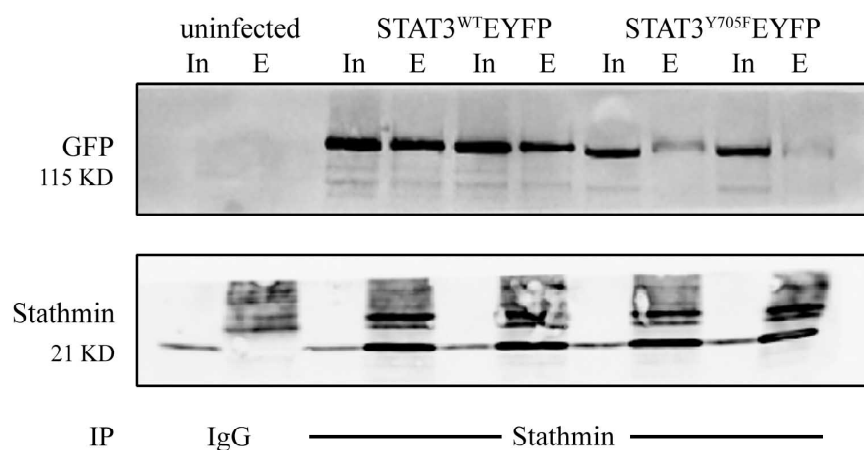


Figure 5.4.4: STAT3 phosphorylation at Y705 is required for its interaction with Stathmin

Immunoprecipitation of Stathmin from primary motoneurons over-expressing wildtype and dominant negative STAT3 (STAT3^{Y705F}EYFP) show loss of STAT3-Stathmin interaction when phosphorylation at Y705 is abolished.

5.5 Stathmin knockdown rescues axonal pathology in *pnn* mutant motoneurons

5.5.1 Lentiviral knockdown of Stathmin in primary motoneurons

Stathmin binds to α/β tubulin heterodimers and thereby reduces the availability of free α/β tubulin heterodimers. This mechanism reduces the kinetics of microtubule polymerization. Co-immunoprecipitation studies showed that STAT3 sequesters Stathmin in a phosphorylation dependent manner and that this results in release of tubulin from Stathmin, which could be available for microtubule polymerization. This raises a question whether the CNTF application to *pnn* mutant motoneurons locally increases the availability of α/β tubulin heterodimers via increase STAT3 Stathmin interaction and thereby increases the axon elongation. To test this hypothesis, we knocked down Stathmin in *pnn* mutant motoneurons by lentiviral RNAi approach and observed whether we could rescue axon elongation in absence of CNTF. Short hairpin RNA for Stathmin and a mismatch control were generated by cloning into pLL 3.7 RNAi vector (Bender.F.L.P, Ph.D thesis). Lentiviruses expressing siRNA for Stathmin and mismatch control were infected in primary motoneurons that were cultured for 5DIV. Immunostaining of Stathmin in these cells showed considerable knockdown of Stathmin. GFP labeling was used to identify the infected motoneurons (Figure 5.5.1B). Knockdown of Stathmin was also validated through westernblot analysis, as shown in figure 5.5.1A Stathmin protein levels were reduced in motoneurons infected with lentivirus expressing siRNA against Stathmin in comparison to uninfected motoneurons. The mismatch control did not reduce indicating that RNAi oligo is indeed specific.

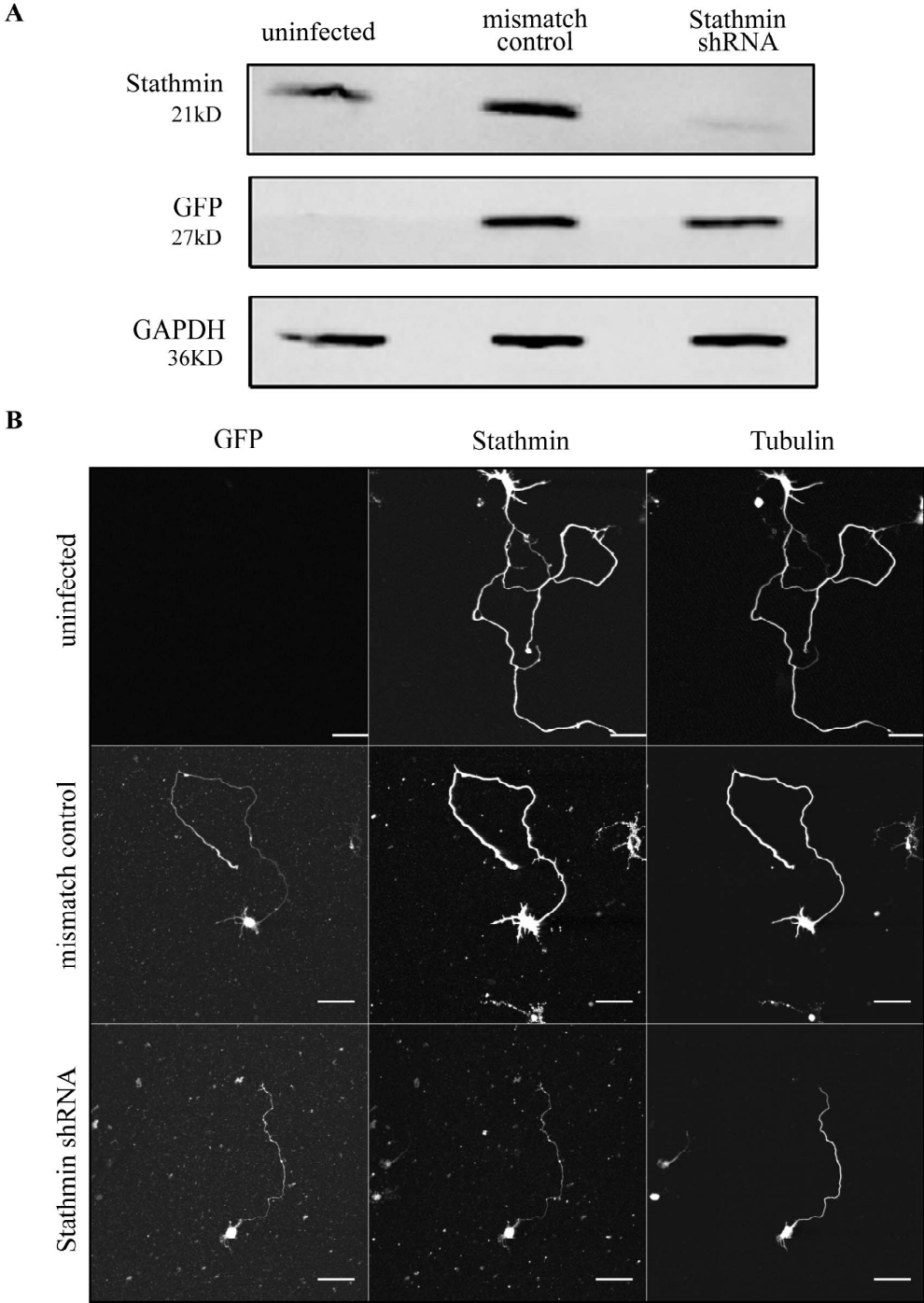


Figure 5.5.1: Lentiviral knockdown of Stathmin in primary motoneurons
(A) Lentiviral transduction of primary motoneurons with Stathmin siRNA oligo and mismatch oligo control for 5 DIV. Western blot analysis from these protein extracts showed reduction of Stathmin protein in cultures treated with Stathmin siRNA. Levels of Stathmin were unaltered in untreated and mismatch oligo treated controls.
(B) Lentiviral knock down of Stathmin was also observed through immunocytochemistry method. Cells were labeled with GFP, Stathmin and α -tubulin. Scale bar: 100 μ m

5.5.2 Stathmin knockdown rescues axon growth defect in *pnn* mutant motoneurons

We then analyzed whether Stathmin knockdown could rescue axonal pathology in *pnn* mutant motoneurons. Wildtype and *pnn* mutant motoneurons infected with Stathmin siRNA and mismatch control were cultured for 5DIV in the presence of BDNF alone. As expected, axon outgrowth of *pnn* mutant motoneurons recovered to wildtype levels upon lentiviral Stathmin knockdown. *Pnn* mutant motoneurons treated with BDNF and mismatch control virus exhibited shorter axons. CNTF addition did not lead to any further increase in axon growth, indicating that Stathmin inhibition is the major pathway how CNTF rescues axon growth in *pnn* mutant motoneurons. Surprisingly, Stathmin knockdown did not alter the axon length of wildtype motoneurons (Figure 5.5.2A-B)

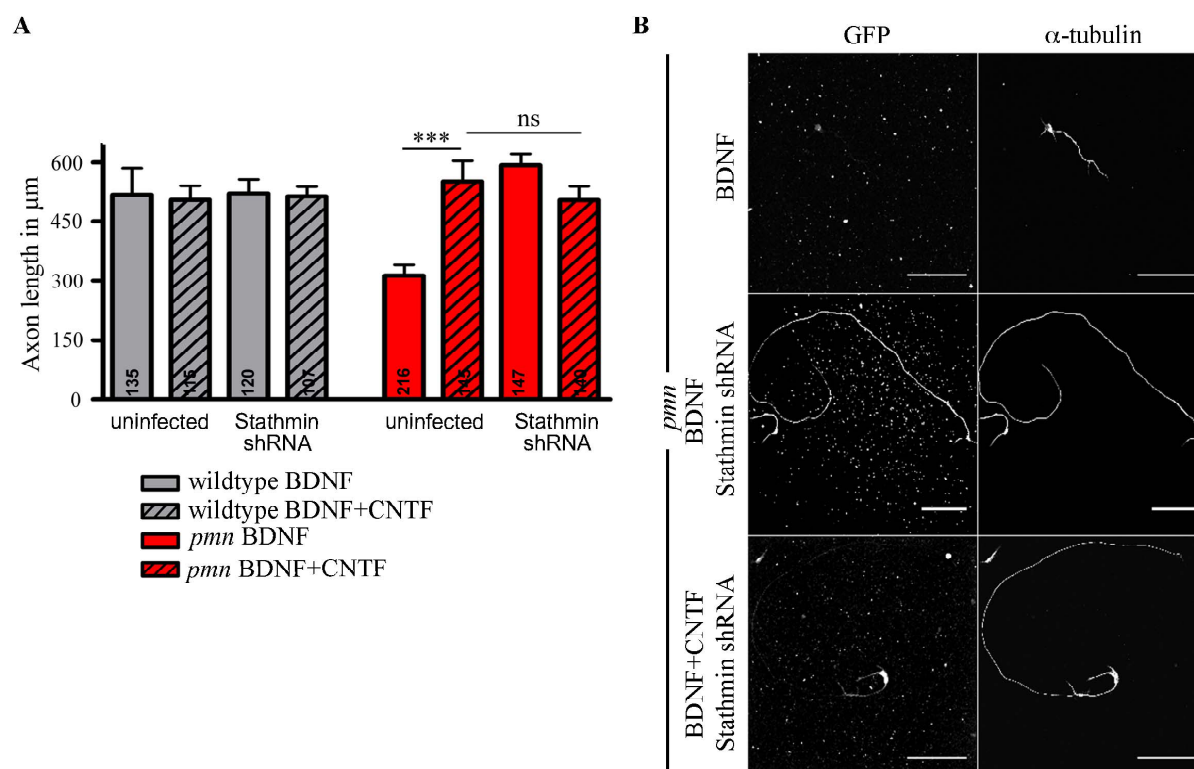


Figure 5.5.2: Stathmin knockdown rescues axonal pathology in *pnn* mutant motoneurons

(A) Axon length is restored in *pnn* mutant motoneurons after lentiviral Stathmin knockdown. Wildtype and *pnn* mutant motoneurons were cultured for 5 DIV. Stathmin knockdown rescues axon length in *pnn* mutant motoneurons. CNTF application did not induce additional axon growth in motoneurons with Stathmin

knockdown. Numbers in bars indicate number of cells measured; Data shown represent mean \pm S.E.M., $n = 3$ independent experiments. *** $P < 0.001$, Kruskal-Wallis with Dunn's multiple comparison test.

(B) Representative images of *pnn* mutant motoneurons after lentiviral Stathmin knockdown. Cells were labelled with GFP, and α -tubulin (Cy-3). Scale bar: 100 μ m.

5.5.3 Stathmin levels are not altered in *pnn* mutant motoneurons

Stathmin has been shown to be upregulated on the protein level in spinal cord and sciatic nerve of *Smn*^{-/-};SMN2^{tg} mice, a mouse model for spinal muscular atrophy (Wen et al., 2010). Since phenotype of *pnn* mice closely resemble to spinal muscular atrophy, it was of high interest to investigate the level of Stathmin in *pnn* mutant motoneurons. Primary motoneurons from wildtype and *pnn* embryos were cultured for 5 DIV with BDNF or BDNF+CNTF. Western blot analysis from these protein lysates showed no alteration in Stathmin protein between wildtype and *pnn* mutant motoneurons. Similarly, addition of CNTF did not change Stathmin protein level (Figure 5.5.3).

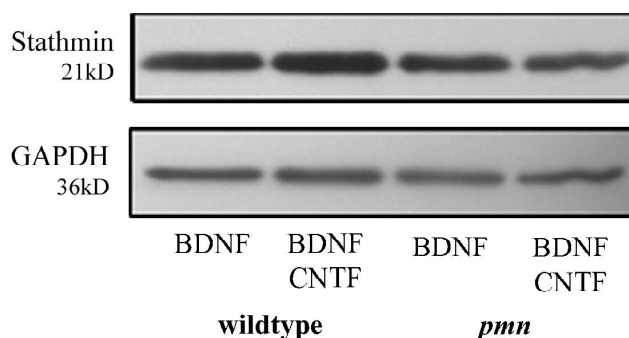


Figure 5.5.3: Stathmin levels are not altered in *pnn* mutant motoneurons

Western blot analysis from primary motoneurons shows that amount Stathmin protein is not altered between wildtype and *pnn*. Levels of Stathmin were same even with application of CNTF

5.6 CNTF alters the microtubule dynamics in *pmn* mutant motoneurons

Active transport along lengthy axons is necessary to replenish materials made in cell body to the farthest region of the axons (example growth cone). Impairment of microtubule dynamics has been reported in many neurodegenerative disorders. The transgenic SOD1^{G93A}, mouse model for ALS, has been reported to show impaired axonal transport accompanied by hyperdynamic microtubules. Moreover stabilization of microtubules via microtubule-modulating agent (MTMA) delayed the symptoms in SOD1^{G93A} mice (Fanara et al., 2007). Cultured *pmn* mutant motoneurons also exhibit impaired mitochondrial transport when compared to wildtype motoneurons. Application of CNTF rescues impaired microtubule based transport. (Bender FLP and Frank N Ph.D thesis). Moreover, recent evidence showing CNTF dependent interaction between Stathmin and STAT3 releases α/β tubulin heterodimers from Stathmin, necessitated to study whether microtubule dynamics is altered in *pmn* mutant motoneurons.

5.6.1 Post-translation modifications in α -tubulin represent microtubule dynamics

Posttranslational modifications in tubulin are known to specify properties and functions of microtubules. Tyrosinated tubulin has been shown as a characteristic feature of nascent and dynamic microtubules (Janke and Bulinski, 2011). Once the α/β tubulin heterodimers are attached to microtubule lattice, they are detyrosinated and thereby resistant to depolymerization. Acetylation of α -tubulin at lysine 40 causes the microtubules to be stabilized and long lived (Janke and Bulinski, 2011). In hippocampal neurons, tyrosinated tubulin is present all over the axon and dendrites and most importantly enriched in the growth cones and protrusions, whereas, acetylated tubulin is predominantly present in axonal shaft and absent in dendrites (Witte et al., 2008). Confirming previous reports with other neuronal cell types (Witte et al., 2008) showing that acetylated tubulin is present in all parts of the axon but relatively excluded from axonal growth cones and dendrites, where most microtubules are thought to be more stable than in distal

parts. Tyrosinated tubulin was in all regions of the neuron, including regions close to the axonal growth cone and in dendrites (Figure 5.6.1)

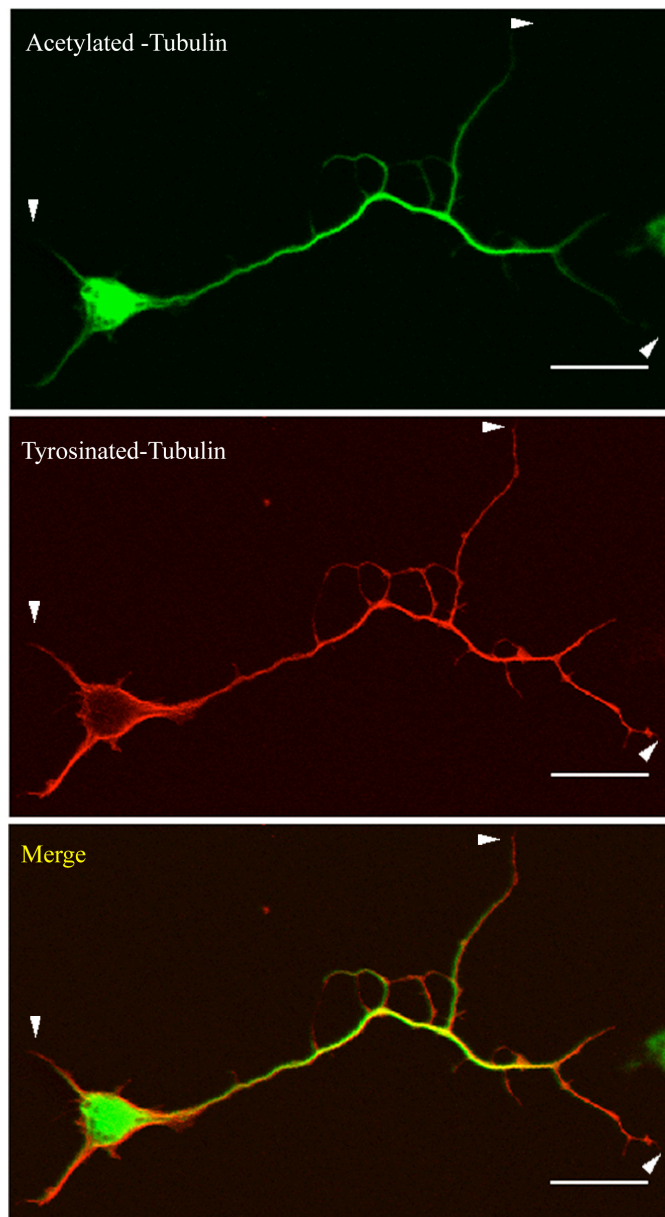


Figure 5.6.1: Localization of different posttranslational modified forms of α -tubulin

Wildtype motoneurons were stained with antibodies against acetylated and tyrosinated α -tubulin. Acetylated tubulin (Cy2) labels stabilized microtubules and is enriched in the axons but relatively excluded from dendrites and axonal growth cones (arrow heads). Tyrosinated tubulin (Cy3) labels dynamic and unstable Microtubules, including those in dendrites and axonal tips as shown by arrowheads. Scale bar: 20 μ m.

Levels of tyrosinated and acetylated tubulin were measured in *pmn* mutant motoneurons. *Pmn* mutant motoneurons cultured in the presence of BDNF showed significantly higher levels of tyrosinated tubulin in axons when compared to wildtype motoneurons, indicating that there are more nascent or dynamic microtubules in axons of *pmn* mutant motoneurons. Addition of CNTF or knockdown of Stathmin significantly reduced the levels of tyrosinated tubulin indicating that CNTF influences dynamics of microtubules and stabilizes them, presumably by counteracting Stathmin activity. Surprisingly, the levels of acetylated tubulin were not statistically different in *pmn* and wildtype motoneurons. Moreover CNTF treatment or Stathmin knockdown did not affect the levels of acetylated tubulin (Figure 5.6.2)

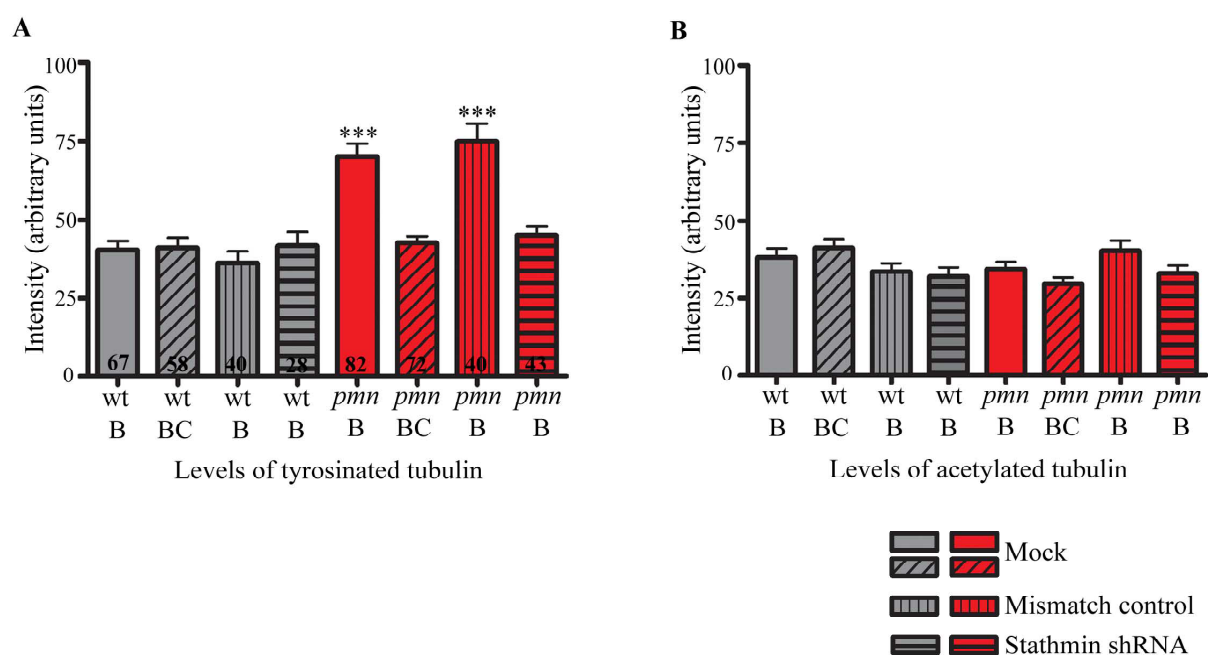


Figure 5.6.2: Levels of tyrosinated and acetylated tubulin in *pmn* mutant motoneurons

(A) Levels of tyrosinated tubulin were increased in *pmn* mutant motoneurons when compared to wildtype motoneurons. CNTF treatment [10 ng/ml] or Stathmin knockdown in *pmn* mutant motoneurons reduced tyrosinated tubulin levels to wildtype levels.

(B) Levels of acetylated tubulin were unchanged under conditions investigated. Numbers in bars indicate number of cells analyzed. BDNF and CNTF are indicated by B and C, respectively. Bars shown represent mean \pm S.E.M from 3 independent experiments. Statistical analysis: *** $P < 0.001$, ANOVA with Bonferroni post-hoc test.

5.6.2 Microtubule fractionation

Microtubule fractionation to isolate polymerized and soluble tubulin is an alternative method to understand microtubule dynamics. Motoneurons cultured for 5 DIV were extracted with microtubule stabilization buffer with 0.5% Triton X-100 for 5 min. Polymerized and soluble tubulin was separated by centrifugation. To control whether fractionation is achieved, cells were treated with paclitaxel (10 μ M) for 2 h to polymerize microtubules. Figure 5.6.3A shows western blot analysis of microtubule fractionation from wildtype motoneurons under physiological condition and after treatment with paclitaxel. Fractionation was analyzed with α -tubulin (detects tubulin irrespective of its post-translational modification), tyrosinated tubulin (detects the nascent form of tubulin) and acetylated tubulin (detects the stable microtubules). Under physiological conditions, α -tubulin was observed in both polymerized and soluble fraction, where as after paclitaxel treatment most of the tubulin was present in polymerized fraction. Immunoblot analysis with tyrosinated tubulin and acetylated tubulin showed they are present mostly in the soluble fraction and polymerized fraction respectively. This confirms that the tubulin fractionation technique can be adopted to analyse with in cultured motoneurons and that antibodies against acetylated and tyrosinated tubulins are specific (Figure 5.6.3A).

Microtubule fractionation was performed on wildtype and *pnn* mutant motoneurons to test whether the altered microtubule dynamics observed reflects in microtubule fractionation. Motoneurons from 4-5 embryos for wildtype and *pnn* embryos were pooled to perform microtubule fractionation assay. Western blot analysis was performed for α -tubulin, tyrosinated tubulin and acetylated tubulin. Histone 3 and GAPDH served as a loading control. Western blot analysis with α -tubulin showed that slight increase in the soluble form of tubulin in *pnn* mutant motoneurons when compared to wildtype motoneurons. This was also confirmed with antibodies for tyrosinated tubulin. This observation indicates that microtubule dynamics is altered in *pnn* mutant motoneurons (Figure 5.6.3B). Since the amount of protein is critical for such a

fractionation experiment, it was difficult to perform this experiment in mutant embryos and therefore could not be tested with CNTF treatment.

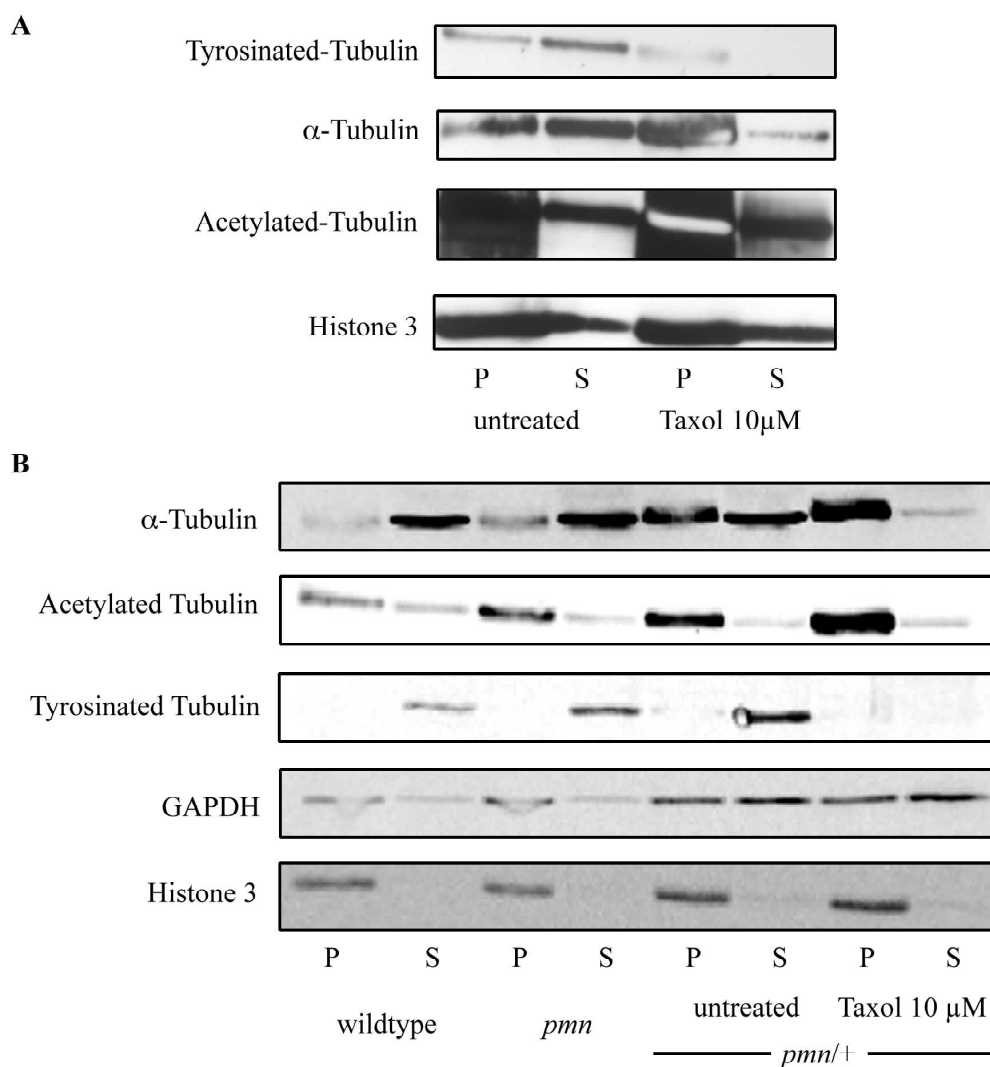


Figure 5.6.3: Microtubule fractionation in primary motoneurons

(A) Primary motoneurons were cultured for 5DIV and microtubules were fractionated to polymerized and soluble form using microtubule stabilization buffer. Western blot analysis against various isoforms of Tubulin indicated that acetylated tubulin was observed predominantly in the polymerized fraction and tyrosinated tubulin was observed in the soluble fraction. As a control, cells treated with taxol to polymerize the microtubules showed absence of tyrosinated α -tubulin and total α -tubulin depletion in the soluble fraction.

(B) Microtubule fraction performed in wildtype and *pmn* mutant motoneurons showed slight increase in the tyrosinated α -tubulin and corresponding increase of total α -tubulin levels in soluble fraction of *pmn* mutant motoneurons. Histone and GAPDH were used as loading controls.

5.6.3 Microtubule stabilization promotes axon growth in *pnn* mutant motoneurons

Since previous results showed that axons of *pnn* mutant motoneurons possessed high levels of nascent and dynamic form of tubulin (tyrosinated tubulin) corresponding to shorter axons, it became essential to test whether stabilization of microtubule is sufficient to promote axon elongation in *pnn* mutant motoneurons. For this experiment, *pnn* and wildtype motoneurons were cultured in the presence of BDNF and 10 nM paclitaxel, a microtubule-stabilizing drug for 5 DIV. Paclitaxel at such a concentration has been reported earlier to promote axon elongation (Witte et al., 2008). Taxol treatment promoted increased axon growth in *pnn* mutant motoneurons comparable to wildtype and *pnn* mutant motoneurons cultured with CNTF (Figure 5.6.4A-B).

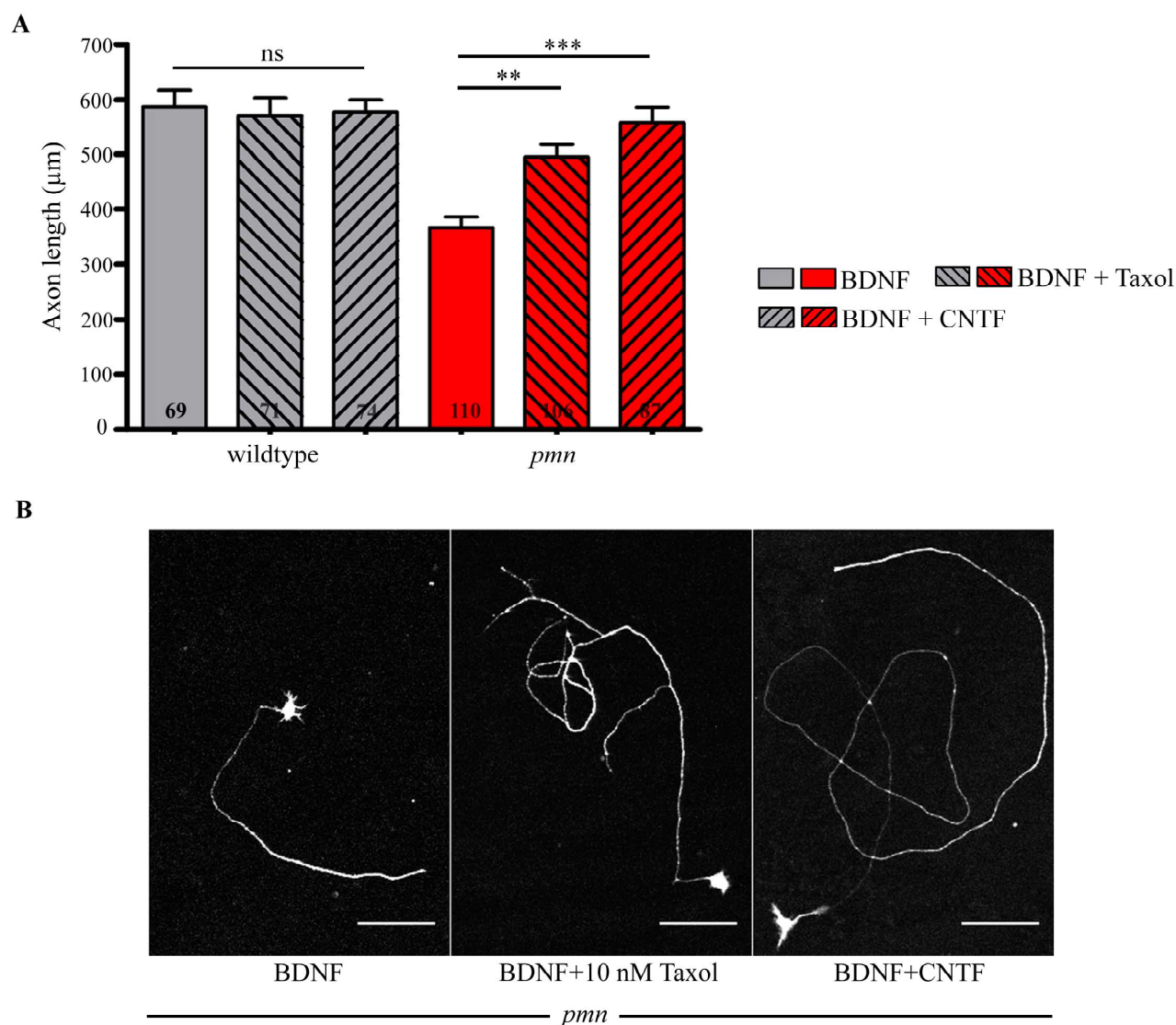


Figure 5.6.4: Stabilization of microtubules with taxol promotes axon growth in *pmn* mutant motoneurons

(A) Representative pictures of *pmn* mutant motoneurons cultured with BDNF, 10 nM taxol, BDNF and CNTF showing increased axon length upon stabilization of microtubules. Scale bar: 100 µm.

(B) Stabilization of microtubules in *pmn* mutant motoneurons in the presence of 10 nM of taxol increased axon length in *pmn* motoneurons to wildtype levels. Numbers in bars represent the number of cells measured. Bars shown represent mean \pm S.E.M from 3 independent experiments. Statistical analysis: ns (not significant), *** $P < 0.001$ ANOVA with Bonferroni post-hoc test.

5.7 CNTF enhances microtubule polymerization in primary cultured motoneurons

Mutation in *TBCE* gene in *pmn* mice contributes to less α/β tubulin heterodimers formation. Previous studies with primary *pmn* mutant motoneurons showed impaired microtubule polymerization (Schaefer et al., 2007). Since CNTF alters the microtubule dynamics in *pmn* mutant motoneurons, it was also suspected whether CNTF could influence microtubule polymerization. To test this hypothesis, microtubule regrowth assay was performed after nocodazole treatment (Ahmad and Baas, 1995; Schaefer et al., 2007). Wildtype and *pmn* mutant motoneurons were plated on coverslips and treated with microtubule destabilizing drug, nocodazole, (10 μ M) for 6h to depolymerize the existing microtubule network (Figure 5.7.1A). Microtubule regrowth after nocodazole washout was observed within 5 minutes. The polymerized microtubules were extracted and subsequently fixed with 2% PFA. Cells were stained with α -tubulin and γ -tubulin to label polymerized microtubule network and microtubule organizing center (MTOC) respectively. To measure the number of microtubules emanating from the MTOC, Sholl analysis was performed with radius increments of 0.25 μ m (Figure 5.7.2A). Graphs were plotted against mean number of intersection and distance from MTOC. As shown in the figure 5.7.1B & 5.7.2B *pmn* mutant motoneurons showed lower number of intersections when compared to wildtype motoneurons, corresponding to less microtubules emanating from MTOC and the microtubules formed were shorter than wildtype. Application of CNTF significantly increased the number of microtubule formed and length of microtubule formed in *pmn* mutant motoneurons (Figure 5.7.1B & 5.7.2C). Interestingly, application of CNTF to wildtype motoneurons significantly increased the microtubule polymerization (Figure 5.7.2F). To understand whether CNTF mediated microtubule polymerization is dependent of STAT3, microtubule regrowth assay was performed with primary motoneurons from $STAT3^{KO/FL};NFL-Cre^{tg}$. $STAT3^{KO/FL};NFL-Cre^{tg}$. These motoneurons showed less intersection when compared to the wildtype. Importantly, the CNTF application did not enhance number of

microtubules formed indicating that STAT3 mediates microtubule polymerization, presumably by counteracting Stathmin (Figure 5.7.2E). Surprisingly, $STAT3^{KO/FL};NFL-Cre^{tg};pnn^{-/-}$ motoneurons exhibited significantly less numbers of microtubules when compared to $STAT3^{KO/FL};NFL-Cre^{tg}$ motoneurons, indicating that two distinct phenomena contribute to an additive effect. Firstly, the TBCE mutation in *pnn* mutant motoneurons leads to less amount of α/β tubulin heterodimers formed and secondly, lack of STAT3 to counteract Stathmin and thereby α/β tubulin heterodimers are not released from Stathmin (Figure 5.7.2E). The average length of microtubule formed was increased upon CNTF stimulation (back calculated from the Sholl analysis described in materials and methods). These data suggests that CNTF and STAT3 plays a novel role in microtubule polymerization and thereby induce axon elongation in *pnn* mutant motoneurons (Figure 5.7.2D).

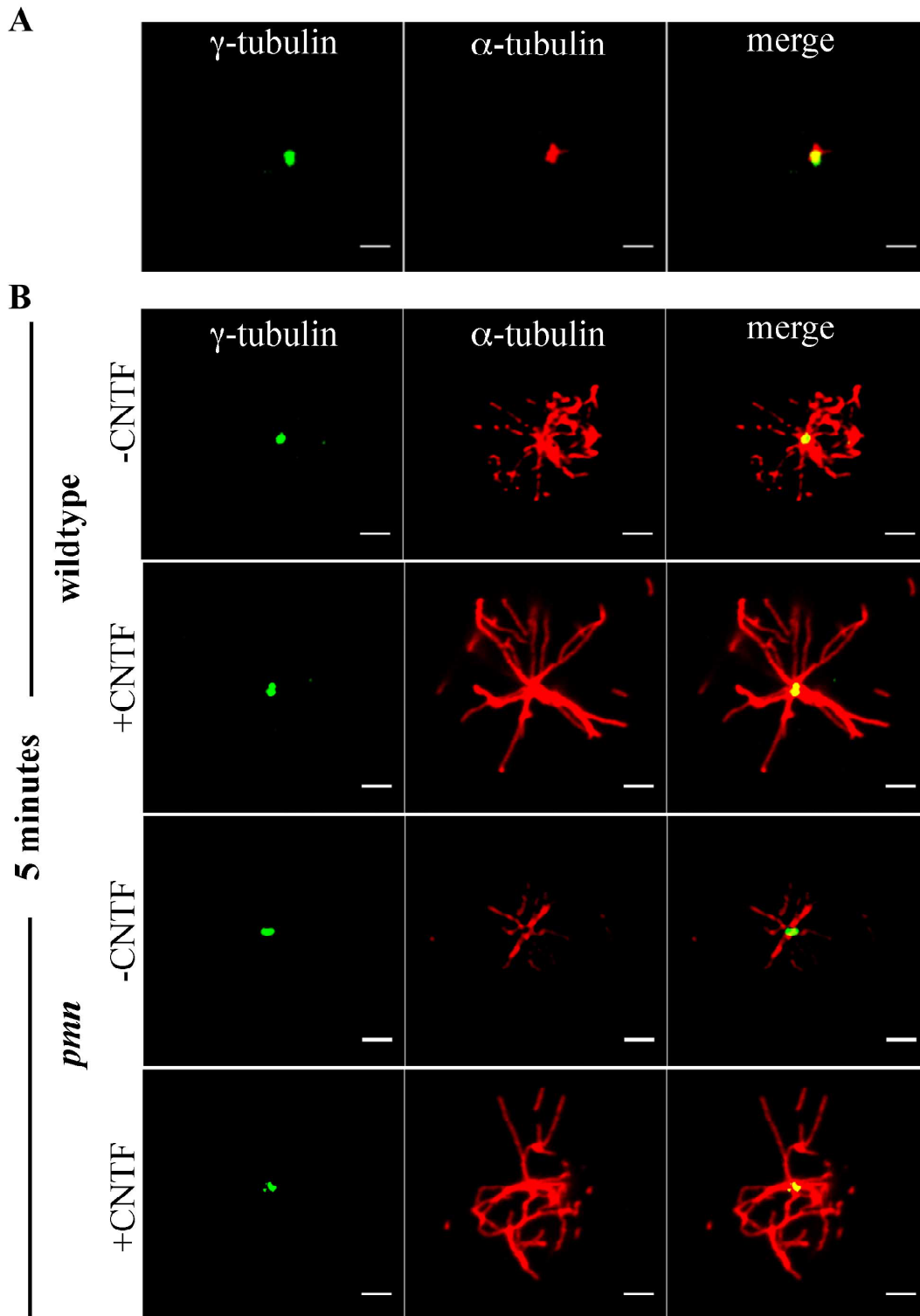


Figure 5.7.1: CNTF enhances microtubule regrowth in cultured motoneurons

Representative images of primary motoneurons analyzed for microtubule regrowth assay. Cells were immunostained with γ -tubulin (Cy2) to label the centrosome and α -tubulin (Cy3) to label microtubules

(A) Microtubules were depolymerized with nocodazole for 6 h. Cells were fixed right after soluble proteins were extracted by washing out with tritonX-100.

(B) Microtubule regrowth analyzed at 5 min after CNTF application in cultured wildtype and *pnn* mutant motoneurons. Scale bar: 2 μ m.

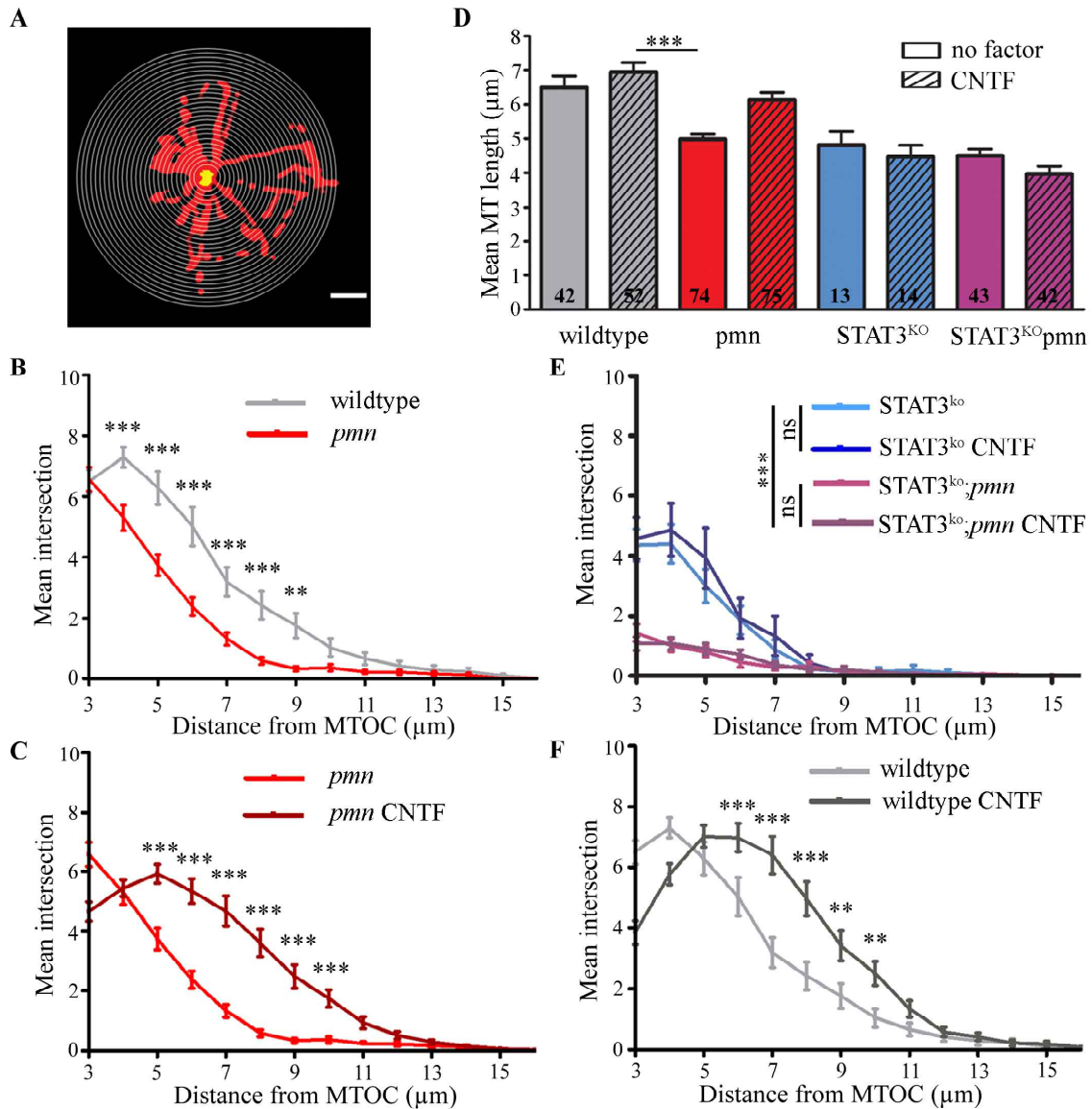


Figure 5.7.2: CNTF enhances microtubule regrowth in cultured motoneurons

(A) Representative image from Sholl analysis performed on primary motoneurons with 0.25 μm step concentric circles. Scale bar: 2 μm .

(B-C, E-F) Graphs obtained from Sholl analysis depicting number of intersections on y-axis and distance from MTOC on x-axis.

(B) Comparison of MT regrowth between *pmn* mutant and wildtype motoneurons.

(C) CNTF enhances MT regrowth in *pmn* mutant motoneurons.

(D) Graphical representation of average length of polymerized MTs formed in wildtype and *pmn* mutant motoneurons with and without CNTF, and in STAT3^{fl/KO};NFL-Cre^{tg} motoneurons. Numbers in columns represent the number of analysed motoneurons. Bars shown represent mean \pm S.E.M from 4 independent experiments. Statistical analysis: ***P<0.001 ANOVA with Bonferroni post-hoc test.

(E) CNTF mediated MT regrowth was abolished in STAT3^{fl/KO};NFL-Cre^{tg} and STAT3^{fl/KO};NFL-Cre^{tg}*pmn* mutant motoneurons.

(F) CNTF enhances MT regrowth in wildtype motoneurons. Statistical analysis: *P<0.05, **P<0.01, ***P<0.001; Two way ANOVA with Bonferroni post-hoc test.

5.8 Stability of TBCE protein

Autosomal recessive mutation in *pnn* mouse was mapped to chromosome 13 (Martin et al., 2001) and the point mutation was identified in the TBCE gene causing a T→G transition at position 1682 which leads to Trp→Gly substitution at the last amino acid of the TBCE protein (Bommel et al., 2002; Martin et al., 2002). Pulse chase experiment of wildtype and mutant TBCE protein after metabolic labeling with ³⁵S labeling showed that mutation in TBCE protein rendered it unstable and more susceptible to trypsin digestion when compared to wildtype protein, indicating putative conformational change due to this amino-acid substitution (Martin et al., 2002). Moreover it has also been shown that overexpression of mutant TBCE in *pnn* mutant motoneurons partially rescued axon length deficit in cultured motoneurons indicating that the mutant TBCE protein is still functional (Bender FLP Ph.D dissertation). These findings raised the question whether CNTF could alter the stability of the TBCE protein and thereby able to rescue axon elongation defect.

5.8.1 Tryptophan to Glycine mutation in TBCE renders it unstable

Firstly, to understand the stability of mutant TBCE protein *in-vitro*, HEK 293T cells (human cell line) and N2A cells (mouse cell line) were transiently transfected with wildtype (TBCE^{WT}) and mutant (TBCE^{W524G}) TBCE expression vector (pcDNA3.1). The overexpressed protein was tagged with HA at the amino terminal end. Co-transfecting the cells with a GFP expressing vector controlled efficiency of transfection. 24 hours post transfection, cells were treated with three different proteasome inhibitors, namely, Lactacystin (5 μM), MG132 (5 μM) and Proteasome Inhibitor 1 (5 μM) for 24 h. The amount of HA-TBCE was analyzed by standard western blot and quantified with Image J software. Amounts of GFP and GAPDH protein were also measured as internal normalization control.

As shown in western blots of Figure 5.8.1, the total amount of HA-TBCE was detected by anti-HA antibody. HA-TBCE^{W524G} was found to be less abundant than the HA-TBCE^{WT} in both cell types studied (HEK 293T and N2A). Relative amount of the HA-TBCE protein was quantified by GFP which was co-transfected and had the same promoter as HA-TBCE (CMV promoter). In HEK 293T cells, the amount of HA-TBCE^{W524G} was reduced by 40% when compared to HA-TBCE^{WT}. The reduction of HA-TBCE^{W524G} in N2A cells was even more striking as the protein was reduced by approximately 60%. To analyze whether this reduction is caused by increased degradation of HA-TBCE^{W524G}, cells were treated with proteasome inhibitors to inhibit ubiquitin proteasome degradation pathway. Upon treatment with proteasome inhibitors, the amount of HA-TBCE^{W524G} was restored to the levels of HA-TBCE^{WT}, indicating HA-TBCE^{W524G} is highly unstable and undergoes proteasomal degradation. The amount of both GFP and GAPDH was found to be reduced after the treatment of proteasome inhibitors possibly due to increased cell death or arrest in cell cycle. Quantification of HA-TBCE^{WT} and HA-TBCE^{W524G} after proteasome inhibitors showed approximately 3 fold increase than the untreated cells, possibly the turnover of TBCE protein is much higher than GFP and GAPDH.

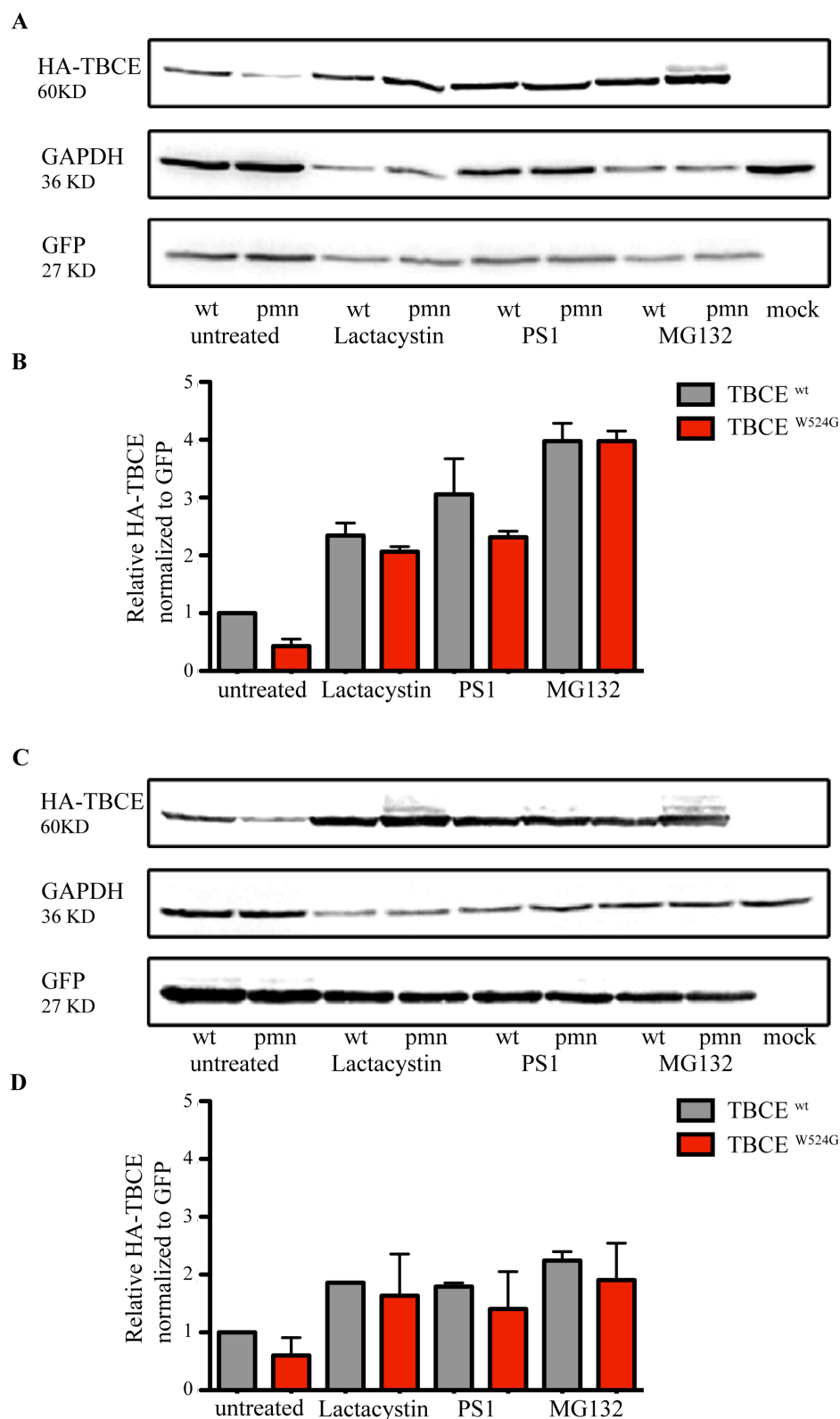


Figure 5.8.1: Tryptophan to Glycine (W-G) substitution in TBCE renders it unstable
 (A, C) Western blot analysis of overexpressed HA-TBCE^{WT} and HA-TBCE^{W524G} in N2A (A) and HEK293T (C) cells showed that amount of HA-TBCE^{W524G} was reduced when compared to HA-TBCE^{WT}. Treatment with proteasome inhibitors restored comparable levels.
 (B, D) Quantification of HA-TBCE^{WT} and HA-TBCE^{W524G} from N2A (B) and HEK293T (D) cells, n=3 independent experiments.

5.8.2 CNTF does not alter the stability of TBCE protein

Previous studies have shown that the neurotrophic factor CNTF prolongs the survival and improves motor function of *pmn* mutant mouse (Sendtner et al., 1992b). In order to understand whether CNTF somehow plays a role in stabilizing the TBCE protein and thereby rescues the phenotype, TBCE protein levels in cultured *pmn* mutant motoneurons were analyzed. Primary motoneurons from wildtype and *pmn* mutant embryos were cultured for 5 days in-vitro in presence and absence of CNTF (10 ng/ml). Approximately $0.1 - 0.2 \times 10^5$ cells were plated per condition. To obtain such large number of cells, cells from different embryos of the same genotype were pooled before plating. Cells were harvested after 5 days for western blot analysis. Figure 5.8.2 shows the levels of TBCE in *pmn* mutant motoneurons. As expected the amount of TBCE protein in *pmn* mutant motoneurons was significantly reduced when compared to wildtype motoneurons. CNTF application to motoneurons for 5 days did not change the levels of TBCE protein in wildtype motoneurons. Similarly, CNTF did not restore the reduced TBCE protein level in *pmn* mutant motoneurons, indicating the CNTF does not rescue the *pmn* mutant mouse by altering the stability of the TBCE protein.

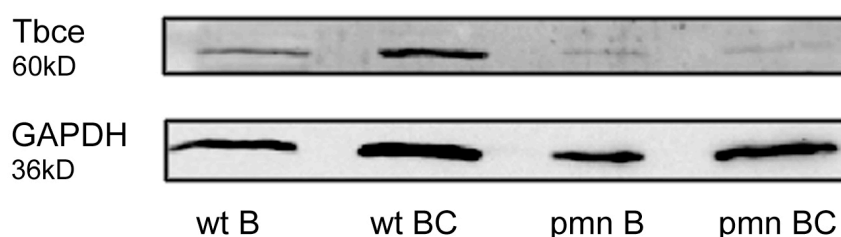


Figure 5.8.2 CNTF does not increase the levels of TBCE

Western blot analysis from wildtype and *pmn* mutant motoneurons showed reduced amount of TBCE protein in *pmn* mutant motoneurons. Addition of CNTF (10 ng/ml) for 5 days did not increase the levels of TBCE in both wildtype and *pmn* mutant motoneurons, indicating CNTF does not alter the stability of TBCE^{W524G}

5.8.3 CNTF does not regulate the expression of *Tbce* gene

STAT3 has been known as a transcription factor and upon activation it increases the expression of various genes such as Bcl-XL, Bcl-2 and SOCS3. This raised the question whether TBCE could possibly be a downstream target of CNTF-STAT3. Therefore, expression of TBCE mRNA upon CNTF activation was analyzed in primary wildtype motoneurons.

Firstly, localization of TBCE mRNA in primary motoneurons was observed by Fluorescent *in-situ* hybridization (FISH) technique. Primary motoneurons were cultured for 5 days *in-vitro*. TBCE mRNA specific antisense (from genedetect) probe was used to detect the TBCE mRNA in primary motoneurons. Sense control and RNase treated sample were used as negative control for *in-situ* hybridization. Immunocytochemistry for tau protein was coupled with FISH to observe the morphology of the motoneuron. TBCE mRNA is localized in dendrites, axons and cell body (relatively less) of primary motoneurons. Treatment of motoneurons with RNase prior to labeling with antisense helped to judge the specificity of the antisense probe. Sense control was used to control the unspecific binding of the probe to RNA (Figure 5.8.3).

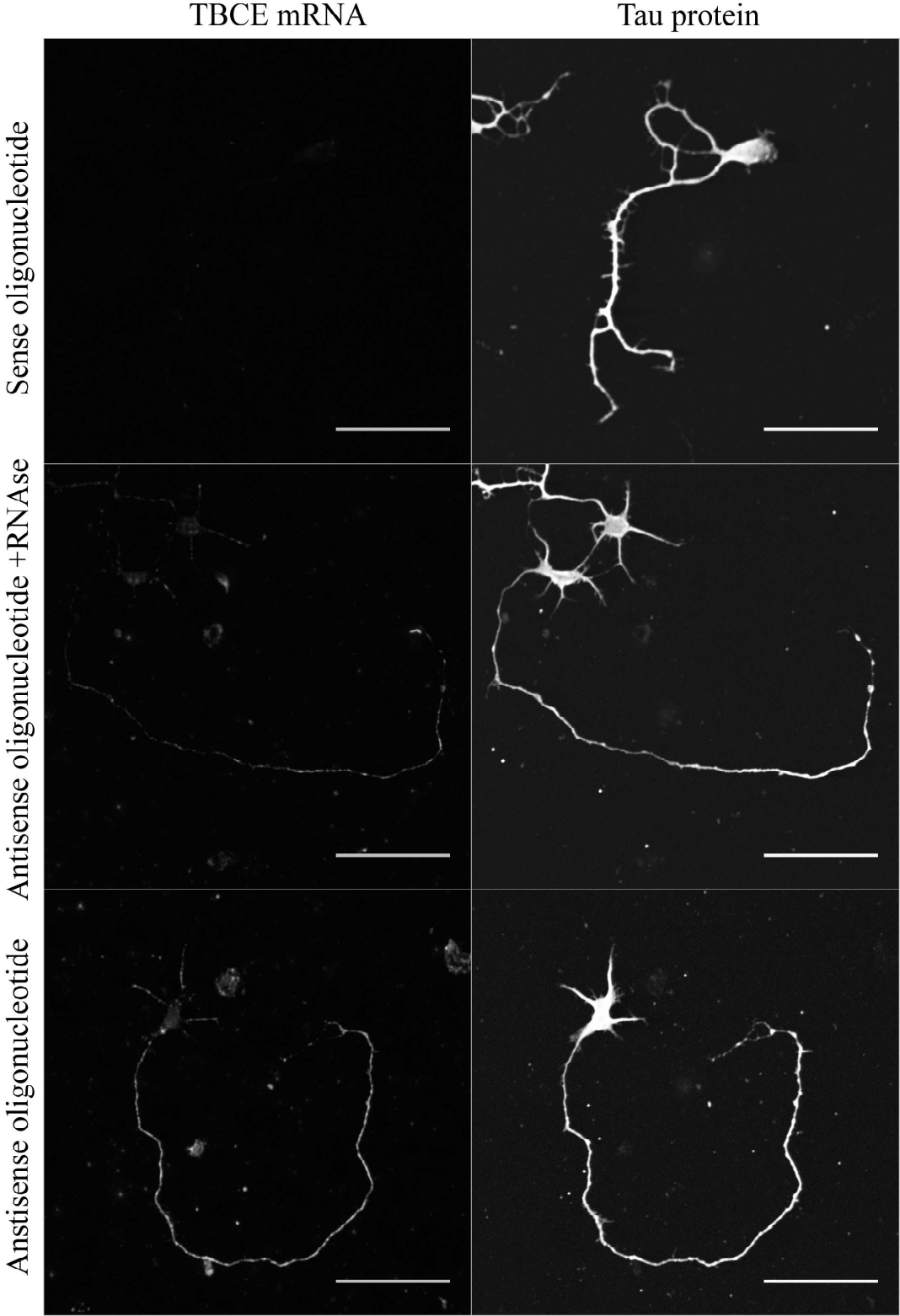


Figure 5.8.3 Localization of TBCE mRNA in primary motoneurons
Primary motoneurons were labeled with antisense oligonucleotide probe specific to TBCE mRNA showing the presence of TBCE mRNA in axon, dendrites and cell body (relatively less). Sense probe and RNase treatment served as negative controls. Immunostaining of Tau was performed to visualize the morphology of the cell. Scale bar: 100 μ m.

Secondly in order to analyze expression of TBCE mRNA upon CNTF activation real time quantitative reverse transcriptase (RT) PCR was performed on primary motoneurons cultured for 5 days *in-vitro* with BDNF (10 ng/ml) and motoneuron cultured with BDNF (10 ng/ml) and CNTF (10 ng/ml). Total RNA was extracted, reverse transcribed to c-DNA and real time quantitative pcr was performed for TBCE and actin c-DNA. Actin was used as a control house keeping gene in this experiment. Relative expression of TBCE was not significantly altered upon CNTF activation in cultured primary motoneurons (Figure 5.8.4)

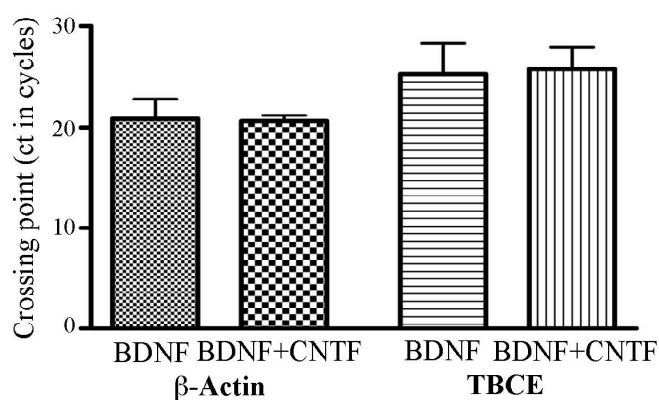


Figure 5.8.4: CNTF does not alter expression of TBCE mRNA in primary motoneurons

Quantitative real time PCR analysis on day 5 primary motoneurons showed no significant difference in TBCE mRNA between BDNF and BDNF+CNTF treated culture. β -Actin mRNA was used as a control house-keeping gene.

5.9 STAT3 activation in sciatic nerve of *pmn* mouse

The sciatic nerve is a large nerve originating from the lumbar spinal cord that extends to the entire length of hind limb. It is a mixed nerve containing both sensory and motor axons. It is widely used to study peripheral nerve regeneration after lesion. Early studies have shown that STAT3 is phosphorylated after sciatic nerve transection and unlike ERK1/2 (which is also activated after injury), p-STAT3^{Y705} was observed more in the proximal site of injury when compared to distal site of injury (Sheu et al., 2000). Furthermore, activated STAT3 has been shown to be retrogradely transported and translocated to the nucleus after injury (Ben-Yaakov et al., 2012) indicating that it might send the signal to nucleus for axonal regeneration. Since sciatic nerve is also affected in *pmn* mice with loss of motor axons, we checked whether phosphorylated STAT3 is altered in sciatic nerve of *pmn* mice. Sciatic nerve from 4 week old wildtype and *pmn* mice was isolated, proteins was extracted and subjected to western blot analysis. As shown in the figure 5.9A the levels of p-STAT3^{Y705} was increased in sciatic nerve of *pmn* mice when compared to wildtype littermates. To check whether the increased level of STAT3 phosphorylation is also observed in pre-symptomatic mice, western blot analysis was performed from postnatal day 10 and 17 old *pmn* mice. Interestingly, the levels of p-STAT3^{Y705} were increased in both the analyzed time points analyzed, indicating this observation is pre-symptomatic (Figure 5.9B). Further analysis needs to be performed to characterize whether CNTF release from Schwann cell is responsible for this phosphorylation.

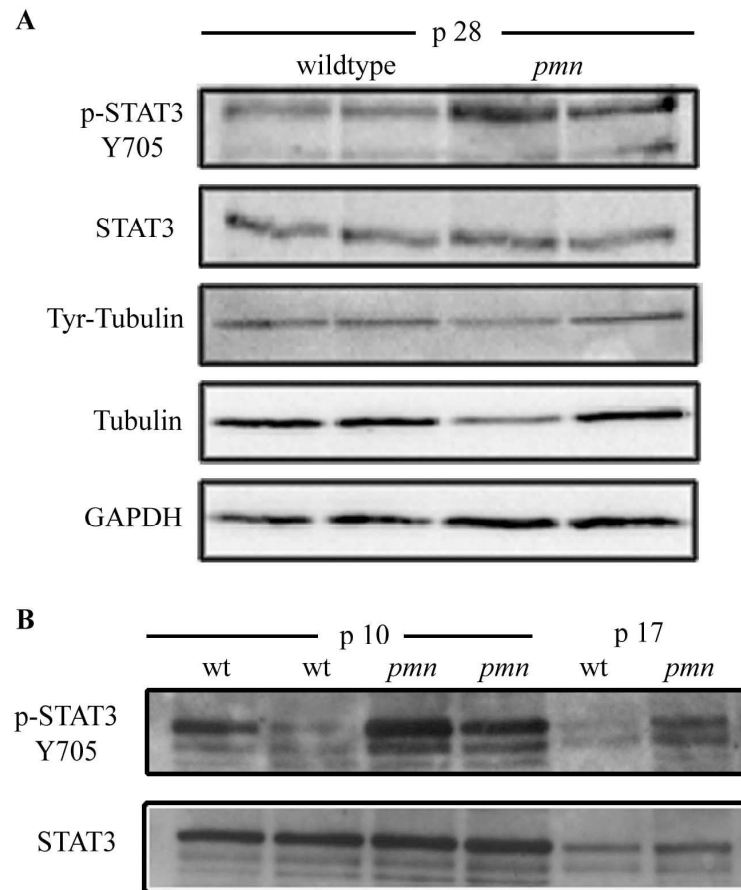


Figure 5.9 pSTAT3^{Y705} is upregulated in sciatic nerves of *pmn* mutant mice

(A) Western blot analysis from sciatic nerve of postnatal day 28 old wildtype and *pmn* mutant mice indicated increased levels of phosphorylation of STAT3 at tyrosine 705

(B) Western blot analysis from sciatic nerve of postnatal day 10 and 17 old wildtype and *pmn* mutant mice indicated increased levels of phosphorylation of STAT3 at tyrosine 705

5.10 Characterization of Synapse associated protein 1 (SYAP1) and interaction with TBCE

Synapse associated protein 47 (SAP47) is a novel drosophila protein identified by screening hybridoma library of several monoclonal antibodies that selectively stain synaptic terminals in immunohistochemical studies (Hofbauer et al., 2009; Reichmuth et al., 1995). SAP47 is expressed in synaptic regions of larval brain. Deletion mutant of SAP47 showed impaired short term plasticity and odorant-tastant associative learning ability (Saumweber et al., 2011). Yeast 2 hybrid studies were performed by Dr. N. Funk to identify the interacting partners for SAP47. One of the interacting partners identified was TBCE like protein (TBCE-L). TBCE-L is a highly conserved protein across several species (Bartolini et al., 2005) and as the name suggests it has high similarity to TBCE. Over expression studies in Hela cells have shown that TBCE-L has microtubule destabilizing activity by degrading α/β heterodimers and thus reduce the availability for microtubule polymerization (Bartolini et al., 2005). Mouse homologue of SAP47 is synapse associated protein 1 (SYAP1). TBCE has been shown to localize in cell body, axons and enriched in the growth cones of motoneurons (Bender F.L.P PhD thesis). This raised a question whether TBCE might have a novel role in the pre-synapse in association with SYAP1. In line with this question, SYAP1 localization and its interaction with TBCE was analyzed in the present study.

5.10.1 Characterization of antibodies against SYAP1

Antibodies are prerequisite for characterization of a protein. Since not many studies have been done on SYAP1, it was necessary to characterize available antibodies against SYAP1. Dr. N. Funk generated a mouse polyclonal serum against SYAP1 using a peptide as an immunogen. Another commercial antibody against SYAP1 was obtained from SIGMA-Aldrich, however this

antibody was raised against the human SYAP1 protein. Sequence similarity between peptide used for immunogen and mouse SYAP1 was around 93%, so this human specific SYAP1 antibody was also tested in this study. To test the specificity of these antibodies, HEK 293T cells were transfected with 2 expression vectors for mouse SYAP1 (pcDNA3 and pGJ3 vector system). SYAP1 was N-terminally tagged with a FLAG amino acid sequence (Dr. N. Funk). Proteins extracts obtained were subjected to western blot analysis for 2 different SYAP1 antibodies and FLAG antibody. Protein extracts from mouse primary motoneurons were also analyzed in parallel. As shown in figure 5.10.1 endogenous SYAP1 in HEK293T cells was observed migrating at approximately 55 kDa when probed with both mouse and human specific antibody. Overexpressed FLAG-SYAP1 in both expression systems was observed to migrate at 60 kDa. Protein extracts were also probed with anti-FLAG antibody to detect overexpressed protein alone and compare the running behaviour observed with the SYAP1 antibodies. The FLAG antibody detected a prominent band at approximately 60 kDa similar to the protein detected by the SYAP1 antibodies. Untransfected cells did not show a positive signal for FLAG antibody. Protein extracts from primary motoneurons also showed a prominent band at 55 kDa similar to HEK 293T cells. Additionally, another band at approximately 45 kDa was detected by human specific SYAP1 antibody, which was absent when detected with mouse SYAP1 antibody. This could be unspecific or reflect another isoform of SYAP1 which needs to be characterized. These results indicated that both SYAP1 antibodies were binding to SYAP1 protein.

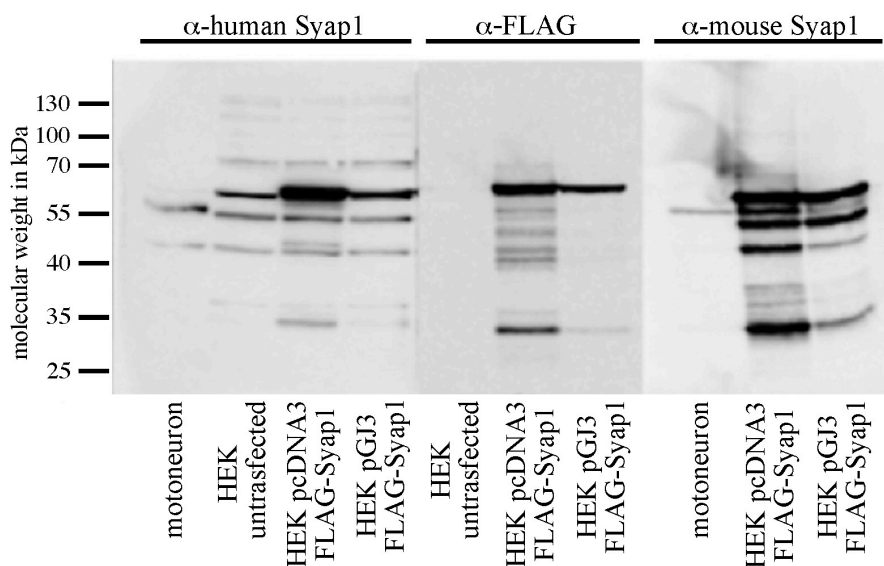


Figure 5.10.1: Characterization of antibodies against SYAP1

Western blot analysis of protein extracts isolated from motoneurons and HEK cells over-expressing with FLAG-SYAP1 and probed with antibodies α -human SYAP1, α -FLAG and α -mouse SYAP1.

5.10.2 Lentiviral knock down of SYAP1 in primary motoneurons

Specificity of the antibody could be tested using a protein knockdown approach. Dr. N. Funk had previously cloned 4 different siRNA oligos against mouse SYAP1 into pLL3.7 lentilox RNAi vector. All four plasmids were tested for their knock down efficiency by western blot analysis. HEK 293 T cells were co-transfected with pcDNA3 FLAG-SYAP1 and 2 different concentrations (0.4 μ g and 0.6 μ g) of pLL3.7 vector containing the knockdown oligo (24 well). As a transfection control pcDNA3 FLAG-SYAP1 and GFP-pLL3.7 vector was used. Western blot analysis was performed and blots were probed for FLAG antibody to detect FLAG-SYAP1 and GFP to measure the rate of transfection. Over-expression of mouse FLAG-SYAP1 was performed to overcome the problem of HEK cells being a human cell line and the associated problem whether knockdown is specific for mouse SYAP1. As shown in the figure 5.10.2A, out of four different oligos generated only oligo 3 was functional for knock down of SYAP1 protein. This positive clone was used to generate lentivirus in order to check the antibody specificity and

to study the function of SYAP1 protein. Lentiviruses expressing SYAP1 knockdown oligo3 were further tested in primary motoneurons. Primary motoneurons were cultured for 5 DIV with neurotrophic factors BDNF and CNTF. SYAP1 oligo 3 virus and control GFP virus were added on the day of plating. Western blot analysis showed a reduction in SYAP1 protein level were SYAP1 oligo 3 virus was added (Figure 5.10.2B)

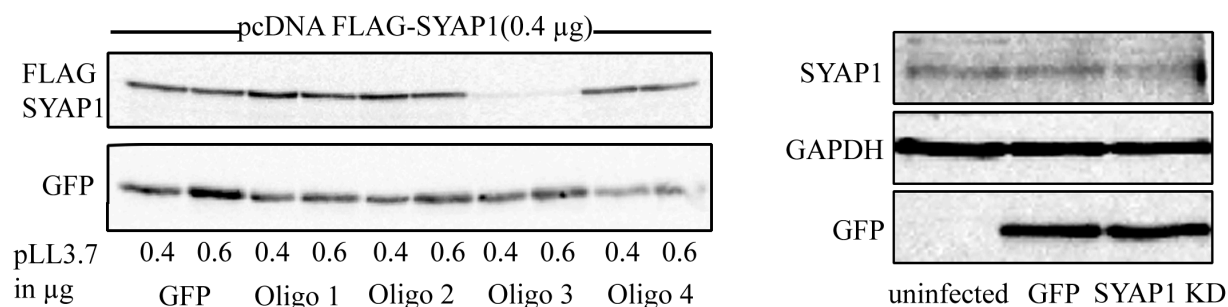


Figure 5.10.2: SYAP1 knockdown in primary motoneurons

(A) SYAP1 knockdown oligos were tested for its efficiency by co-transfection of pcDNA FLAG SYAP1 and pLL3.7 SYAP1 oligos in HEK 293T cells

(B) Lentivirus knockdown of SYAP1 (oligo 3) in primary motoneurons.

5.10.3 Colocalization of Tbce and SYAP1

Localization of TBCE in primary motoneurons was previously studied by Dr. Florian Bender (Bender FLP PhD thesis). TBCE was observed to be localized in centrosome, golgi apparatus, axon and also enriched in growth cone of primary motoneurons. To understand whether SYAP1 and TBCE colocalize with each other, primary motoneurons were stained with antibody against TBCE (rabbit anti-TBCE) and SYAP1 (mouse anti-SYAP1). Immunocytochemistry analysis showed that both TBCE and SYAP1 colocalize in distinct perinuclear region, supposedly in the golgi apparatus and are enriched in the growth cones of primary motoneurons pointing to an alternative function of TBCE other than its classical chaperone activity (Figure 5.10.3).

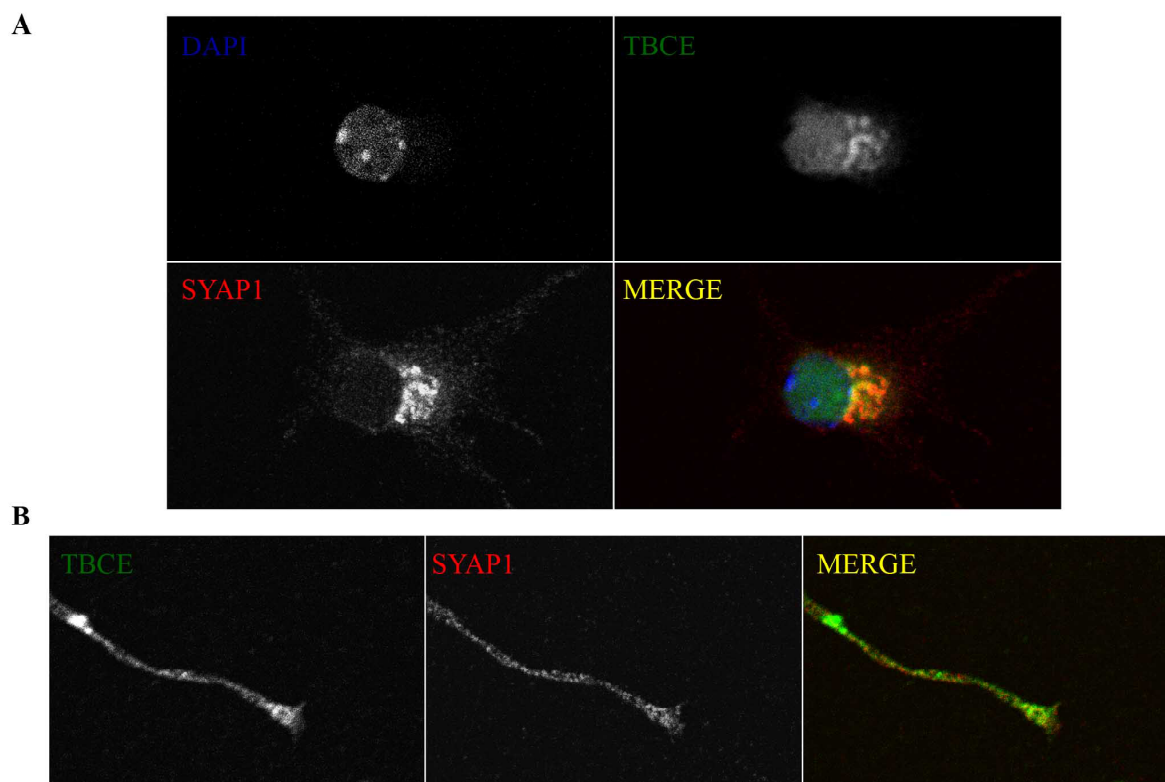


Figure 5.10.3: Co-localization of TBCE and SYAP1 in primary motoneurons

Primary motoneurons cultured for 5 DIV were labeled with rabbit TBCE and mouse SYAP1 antibody. Both proteins colocalized near the cell body presumably in the Golgi apparatus and are enriched in growth cones of axons of primary motoneurons.

5.10.4 SYAP1 interaction with TBCE

Since previous results through colocalization studies and Yeast 2 hybrid screens suggests that TBCE and SYAP1 might interact with each other, it was inevitable to study whether these protein interact through immunoprecipitation studies. Moreover, since TBCE mutation (TBCE^{W524G}) at the last amino acid causes progressive neurodegeneration in *pmn* mouse, it was analyzed if the mutation has any functional relevance in interaction with SYAP1. Immunoprecipitation study was performed in HEK 293T cells. HEK cells were over-expressed with FLAG-SYAP1 (pcDNA3) and HA-TBCE^{WT} (pcDNA3) or HA-TBCE^{W524G} (pcDNA3). Proteins were isolated and subjected to immunoprecipitation with anti-FLAG antibody. Western blot was performed using FLAG and HA antibodies to detect the amount of FLAG-SYAP1 and

HA-TBCE immunoprecipitated respectively. As shown in the figure 5.10.4, input levels of both FLAG-SYAP1 and HA-TBCE (wt and W524G) were similar in both conditions indicating equal amounts of protein were used for immunoprecipitation. Amount of FLAG-SYAP1 immunoprecipitated (eluate) were also similar in both the conditions validating equal amount of FLAG-SYAP1 has been immunoprecipitated by the anti-FLAG antibody. Westernblot analysis with anti-HA antibody showed TBCE is co-precipitated along with SYAP1. Interestingly, the interaction between TBCE^{W524G} and SYAP1 was reduced when compared to wildtype TBCE, indicating C-terminal region of TBCE is required for interaction with SYAP1. Absence of GAPDH in the eluate lanes showed the specificity of anti-FLAG antibody in immunoprecipitating the FLAG tagged proteins.

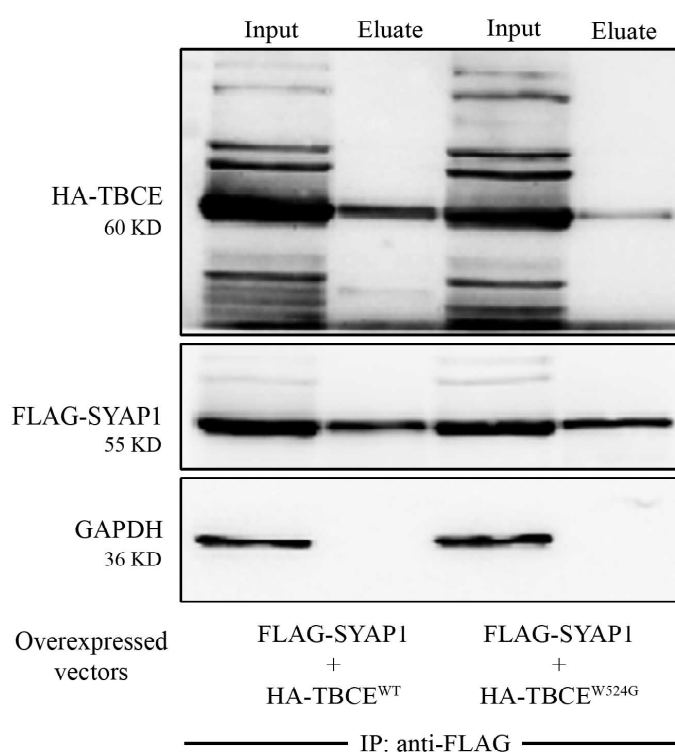


Figure 5.10.4: SYAP1 interaction with TBCE

Immunoprecipitation studies were performed in HEK 293T cells co-transfected with FLAG-SYAP1 and HA-TBCE (WT or W524G mutant). α -FLAG antibody was used to immunoprecipitate SYAP1. HA-TBCE was co-immunoprecipitated along with FLAG-SYAP1 and the interaction of FLAG-SYAP1 to HA-TBCE^{W524G} was reduced when compared to HA-TBCE^{WT}

6. DISCUSSION

Neurotrophic factors are a major class of growth factors, which influence proliferation, survival, and maintenance of neurons, differentiation and apoptosis of both neuronal and non-neuronal cells. They also regulate synaptic plasticity in mature neurons. In this present study, we investigated the mechanism how ciliary neurotrophic factor (CNTF), in contrast to other neurotrophic factors such as BDNF and GDNF, supports motoneuron axon maintenance in *progressive motor neuronopathy* mice, a model of motoneuron disease caused by a mutation in the *Tbce* gene. The *Tbce* gene codes for a chaperone that is involved in the formation of α/β -tubulin heterodimers. Activation of STAT3 by CNTF stimulates microtubule formation in *pnn* mutant motoneurons. Activated STAT3 sequesters Stathmin, a microtubule destabilizing protein that binds α/β -tubulin heterodimers (Ng et al., 2006), and thereby increases the availability of α/β -tubulin heterodimers for microtubule formation.

6.1 CNTF has a specific role in axon maintenance

Neurotrophic factors from several gene families, including BDNF, GDNF and CNTF have originally been identified as potent survival factors for embryonic motoneurons (Arakawa et al., 1990; Henderson et al., 1994; Sendtner et al., 1996; Sendtner et al., 1992a; Sendtner et al., 1990). These neurotrophic factors were able to prevent motoneuron cell death after nerve lesion in early stages after birth (Sendtner et al., 1990). Moreover, when both BDNF and GDNF were applied together survival of the motoneurons was increased reflecting the presence of an heterogeneous population of motoneurons in the spinal cord responding to different neurotrophic factors. (Vejsada et al., 1998). Although these neurotrophic factors converge similarly in survival of motoneurons during development and neonatal stage, they tend to differ in their capacity to maintain axons after injury. For instance, CNTF, but not other neurotrophic factors, such as bFGF, BDNF, GDNF, was not able to regenerate lesioned retinal ganglion cell axons (Cui et al.,

1999). Another recent study showed that Schwann cells localized CNTF compensates for loss of motoneurons in *Smn*^{+/-} mice, a mouse model of type-III SMA, by increasing axonal sprouting and thereby increase the size of motor units in skeletal muscle of *Smn*^{+/-} mice before the disease phenotype becomes apparent (Simon et al., 2010). It remained open from these studies whether signaling cascades for neuron survival and maintenance of axons are similar. Treatment of *pnn* mutant mice with CNTF or GDNF results in different effects on survival of these mice, despite similar survival effects these two neurotrophic factors for motoneuron cell bodies (Sagot et al., 1996; Sendtner et al., 1992b). This distinct and specific effect of CNTF but not GDNF was the basis of our study with *pnn* mutant mice that was designed to understand the mechanism how CNTF treatment results in axon maintenance.

Primary motoneurons from *pnn* mutant mice exhibit shorter axons with increased number of axonal swellings when compared to wildtype motoneurons (Bommel et al., 2002). All three neurotrophic factors (BDNF, CNTF, GDNF) investigated in this study were potent for survival of *pnn* mutant motoneurons. Interestingly, similar to the *in-vivo* observation, CNTF but not BDNF or GDNF was able to rescue axon elongation *in-vitro* (Figure 5.1.1 and 5.1.2). This points to a specific role of CNTF in axonal maintenance of primary motoneurons. CNTF is expressed in Schwann cells of the peripheral nervous system and in astrocytes of central nervous system (Sendtner et al., 1992c; Stockli et al., 1991). Expression of CNTF is observed around first postnatal week and reaches a maximum by 4 weeks after birth correlating with the maturation of Schwann cells. The amount of CNTF produced by Schwann cells in the peripheral nervous system did not differ between 4 week old wildtype and *pnn* mutant mice (Sendtner et al., 1997). This opened a question why endogenous CNTF produced by *pnn* mice could not rescue the observed motoneuron degeneration. The plausible explanation for this is that the CNTF that is expressed in Schwann cells at 4 weeks after birth is not available to degenerating motoneurons and thus cannot to overcome the symptoms observed in this mouse model. This can only be

explained by the fact that CNTF is not secreted by Schwann cells at sufficient amounts. CNTF is a soluble protein lacking a conventional hydrophobic leader sequence and therefore seems to be released at high amounts only after injury (Stockli et al., 1991). Alternatively, when *pmn* mice were treated with NGF leader sequence /CNTF expressing D3 cells at postnatal day 20 the survival of the mice was prolonged when compared to untreated littermates (Sendtner et al., 1992b) indicating that CNTF is a lesion factor.

4.2 Local function of STAT3 is necessary for CNTF mediated axon outgrowth in *pmn* motoneurons

CNTF binds to a tripartite receptor complex containing LIFR β , GP130 and CNTFR α and activates signal transduction through the transcription factor STAT3 (Stahl et al., 1995). Conditional ablation of STAT3 in motoneurons does not have influence on survival of spinal motoneurons during embryonic development and after birth. However, after axotomy STAT3 is necessary for survival (Schweizer et al., 2002) and axon regeneration (Sun et al., 2011) of neurons in the peripheral nervous system. Recent studies have shown that transcriptional effects of STAT3 through upregulation of Bcl-xl and Reg-2 expression is required for survival of facial motoneurons (Schweizer et al., 2002) and dorsal root ganglionic neurons after axotomy (Ben-Yaakov et al., 2012; Nishimune et al., 2000). Nevertheless, it remained open whether transcriptional effects of STAT3 are required for axon regeneration and maintenance. In cultured primary motoneurons CNTF mediated STAT3 at tyrosine 705, surprisingly did not lead to nuclear accumulation of activated STAT3. As shown by nuclear fractionation of primary motoneurons, most of the activated STAT3 was observed in the cytoplasm at any point of time and was not transported to the nucleus (Selvaraj et al., 2012). These results indicated that an alternative cytoplasmic function of STAT3 might be responsible for STAT3 dependent axon growth in *pmn* mutant motoneurons.

CNTF mediated rescue of axon outgrowth in *pmn* mutant motoneurons was dependent on STAT3. STAT3^{KO};*pmn* motoneurons exhibited short axons. Lentiviral over-expression of either wildtype STAT3 or DNA binding mutant of STAT3 in STAT3 deficient motoneurons did not abolish the effects of CNTF on axon growth in *pmn* mutant motoneurons. Interestingly, in the absence of CNTF both over-expression of wildtype and DNA binding mutant STAT3 marginally increased axon length of STAT3^{KO};*pmn* motoneurons. The observed increase was statistically significant, $p < 0.05$, (although significantly shorter than wildtype motoneurons). This moderate increase reflects a rescue effect of STAT3, signifying that STAT3 is important for axon elongation in primary motoneurons. However, phosphorylation of STAT3 was important for the rescue of axon elongation observed in *pmn* mutant motoneurons. Over-expression of tyrosine phosphorylation mutant of STAT3 in STAT3^{KO};*pmn* motoneurons did not increase axon elongation. Moreover the tyrosine mutant of STAT3 was observed to be dominant negative as it reduced the effect of endogenous STAT3 protein on axon elongation of wildtype motoneurons.

A Cytoplasmic function of STAT3 has been reported in few recent studies, cytoplasmic STAT3 is involved in regulating synaptic plasticity in the hippocampus (Nicolas et al., 2012) although its mechanism of function still remains elusive. Another study by Verma et al., showed that STAT3 interaction with Stathmin was critical for T-cell migration (Verma et al., 2009). Taken together, these studies suggest that local signaling pathways could be involved for STAT3 effects on axon stability and maintenance.

6.3 Stathmin - a downstream target of STAT3

Stathmin is a member of a family of microtubule destabilizing proteins; other members include superior cervical ganglion protein 10 (SCG10), SCG10 like protein (SCLIP) and RB3, all sharing a conserved C-terminal domain and an amino terminal domain of varying lengths (Charbaut et al., 2001). Stathmin functions primarily in binding to two molecules of α/β tubulin heterodimers and sequestering them from microtubule polymerization. p-STAT3^{Y705}-Stathmin

interaction has been observed upon cytokine stimulation in a number of cell types, including T-lymphocytes (Verma et al., 2009) and various cell lines (Ng et al., 2006). These studies showed that STAT3, when over-expressed together with Stathmin, binds to its C-terminus, the same region that also interacts with tubulin heterodimers (Ng et al., 2006). Our results from primary motoneurons confirm that STAT3 and Stathmin interact with each other in a phosphorylation dependent manner. Since STAT3 binds to the C-terminal end of Stathmin, the same region where tubulin heterodimers, it is likely both STAT3 and tubulin heterodimers compete with each other for binding with Stathmin. This was evident in our co-immunoprecipitation analysis. After CNTF treatment Stathmin interaction with tubulin was reduced by 40%. The released tubulin heterodimers from Stathmin presumably increases the pool of available tubulin dimers for polymerization of microtubules and thereby shifting the dynamics towards polymerization. Alternatively, when Stathmin was depleted from *pmn* mutant primary motoneurons, axon outgrowth was rescued to wildtype levels. The fact that we did not observe an additional effect upon CNTF treatment suggests that Stathmin is the downstream molecule of CNTF-STAT3 mediated axon elongation in *pmn* mutant motoneurons. Surprisingly, depletion of Stathmin in wildtype motoneurons did not enhance axon growth suggesting that Stathmin dependent tubulin dynamics is tightly regulated to maintain the status quo. Recent studies showed that over-expression of Tbc1e and Tbc1e like protein degrades tubulin heterodimers (Bartolini et al., 2005; Voloshin et al., 2010) and that Stathmin counteracts and protects the degradation of tubulin heterodimers (Sellin et al., 2008). Stathmin depletion thus shifts the balance between preservation of α/β -tubulin heterodimers to degradation. Our study and previous studies have identified that the mutation caused in *Tbce* gene in *pmn* mice renders TBCE protein unstable and prone to proteasomal degradation (Martin et al., 2002) when compared to the wildtype TBCE. This could explain why effect of Stathmin depletion on axon outgrowth is highly pronounced in *pmn* mutant motoneurons.

6.4 Role of Stathmin in neuronal differentiation

Recent reports suggested that Stathmin is involved in maintenance of axons and neuromuscular junctions and that disturbances of Stathmin function are also associated with different neurodegenerative processes in disease models. Despite Stathmin is expressed in higher levels during development, Stathmin^{-/-} mice did not show any development phenotype. However, Stathmin^{-/-} adult mice develop both central and peripheral axonopathy suggesting Stathmin could play a major role in axon maintenance (Liedtke et al., 2002). Stathmin null mutants in *Drosophila melanogaster* exhibit synapse retraction and reduced size of NMJ (Graf et al., 2011). On the contrary, in the Smn^{-/-};SMN2 mouse model of spinal muscular atrophy where impaired maturation of NMJ is also observed Stathmin levels were significantly upregulated in both central and peripheral nervous system (Wen et al., 2010). In this present study, we did not find difference in expression of Stathmin in *pmn* mutant motoneurons. These discrepancies indicate that Stathmin dynamics are tightly regulated and play a vital role in axon maintenance. Moreover, additional regulatory mechanism might be involved in fine-tuning Stathmin activity. One such regulatory mechanism is the phosphorylation of Stathmin by serine kinases at 4 different sites (Curmi et al., 1999). Stathmin phosphorylation inactivates its microtubule destabilizing activity and thereby plays an essential role in neuronal polarity and other developmental aspects in neurons. Two recent studies have shown inactivation of Stathmin by serine phosphorylation is vital for generating normal axons and dendrites in hippocampal neurons and essential for inducing axonal branching. Stathmin phosphorylation in a Rac dependent manner via DOCK7 in the leading edge of axonal tips is necessary to form polarized neurons (Watabe-Uchida et al., 2006). Similarly, BDNF induced axon branching in cortical neurons by MAP kinase phosphatase-1 involves downstream suppression of Stathmin activity by negatively regulating c-Jun N-terminal Kinase (Jeanneteau et al., 2010). In summary, regulation of Stathmin by altering expression level or inactivation of its activity by phosphorylation is key in development of axons and forming proper synaptic contacts.

6.5 Microtubule dynamics in neurodegenerative diseases

Microtubules dynamics play a vital role in many neurodegenerative diseases. Altered axonal microtubule dynamics was reported in sciatic nerve, spinal cord and cortex of SOD1^{G93A} mouse model of ALS. Moreover, when SOD1^{G93A} mice were treated with noscapine, a microtubule-modulating agent, delayed the onset of symptoms while prolonging survival (Fanara et al., 2007). Similarly stabilization of microtubules by paclitaxel increases total polymerized tubulin and decreases tyrosinated tubulin after axonal lesion, and thus promotes regeneration of dorsal root sensory nerve fibers after spinal cord lesion (Hellal et al., 2011). These findings indicate that mechanisms modifying the turnover and stability of microtubules could play a central role under conditions when axons regenerate and possibly also under conditions of axonal degeneration, such as in motoneuron disease. In *pnn* mutant motoneurons, we observed enhanced level of tyrosinated tubulin in axons, a marker for highly dynamic and newly synthesized tubulin, and it was normalized to wildtype level upon treatment with either CNTF or by depleting its downstream target Stathmin.

Similarly, our data and previous work from Schaefer et al., also confirmed that the amount of soluble unpolymerized tubulin was increased in *pnn* mutant motoneurons and in TBCE depleted NSC34 cells (Schaefer et al., 2007). These results suggest that microtubule dynamics is impaired in *pnn* motoneurons. Moreover, application of paclitaxel rescued axon elongation in *pnn* motoneurons indicating that microtubule stabilization is sufficient that STAT3-Stathmin interaction could alter the dynamics of microtubules towards polymerization, thus increasing axon growth, stabilization and maintenance.

6.6 Microtubule dynamics observed in *pmn* mutant motoneurons

The *in-vitro* microtubule growth assay used in our study (Selvaraj et al., 2012) is a fast and a precise tool to study microtubule dynamics in isolated *pmn* motoneurons. It allows to assess the rate of microtubule polymerization. In *pmn* mutant motoneurons the rate of α/β heterodimer formation is impaired due to reduced amount of functional TBCE. This is reflected in the microtubule regrowth assay, as the number of microtubules emanating from MTOC and the length of the polymerized microtubule in *pmn* motoneurons were lower when compared to wildtype motoneurons (Schaefer et al., 2007; Selvaraj et al., 2012). A distinct fraction of α/β heterodimers is bound to Stathmin. Since the amount of Stathmin is not dysregulated in *pmn* motoneurons, it is likely that similar proportion of α/β tubulin heterodimers are bound to Stathmin in wildtype and *pmn* motoneurons and that remaining α/β tubulin heterodimers are freely available for microtubule polymerization. Therefore, the amount of freely available α/β tubulin heterodimers is reduced in *pmn* mutant motoneurons. CNTF addition activates STAT3 phosphorylation, subsequent interaction of p-STAT3 with Stathmin releases bound α/β heterodimers, thereby increasing the pool of available α/β heterodimers for polymerization and this induces increased number and average length of polymerized microtubules. STAT3 depleted motoneurons also showed reduced numbers of polymerized microtubules due reduced Stathmin interaction. Thus α/β tubulin heterodimers are not released for polymerization. Therefore, enriching the freely available pool of α/β heterodimers either by normalized activity of TBCE or release of bound α/β heterodimers from Stathmin induces microtubule polymerization. These two mechanisms are independent of each other as $STAT3^{FL/KO};pmn$ motoneurons showed further reduction in number of polymerized microtubules formed when compared to $STAT3^{KO}$ and *pmn* motoneurons (Figure 6.1).

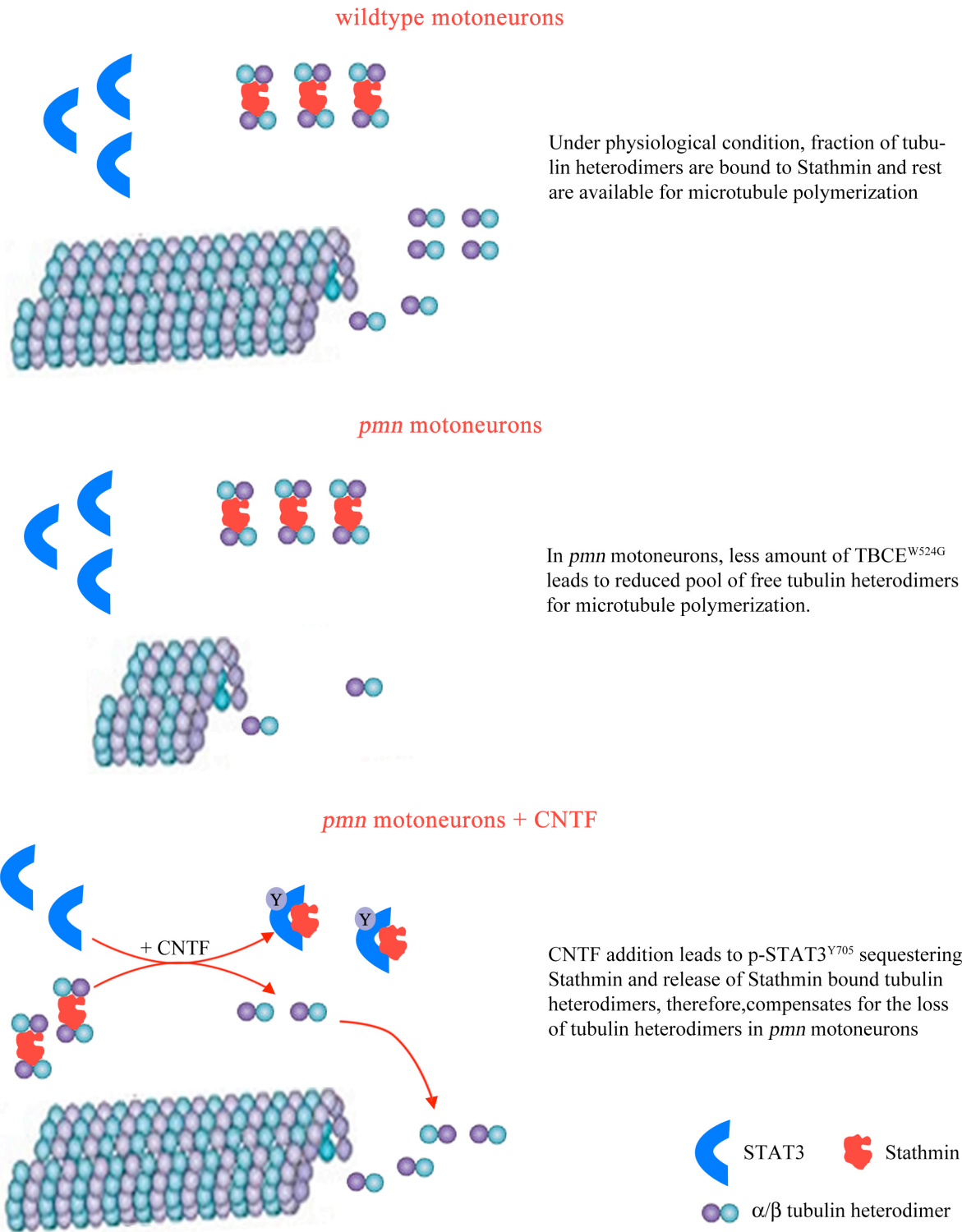


Figure 6.1: Scheme of CNTF mediated microtubules observed in *pmn* mutant motoneurons

6.7 TBCE^{W524G} protein is functional but highly unstable

Tubulin binding chaperone E is an important protein for generation of tubulin heterodimers. TBCE along with TBCB binds to α -tubulin and functions as a chaperone in formation of α/β tubulin heterodimers (Tian et al., 1996). Microtubule formation is critical in various cellular events such as mitosis, maintenance of cellular architecture, transport etc. The mutation in the *Tbce* gene that is responsible for the disease is found in the last coding exon and leads to an amino acid exchange from tryptophan to glycine (TBCE^{W524G}). Our data and previous study has shown that the mutant TBCE (TBCE^{W524G}) is highly unstable (Martin et al., 2002) and is degraded by proteasome dependent degradation, and therefore results in instable microtubules that cause a neurodegenerative disease that predominantly affects motoneurons. It is still unclear why this mutation in *Tbce* gene affects motoneurons predominantly and not the other type of cells. Interestingly, over-expression of mutant TBCE^{W524G} in *pnn* mutant motoneurons was sufficient for normalizing axon outgrowth to the same levels as observed in cultured wildtype motoneurons (Bender FLP, Ph.D thesis) indicating that the amount of TBCE^{W524G} is critical in *pnn* mutant motoneurons and that the enzymatic function is still retained. This could explain why the mutation in *Tbce* gene affects motoneurons specifically and not the other type of cells. One possibility could be that the amount of α/β tubulin heterodimers required for motoneuron is higher when compared to other proliferating cells. Therefore, when the amount of TBCE^{W524G} is too low in *pnn* mutant motoneurons this results in less α/β tubulin heterodimers in proximal part of axons and less axon growth (Selvaraj et al., 2012). The same mutation or mutations in the last coding exon of *TBCE* were not observed in more than 700 patients with sporadic and familial forms of motoneuron disease (M. Beck, F. Bender and M. Sendtner, unpublished results). Therefore, mutation in *Tbce* gene in *pnn* mice provides a valuable model to study the role of microtubules in motoneuron diseases.

6.8 Possible role of TBCE in synapse maintenance

Microtubules and microfilaments are the main source of anchor for synaptic vesicles in the pre-synaptic compartment and also essential for release of neurotransmitters into the synaptic cleft. Depolymerization of microtubule and microfilaments by colchicine and cytochalasin-D respectively, attenuates tetanus toxin induced blockage of neurotransmitter release (Ashton and Dolly, 1997) suggesting that alterations of microtubule and microfilament dynamics are prerequisite for release of bound synaptic vesicles. *Drosophila* TBCE in presynaptic neurons regulates NMJ development and its precise expression is necessary for neurotransmission (Jin et al., 2009). Interaction of the presynaptic protein SAP47 with TBCE like (E-Like) protein in *Drosophila* led to this study to identify whether TBCE has another novel role in synapse maturation or neurotransmitter release. Preliminary work performed in this study shows that SYAP1, mouse homologue of SAP47, is expressed in motoneurons and localized in the golgi apparatus as well as in axons and it is also enriched in growth cones. The mouse anti-serum generated by Dr. N.Funk was specific and detected SYAP1 protein at a size of 55 kDa. We also tested another commercial antibody from SIGMA due to the scarce availability of mouse anti-serum. This antibody also detected a 55 kDa band and an additional unknown 40 kDa band. Further analysis has to be performed to check the specificity of this antibody. Our data also confirms interaction of SYAP1 with TBCE. Interestingly this interaction is weaker with mutant TBCE possibly due to the structural alteration in mutant TBCE. It would be interesting to know whether TBCE has a novel function in synapse. Using lentiviral knockdown of SYAP1 generated in this study, it will be feasible to study the function of the SYAP1 protein in this context. One such functional study would be to study the role of SYAP1 and TBCE in synaptic vesicle recycling using FM1-43 lipophilic dye in motoneurons or hippocampal neurons. Recent report has elucidated a functional role of SYAP1 in stimulating growth factor dependent adipocyte differentiation by promoting mTORC2 mediated phosphorylation of Akt (Yao et al., 2013). SYAP1 interacts with mTORC2 and Akt and facilitates Akt phosphorylation at serine

473. mTORC2 has been shown as a key regulator in polarization of actin cytoskeleton (Liu et al., 2010). These findings suggest that SYAP1 might be a key signaling molecule mediating growth factor induced receptor tyrosine kinase signaling in altering actin cytoskeleton and synaptic plasticity.

7. REFERENCE

- Adler, R., K.B. Landa, M. Manthorpe, and S. Varon. 1979. Cholinergic neuronotrophic factors: intraocular distribution of trophic activity for ciliary neurons. *Science*. 204:1434-1436.
- Ahmad, F.J., and P.W. Baas. 1995. Microtubules released from the neuronal centrosome are transported into the axon. *J Cell Sci*. 108 (Pt 8):2761-2769.
- Akira, S., Y. Nishio, M. Inoue, X.J. Wang, S. Wei, T. Matsusaka, K. Yoshida, T. Sudo, M. Naruto, and T. Kishimoto. 1994. Molecular cloning of APRF, a novel IFN-stimulated gene factor 3 p91-related transcription factor involved in the gp130-mediated signaling pathway. *Cell*. 77:63-71.
- Andrus, P.K., T.J. Fleck, M.E. Gurney, and E.D. Hall. 1998. Protein oxidative damage in a transgenic mouse model of familial amyotrophic lateral sclerosis. *J Neurochem*. 71:2041-2048.
- Arakawa, Y., M. Sendtner, and H. Thoenen. 1990. Survival effect of ciliary neurotrophic factor (CNTF) on chick embryonic motoneurons in culture: comparison with other neurotrophic factors and cytokines. *J Neurosci*. 10:3507-3515.
- Ashton, A.C., and J.O. Dolly. 1997. Microtubules and microfilaments participate in the inhibition of synaptosomal noradrenaline release by tetanus toxin. *J Neurochem*. 68:649-658.
- Atlas, R., L. Behar, E. Elliott, and I. Ginzburg. 2004. The insulin-like growth factor mRNA binding-protein IMP-1 and the Ras-regulatory protein G3BP associate with tau mRNA and HuD protein in differentiated P19 neuronal cells. *J Neurochem*. 89:613-626.
- Barra, H.S., J.A. Rodriguez, C.A. Arce, and R. Caputto. 1973. A soluble preparation from rat brain that incorporates into its own proteins (14 C)arginine by a ribonuclease-sensitive system and (14 C)tyrosine by a ribonuclease-insensitive system. *J Neurochem*. 20:97-108.
- Bartolini, F., G. Tian, M. Piehl, L. Cassimeris, S.A. Lewis, and N.J. Cowan. 2005. Identification of a novel tubulin-destabilizing protein related to the chaperone cofactor E. *J Cell Sci*. 118:1197-1207.
- Bazan, J.F. 1990. Structural design and molecular evolution of a cytokine receptor superfamily. *Proc Natl Acad Sci U S A*. 87:6934-6938.
- Bazan, J.F. 1991. Neuropoietic cytokines in the hematopoietic fold. *Neuron*. 7:197-208.
- Beal, M.F., R.J. Ferrante, S.E. Browne, R.T. Matthews, N.W. Kowall, and R.H. Brown, Jr. 1997. Increased 3-nitrotyrosine in both sporadic and familial amyotrophic lateral sclerosis. *Ann Neurol*. 42:644-654.

- Ben-Yaakov, K., S.Y. Dagan, Y. Segal-Ruder, O. Shalem, D. Vuppalachchi, D.E. Willis, D. Yudin, I. Rishal, F. Rother, M. Bader, A. Blesch, Y. Pilpel, J.L. Twiss, and M. Fainzilber. 2012. Axonal transcription factors signal retrogradely in lesioned peripheral nerve. *EMBO J.* 31:1350-1363.
- Beretta, L., T. Dobransky, and A. Sobel. 1993. Multiple phosphorylation of stathmin. Identification of four sites phosphorylated in intact cells and in vitro by cyclic AMP-dependent protein kinase and p34cdc2. *J Biol Chem.* 268:20076-20084.
- Bommel, H., G. Xie, W. Rossoll, S. Wiese, S. Jablonka, T. Boehm, and M. Sendtner. 2002. Missense mutation in the tubulin-specific chaperone E (Tbce) gene in the mouse mutant progressive motor neuronopathy, a model of human motoneuron disease. *J Cell Biol.* 159:563-569.
- BROOKES, B.R., M. SANJAK, H. MITSUMOTO, K. SZIRONY, H. NEVILLE, S. RINGEL, J. BRJNKMANN, A. PESTRONK, J. FLORENCE, J. CEDARBAUM, C. M., N. STAMBLER, J. WITTES, and E. BRITAIN. 1993a. Recombinant human ciliary neurotrophic factor (rhCNTF) In amyotrophic lateral sclerosis (ALS) patients: Dose selection strategy in phase I-II safety, tolerability and pharmacokinetic studies. *Can.J. Neurol. Sci.* 20:83.
- BROOKES, B.R., M. SANJAK, H. MITSUMOTO, K. SZIRONY, H. NEVILLE, S. RINGEL, J. BRJNKMANN, A. PESTRONK, J. FLORENCE, J. CEDARBAUM, C. M., N. STAMBLER, J. WITTES, and E. BRITAIN. 1993b. Recombinant human ciliary neurotrophic factor (rhCNTF) In amyotrophic lateral sclerosis (ALS) patients: Dose selection strategy in phase I-II safety, tolerability and pharmacokinetic studies. *Can.J. Neurol. Sci.* 20:83.
- Bruijn, L.I., M.W. Becher, M.K. Lee, K.L. Anderson, N.A. Jenkins, N.G. Copeland, S.S. Sisodia, J.D. Rothstein, D.R. Borchelt, D.L. Price, and D.W. Cleveland. 1997. ALS-linked SOD1 mutant G85R mediates damage to astrocytes and promotes rapidly progressive disease with SOD1-containing inclusions. *Neuron.* 18:327-338.
- Burghes, A.H., and C.E. Beattie. 2009. Spinal muscular atrophy: why do low levels of survival motor neuron protein make motor neurons sick? *Nat Rev Neurosci.* 10:597-609.
- Bussaglia, E., O. Clermont, E. Tizzano, S. Lefebvre, L. Burglen, C. Cruaud, J.A. Urtizbarea, J. Colomer, A. Munnich, M. Baiget, and et al. 1995. A frame-shift deletion in the survival motor neuron gene in Spanish spinal muscular atrophy patients. *Nat Genet.* 11:335-337.
- Carrel, T.L., M.L. McWhorter, E. Workman, H. Zhang, E.C. Wolstencroft, C. Lorson, G.J. Bassell, A.H. Burghes, and C.E. Beattie. 2006. Survival motor neuron function in motor axons is independent of functions required for small nuclear ribonucleoprotein biogenesis. *J Neurosci.* 26:11014-11022.
- Cashman, N.R., H.D. Durham, J.K. Blusztajn, K. Oda, T. Tabira, I.T. Shaw, S. Dahrouge, and J.P. Antel. 1992. Neuroblastoma x spinal cord (NSC) hybrid cell lines resemble developing motor neurons. *Dev Dyn.* 194:209-221.

- Charbaut, E., P.A. Curmi, S. Ozon, S. Lachkar, V. Redeker, and A. Sobel. 2001. Stathmin family proteins display specific molecular and tubulin binding properties. *J Biol Chem.* 276:16146-16154.
- Chen, Y.Z., C.L. Bennett, H.M. Huynh, I.P. Blair, I. Puls, J. Irobi, I. Dierick, A. Abel, M.L. Kennerson, B.A. Rabin, G.A. Nicholson, M. Auer-Grumbach, K. Wagner, P. De Jonghe, J.W. Griffin, K.H. Fischbeck, V. Timmerman, D.R. Cornblath, and P.F. Chance. 2004. DNA/RNA helicase gene mutations in a form of juvenile amyotrophic lateral sclerosis (ALS4). *Am J Hum Genet.* 74:1128-1135.
- Christensen, P.B., E. Hojer-Pedersen, and N.B. Jensen. 1990. Survival of patients with amyotrophic lateral sclerosis in 2 Danish counties. *Neurology.* 40:600-604.
- Conde, C., and A. Caceres. 2009. Microtubule assembly, organization and dynamics in axons and dendrites. *Nat Rev Neurosci.* 10:319-332.
- Creppe, C., L. Malinouskaya, M.L. Volvert, M. Gillard, P. Close, O. Malaise, S. Laguesse, I. Cornez, S. Rahmouni, S. Ormenese, S. Belachew, B. Malgrange, J.P. Chapelle, U. Siebenlist, G. Moonen, A. Chariot, and L. Nguyen. 2009. Elongator controls the migration and differentiation of cortical neurons through acetylation of alpha-tubulin. *Cell.* 136:551-564.
- Cui, Q., Q. Lu, K.F. So, and H.K. Yip. 1999. CNTF, not other trophic factors, promotes axonal regeneration of axotomized retinal ganglion cells in adult hamsters. *Invest Ophthalmol Vis Sci.* 40:760-766.
- Curmi, P.A., S.S. Andersen, S. Lachkar, O. Gavet, E. Karsenti, M. Knossow, and A. Sobel. 1997. The stathmin/tubulin interaction in vitro. *J Biol Chem.* 272:25029-25036.
- Curmi, P.A., O. Gavet, E. Charbaut, S. Ozon, S. Lachkar-Colmerauer, V. Manceau, S. Siavoshian, A. Maucuer, and A. Sobel. 1999. Stathmin and its phosphoprotein family: general properties, biochemical and functional interaction with tubulin. *Cell Struct Funct.* 24:345-357.
- Dale, J.M., H. Shen, D.M. Barry, V.B. Garcia, F.F. Rose, Jr., C.L. Lorson, and M.L. Garcia. 2011. The spinal muscular atrophy mouse model, SMADelta7, displays altered axonal transport without global neurofilament alterations. *Acta Neuropathol.* 122:331-341.
- Darnell, J.E., Jr., I.M. Kerr, and G.R. Stark. 1994. Jak-STAT pathways and transcriptional activation in response to IFNs and other extracellular signaling proteins. *Science.* 264:1415-1421.
- Davis, S., T.H. Aldrich, N. Stahl, L. Pan, T. Taga, T. Kishimoto, N.Y. Ip, and G.D. Yancopoulos. 1993. LIFR beta and gp130 as heterodimerizing signal transducers of the tripartite CNTF receptor. *Science.* 260:1805-1808.
- Davis, S., T.H. Aldrich, D.M. Valenzuela, V.V. Wong, M.E. Furth, S.P. Squinto, and G.D. Yancopoulos. 1991. The receptor for ciliary neurotrophic factor. *Science.* 253:59-63.

- DeChiara, T.M., R. Vejsada, W.T. Poueymirou, A. Acheson, C. Suri, J.C. Conover, B. Friedman, J. McClain, L. Pan, N. Stahl, N.Y. Ip, and G.D. Yancopoulos. 1995. Mice lacking the CNTF receptor, unlike mice lacking CNTF, exhibit profound motor neuron deficits at birth. *Cell*. 83:313-322.
- DeJesus-Hernandez, M., I.R. Mackenzie, B.F. Boeve, A.L. Boxer, M. Baker, N.J. Rutherford, A.M. Nicholson, N.A. Finch, H. Flynn, J. Adamson, N. Kouri, A. Wojtas, P. Sengdy, G.Y. Hsiung, A. Karydas, W.W. Seeley, K.A. Josephs, G. Coppola, D.H. Geschwind, Z.K. Wszolek, H. Feldman, D.S. Knopman, R.C. Petersen, B.L. Miller, D.W. Dickson, K.B. Boylan, N.R. Graff-Radford, and R. Rademakers. 2011. Expanded GGGGCC hexanucleotide repeat in noncoding region of C9ORF72 causes chromosome 9p-linked FTD and ALS. *Neuron*. 72:245-256.
- Di Paolo, G., B. Antonsson, D. Kassel, B.M. Riederer, and G. Grenningloh. 1997. Phosphorylation regulates the microtubule-destabilizing activity of stathmin and its interaction with tubulin. *FEBS Lett*. 416:149-152.
- Donaghy, M. 1999. Classification and clinical features of motor neurone diseases and motor neuropathies in adults. *J Neurol*. 246:331-333.
- Drepper, C., T. Herrmann, C. Wessig, M. Beck, and M. Sendtner. 2011. C-terminal FUS/TLS mutations in familial and sporadic ALS in Germany. *Neurobiol Aging*. 32:548 e541-544.
- DuBridg, R.B., P. Tang, H.C. Hsia, P.M. Leong, J.H. Miller, and M.P. Calos. 1987. Analysis of mutation in human cells by using an Epstein-Barr virus shuttle system. *Mol Cell Biol*. 7:379-387.
- Falconer, M.M., U. Vielkind, and D.L. Brown. 1989. Establishment of a stable, acetylated microtubule bundle during neuronal commitment. *Cell Motil Cytoskeleton*. 12:169-180.
- Fallini, C., G.J. Bassell, and W. Rossoll. 2012. Spinal muscular atrophy: the role of SMN in axonal mRNA regulation. *Brain Res*. 1462:81-92.
- Fanara, P., J. Banerjee, R.V. Hueck, M.R. Harper, M. Awada, H. Turner, K.H. Husted, R. Brandt, and M.K. Hellerstein. 2007. Stabilization of hyperdynamic microtubules is neuroprotective in amyotrophic lateral sclerosis. *J Biol Chem*. 282:23465-23472.
- Ferraiuolo, L., J. Kirby, A.J. Grierson, M. Sendtner, and P.J. Shaw. 2011. Molecular pathways of motor neuron injury in amyotrophic lateral sclerosis. *Nat Rev Neurol*. 7:616-630.
- Ferrante, R.J., S.E. Browne, L.A. Shinobu, A.C. Bowling, M.J. Baik, U. MacGarvey, N.W. Kowall, R.H. Brown, Jr., and M.F. Beal. 1997. Evidence of increased oxidative damage in both sporadic and familial amyotrophic lateral sclerosis. *J Neurochem*. 69:2064-2074.
- Fink, J.K., S.M. Jones, G.B. Sharp, B.M. Lange, B. Otterud, and M. Leppert. 1996. Hereditary spastic paraplegia linked to chromosome 15q: Analysis of candidate genes. *Neurology*. 46:835-836.

- Friedman, B., S.S. Scherer, J.S. Rudge, M. Helgren, D. Morrissey, J. McClain, D.Y. Wang, S.J. Wiegand, M.E. Furth, R.M. Lindsay, and et al. 1992. Regulation of ciliary neurotrophic factor expression in myelin-related Schwann cells in vivo. *Neuron*. 9:295-305.
- Gabanella, F., M.E. Butchbach, L. Saieva, C. Carissimi, A.H. Burghes, and L. Pellizzoni. 2007. Ribonucleoprotein assembly defects correlate with spinal muscular atrophy severity and preferentially affect a subset of spliceosomal snRNPs. *PLoS One*. 2:e921.
- Gao, Y., I.E. Vainberg, R.L. Chow, and N.J. Cowan. 1993. Two cofactors and cytoplasmic chaperonin are required for the folding of alpha- and beta-tubulin. *Mol Cell Biol*. 13:2478-2485.
- Glinka, M., T. Herrmann, N. Funk, S. Havlicek, W. Rossoll, C. Winkler, and M. Sendtner. 2010. The heterogeneous nuclear ribonucleoprotein-R is necessary for axonal beta-actin mRNA translocation in spinal motor neurons. *Hum Mol Genet*. 19:1951-1966.
- Gotz, R., S. Wiese, S. Takayama, G.C. Camarero, W. Rossoll, U. Schweizer, J. Troppmair, S. Jablonka, B. Holtmann, J.C. Reed, U.R. Rapp, and M. Sendtner. 2005. Bag1 is essential for differentiation and survival of hematopoietic and neuronal cells. *Nat Neurosci*. 8:1169-1178.
- Gouilleux-Gruart, V., F. Gouilleux, C. Desaint, J.F. Claisse, J.C. Capiod, J. Delobel, R. Weber-Nordt, I. Dusanter-Fourt, F. Dreyfus, B. Groner, and L. Prin. 1996. STAT-related transcription factors are constitutively activated in peripheral blood cells from acute leukemia patients. *Blood*. 87:1692-1697.
- Graf, E.R., H.M. Heerssen, C.M. Wright, G.W. Davis, and A. DiAntonio. 2011. Stathmin is required for stability of the *Drosophila* neuromuscular junction. *J Neurosci*. 31:15026-15034.
- Grynberg, M., L. Jaroszewski, and A. Godzik. 2003. Domain analysis of the tubulin cofactor system: a model for tubulin folding and dimerization. *BMC Bioinformatics*. 4:46.
- Gu, W., F. Pan, H. Zhang, G.J. Bassell, and R.H. Singer. 2002. A predominantly nuclear protein affecting cytoplasmic localization of beta-actin mRNA in fibroblasts and neurons. *J Cell Biol*. 156:41-51.
- Gurney, M.E., H. Pu, A.Y. Chiu, M.C. Dal Canto, C.Y. Polchow, D.D. Alexander, J. Caliendo, A. Hentati, Y.W. Kwon, H.X. Deng, and et al. 1994. Motor neuron degeneration in mice that express a human Cu,Zn superoxide dismutase mutation. *Science*. 264:1772-1775.
- Haase, G., P. Kennel, B. Pettmann, E. Vigne, S. Akli, F. Revah, H. Schmalbruch, and A. Kahn. 1997. Gene therapy of murine motor neuron disease using adenoviral vectors for neurotrophic factors. *Nat Med*. 3:429-436.
- Hafezparast, M., R. Klocke, C. Ruhrberg, A. Marquardt, A. Ahmad-Annur, S. Bowen, G. Lalli, A.S. Witherden, H. Hummerich, S. Nicholson, P.J. Morgan, R. Oozageer, J.V. Priestley, S. Averill, V.R. King, S. Ball, J. Peters, T. Toda, A. Yamamoto, Y. Hiraoka, M.

- Augustin, D. Korthaus, S. Wattler, P. Wabnitz, C. Dickneite, S. Lampel, F. Boehme, G. Peraus, A. Popp, M. Rudelius, J. Schlegel, H. Fuchs, M. Hrabe de Angelis, G. Schiavo, D.T. Shima, A.P. Russ, G. Stumm, J.E. Martin, and E.M. Fisher. 2003. Mutations in dynein link motor neuron degeneration to defects in retrograde transport. *Science*. 300:808-812.
- Hahnen, E., I.Y. Eyupoglu, L. Brichta, K. Haastert, C. Trankle, F.A. Siebzehnruhl, M. Riessland, I. Holker, P. Claus, J. Romstock, R. Buslei, B. Wirth, and I. Blumcke. 2006. In vitro and ex vivo evaluation of second-generation histone deacetylase inhibitors for the treatment of spinal muscular atrophy. *J Neurochem*. 98:193-202.
- Heinrich, P.C., I. Behrmann, G. Muller-Newen, F. Schaper, and L. Graeve. 1998. Interleukin-6-type cytokine signalling through the gp130/Jak/STAT pathway. *Biochem J*. 334 (Pt 2):297-314.
- Helgren, M.E., S.P. Squinto, H.L. Davis, D.J. Parry, T.G. Boulton, C.S. Heck, Y. Zhu, G.D. Yancopoulos, R.M. Lindsay, and P.S. DiStefano. 1994. Trophic effect of ciliary neurotrophic factor on denervated skeletal muscle. *Cell*. 76:493-504.
- Hellal, F., A. Hurtado, J. Ruschel, K.C. Flynn, C.J. Laskowski, M. Umlauf, L.C. Kapitein, D. Strikis, V. Lemmon, J. Bixby, C.C. Hoogenraad, and F. Bradke. 2011. Microtubule stabilization reduces scarring and causes axon regeneration after spinal cord injury. *Science*. 331:928-931.
- Henderson, C.E., H.S. Phillips, R.A. Pollock, A.M. Davies, C. Lemeulle, M. Armanini, L. Simmons, B. Moffet, R.A. Vandlen, L.C. Simpson, and et al. 1994. GDNF: a potent survival factor for motoneurons present in peripheral nerve and muscle. *Science*. 266:1062-1064.
- Hirano, T., K. Nakajima, and M. Hibi. 1997. Signaling mechanisms through gp130: a model of the cytokine system. *Cytokine Growth Factor Rev*. 8:241-252.
- Hofbauer, A., T. Ebel, B. Waltenspiel, P. Oswald, Y.C. Chen, P. Halder, S. Biskup, U. Lewandrowski, C. Winkler, A. Sickmann, S. Buchner, and E. Buchner. 2009. The Wuerzburg hybridoma library against Drosophila brain. *J Neurogenet*. 23:78-91.
- Horvath, C.M., Z. Wen, and J.E. Darnell, Jr. 1995. A STAT protein domain that determines DNA sequence recognition suggests a novel DNA-binding domain. *Genes Dev*. 9:984-994.
- Hubbert, C., A. Guardiola, R. Shao, Y. Kawaguchi, A. Ito, A. Nixon, M. Yoshida, X.F. Wang, and T.P. Yao. 2002. HDAC6 is a microtubule-associated deacetylase. *Nature*. 417:455-458.
- Ip, N.Y., S.H. Nye, T.G. Boulton, S. Davis, T. Taga, Y. Li, S.J. Birren, K. Yasukawa, T. Kishimoto, D.J. Anderson, and et al. 1992. CNTF and LIF act on neuronal cells via shared signaling pathways that involve the IL-6 signal transducing receptor component gp130. *Cell*. 69:1121-1132.

- Jablonka, S., M. Beck, B.D. Lechner, C. Mayer, and M. Sendtner. 2007. Defective Ca²⁺ channel clustering in axon terminals disturbs excitability in motoneurons in spinal muscular atrophy. *J Cell Biol.* 179:139-149.
- Janke, C., and J.C. Bulinski. 2011. Post-translational regulation of the microtubule cytoskeleton: mechanisms and functions. *Nat Rev Mol Cell Biol.* 12:773-786.
- Jeanneteau, F., K. Deinhardt, G. Miyoshi, A.M. Bennett, and M.V. Chao. 2010. The MAP kinase phosphatase MKP-1 regulates BDNF-induced axon branching. *Nat Neurosci.* 13:1373-1379.
- Jessen, K.R., and R. Mirsky. 1992. Schwann cells: early lineage, regulation of proliferation and control of myelin formation. *Curr Opin Neurobiol.* 2:575-581.
- Jin, S., L. Pan, Z. Liu, Q. Wang, Z. Xu, and Y.Q. Zhang. 2009. Drosophila Tubulin-specific chaperone E functions at neuromuscular synapses and is required for microtubule network formation. *Development.* 136:1571-1581.
- Johnson, J.O., J. Mandrioli, M. Benatar, Y. Abramzon, V.M. Van Deerlin, J.Q. Trojanowski, J.R. Gibbs, M. Brunetti, S. Gronka, J. Wu, J. Ding, L. McCluskey, M. Martinez-Lage, D. Falcone, D.G. Hernandez, S. Arepalli, S. Chong, J.C. Schymick, J. Rothstein, F. Landi, Y.D. Wang, A. Calvo, G. Mora, M. Sabatelli, M.R. Monsurro, S. Battistini, F. Salvi, R. Spataro, P. Sola, G. Borghero, G. Galassi, S.W. Scholz, J.P. Taylor, G. Restagno, A. Chio, and B.J. Traynor. 2010. Exome sequencing reveals VCP mutations as a cause of familial ALS. *Neuron.* 68:857-864.
- Jourdain, L., P. Curmi, A. Sobel, D. Pantaloni, and M.F. Carlier. 1997. Stathmin: a tubulin-sequestering protein which forms a ternary T2S complex with two tubulin molecules. *Biochemistry.* 36:10817-10821.
- Kaptein, A., V. Paillard, and M. Saunders. 1996. Dominant negative stat3 mutant inhibits interleukin-6-induced Jak-STAT signal transduction. *J Biol Chem.* 271:5961-5964.
- Konishi, Y., and M. Setou. 2009. Tubulin tyrosination navigates the kinesin-1 motor domain to axons. *Nat Neurosci.* 12:559-567.
- Kretschmar, A.K., M.C. Dinger, C. Henze, K. Brocke-Heidrich, and F. Horn. 2004. Analysis of Stat3 (signal transducer and activator of transcription 3) dimerization by fluorescence resonance energy transfer in living cells. *Biochem J.* 377:289-297.
- L'Hernault, S.W., and J.L. Rosenbaum. 1985. Chlamydomonas alpha-tubulin is posttranslationally modified by acetylation on the epsilon-amino group of a lysine. *Biochemistry.* 24:473-478.
- Lefebvre, S., L. Burglen, S. Reboullet, O. Clermont, P. Burlet, L. Viollet, B. Benichou, C. Cruaud, P. Millasseau, M. Zeviani, and et al. 1995. Identification and characterization of a spinal muscular atrophy-determining gene. *Cell.* 80:155-165.

- Lewis, S.A., G. Tian, and N.J. Cowan. 1997. The alpha- and beta-tubulin folding pathways. *Trends Cell Biol.* 7:479-484.
- Lewis, S.A., G. Tian, I.E. Vainberg, and N.J. Cowan. 1996. Chaperonin-mediated folding of actin and tubulin. *J Cell Biol.* 132:1-4.
- Liedtke, W., E.E. Leman, R.E. Fyffe, C.S. Raine, and U.K. Schubart. 2002. Stathmin-deficient mice develop an age-dependent axonopathy of the central and peripheral nervous systems. *Am J Pathol.* 160:469-480.
- Lillien, L.E., and M.C. Raff. 1990. Differentiation signals in the CNS: type-2 astrocyte development in vitro as a model system. *Neuron.* 5:111-119.
- Lin, L.F., D. Mismar, J.D. Lile, L.G. Armes, E.T. Butler, 3rd, J.L. Vannice, and F. Collins. 1989. Purification, cloning, and expression of ciliary neurotrophic factor (CNTF). *Science.* 246:1023-1025.
- Liu, L., S. Das, W. Losert, and C.A. Parent. 2010. mTORC2 regulates neutrophil chemotaxis in a cAMP- and RhoA-dependent fashion. *Dev Cell.* 19:845-857.
- Liu, L., K.M. McBride, and N.C. Reich. 2005. STAT3 nuclear import is independent of tyrosine phosphorylation and mediated by importin-alpha3. *Proc Natl Acad Sci U S A.* 102:8150-8155.
- Lutticken, C., P. Coffer, J. Yuan, C. Schwartz, E. Caldenhoven, C. Schindler, W. Kruijjer, P.C. Heinrich, and F. Horn. 1995. Interleukin-6-induced serine phosphorylation of transcription factor APRF: evidence for a role in interleukin-6 target gene induction. *FEBS Lett.* 360:137-143.
- Lutticken, C., U.M. Wegenka, J. Yuan, J. Buschmann, C. Schindler, A. Ziemiecki, A.G. Harpur, A.F. Wilks, K. Yasukawa, T. Taga, and et al. 1994. Association of transcription factor APRF and protein kinase Jak1 with the interleukin-6 signal transducer gp130. *Science.* 263:89-92.
- Mackenzie, I.R., R. Rademakers, and M. Neumann. 2010. TDP-43 and FUS in amyotrophic lateral sclerosis and frontotemporal dementia. *Lancet Neurol.* 9:995-1007.
- Marinkovic, P., M.S. Reuter, M.S. Brill, L. Godinho, M. Kerschensteiner, and T. Miggeld. 2012. Axonal transport deficits and degeneration can evolve independently in mouse models of amyotrophic lateral sclerosis. *Proc Natl Acad Sci U S A.* 109:4296-4301.
- Martin, N., J. Jaubert, P. Glaser, M. Szatanik, and J.L. Guenet. 2001. Genetic and physical delineation of the region overlapping the progressive motor neuropathy (pmn) locus on mouse chromosome 13. *Genomics.* 75:9-16.
- Martin, N., J. Jaubert, P. Gounon, E. Salido, G. Haase, M. Szatanik, and J.L. Guenet. 2002. A missense mutation in Tbc causes progressive motor neuronopathy in mice. *Nat Genet.* 32:443-447.

- Masu, Y., E. Wolf, B. Holtmann, M. Sendtner, G. Brem, and H. Thoenen. 1993. Disruption of the CNTF gene results in motor neuron degeneration. *Nature*. 365:27-32.
- Matusica, D., M.P. Fenech, M.L. Rogers, and R.A. Rush. 2008. Characterization and use of the NSC-34 cell line for study of neurotrophin receptor trafficking. *J Neurosci Res*. 86:553-565.
- Maucuer, A., J. Moreau, M. Mechali, and A. Sobel. 1993. Stathmin gene family: phylogenetic conservation and developmental regulation in *Xenopus*. *J Biol Chem*. 268:16420-16429.
- Mitsumoto, H., K. Ikeda, T. Holmlund, T. Greene, J.M. Cedarbaum, V. Wong, and R.M. Lindsay. 1994a. The effects of ciliary neurotrophic factor on motor dysfunction in wobbler mouse motor neuron disease. *Ann Neurol*. 36:142-148.
- Mitsumoto, H., K. Ikeda, B. Klinkosz, J.M. Cedarbaum, V. Wong, and R.M. Lindsay. 1994b. Arrest of motor neuron disease in wobbler mice cotreated with CNTF and BDNF. *Science*. 265:1107-1110.
- Monani, U.R., M. Sendtner, D.D. Covert, D.W. Parsons, C. Andreassi, T.T. Le, S. Jablonka, B. Schrank, W. Rossoll, T.W. Prior, G.E. Morris, and A.H. Burghes. 2000. The human centromeric survival motor neuron gene (SMN2) rescues embryonic lethality in *Smn(-/-)* mice and results in a mouse with spinal muscular atrophy. *Hum Mol Genet*. 9:333-339.
- Neumann, M., D.M. Sampathu, L.K. Kwong, A.C. Truax, M.C. Micsenyi, T.T. Chou, J. Bruce, T. Schuck, M. Grossman, C.M. Clark, L.F. McCluskey, B.L. Miller, E. Masliah, I.R. Mackenzie, H. Feldman, W. Feiden, H.A. Kretschmar, J.Q. Trojanowski, and V.M. Lee. 2006. Ubiquitinated TDP-43 in frontotemporal lobar degeneration and amyotrophic lateral sclerosis. *Science*. 314:130-133.
- Ng, D.C., B.H. Lin, C.P. Lim, G. Huang, T. Zhang, V. Poli, and X. Cao. 2006. Stat3 regulates microtubules by antagonizing the depolymerization activity of stathmin. *J Cell Biol*. 172:245-257.
- Nicolas, C.S., S. Peineau, M. Amici, Z. Csaba, A. Fafouri, C. Javalet, V.J. Collett, L. Hildebrandt, G. Seaton, S.L. Choi, S.E. Sim, C. Bradley, K. Lee, M. Zhuo, B.K. Kaang, P. Gressens, P. Dournaud, S.M. Fitzjohn, Z.A. Bortolotto, K. Cho, and G.L. Collingridge. 2012. The Jak/STAT pathway is involved in synaptic plasticity. *Neuron*. 73:374-390.
- Ning, K., C. Drepper, C.F. Valori, M. Ahsan, M. Wyles, A. Higginbottom, T. Herrmann, P. Shaw, M. Azzouz, and M. Sendtner. 2010. PTEN depletion rescues axonal growth defect and improves survival in SMN-deficient motor neurons. *Hum Mol Genet*. 19:3159-3168.
- Nishimune, H., S. Vasseur, S. Wiese, M.C. Birling, B. Holtmann, M. Sendtner, J.L. Iovanna, and C.E. Henderson. 2000. Reg-2 is a motoneuron neurotrophic factor and a signalling intermediate in the CNTF survival pathway. *Nat Cell Biol*. 2:906-914.
- North, B.J., B.L. Marshall, M.T. Borra, J.M. Denu, and E. Verdin. 2003. The human Sir2 ortholog, SIRT2, is an NAD⁺-dependent tubulin deacetylase. *Mol Cell*. 11:437-444.

- Ohkawa, N., K. Fujitani, E. Tokunaga, S. Furuya, and K. Inokuchi. 2007. The microtubule destabilizer stathmin mediates the development of dendritic arbors in neuronal cells. *J Cell Sci.* 120:1447-1456.
- Ohkawa, N., S. Sugisaki, E. Tokunaga, K. Fujitani, T. Hayasaka, M. Setou, and K. Inokuchi. 2008. N-acetyltransferase ARD1-NAT1 regulates neuronal dendritic development. *Genes Cells.* 13:1171-1183.
- Parvari, R., E. HersHKovitz, N. Grossman, R. Gorodischer, B. Loeys, A. Zecic, G. Mortier, S. Gregory, R. Sharony, M. Kambouris, N. Sakati, B.F. Meyer, A.I. Al Aqeel, A.K. Al Humaidan, F. Al Zahrani, A. Al Swaid, J. Al Othman, G.A. Diaz, R. Weiner, K.T. Khan, R. Gordon, and B.D. Gelb. 2002. Mutation of TBCE causes hypoparathyroidism-retardation-dysmorphism and autosomal recessive Kenny-Caffey syndrome. *Nat Genet.* 32:448-452.
- Polymenidou, M., C. Lagier-Tourenne, K.R. Hutt, C.F. Bennett, D.W. Cleveland, and G.W. Yeo. 2012. Misregulated RNA processing in amyotrophic lateral sclerosis. *Brain Res.* 1462:3-15.
- Puls, I., C. Jonnakuty, B.H. LaMonte, E.L. Holzbaur, M. Tokito, E. Mann, M.K. Floeter, K. Bidus, D. Drayna, S.J. Oh, R.H. Brown, Jr., C.L. Ludlow, and K.H. Fischbeck. 2003. Mutant dynactin in motor neuron disease. *Nat Genet.* 33:455-456.
- Rajan, P., and R.D. McKay. 1998. Multiple routes to astrocytic differentiation in the CNS. *J Neurosci.* 18:3620-3629.
- Rathod, R., S. Havlicek, N. Frank, R. Blum, and M. Sendtner. 2012. Laminin induced local axonal translation of beta-actin mRNA is impaired in SMN-deficient motoneurons. *Histochem Cell Biol.* 138:737-748.
- Raybin, D., and M. Flavin. 1977. Enzyme which specifically adds tyrosine to the alpha chain of tubulin. *Biochemistry.* 16:2189-2194.
- Reich, N.C., and L. Liu. 2006. Tracking STAT nuclear traffic. *Nat Rev Immunol.* 6:602-612.
- Reichmuth, C., S. Becker, M. Benz, K. Debel, D. Reisch, G. Heimbeck, A. Hofbauer, B. Klagges, G.O. Pflugfelder, and E. Buchner. 1995. The sap47 gene of *Drosophila melanogaster* codes for a novel conserved neuronal protein associated with synaptic terminals. *Brain Res Mol Brain Res.* 32:45-54.
- Reid, E., M. Kloos, A. Ashley-Koch, L. Hughes, S. Bevan, I.K. Svenson, F.L. Graham, P.C. Gaskell, A. Dearlove, M.A. Pericak-Vance, D.C. Rubinsztein, and D.A. Marchuk. 2002. A kinesin heavy chain (KIF5A) mutation in hereditary spastic paraplegia (SPG10). *Am J Hum Genet.* 71:1189-1194.
- Renton, A.E., E. Majounie, A. Waite, J. Simon-Sanchez, S. Rollinson, J.R. Gibbs, J.C. Schymick, H. Laaksovirta, J.C. van Swieten, L. Myllykangas, H. Kalimo, A. Paetau, Y. Abramzon, A.M. Remes, A. Kaganovich, S.W. Scholz, J. Duckworth, J. Ding, D.W.

- Harmer, D.G. Hernandez, J.O. Johnson, K. Mok, M. Ryten, D. Tratzuni, R.J. Guerreiro, R.W. Orrell, J. Neal, A. Murray, J. Pearson, I.E. Jansen, D. Sondervan, H. Seelaar, D. Blake, K. Young, N. Halliwell, J.B. Callister, G. Toulson, A. Richardson, A. Gerhard, J. Snowden, D. Mann, D. Neary, M.A. Nalls, T. Peuralinna, L. Jansson, V.M. Isoviita, A.L. Kaivorinne, M. Holtta-Vuori, E. Ikonen, R. Sulkava, M. Benatar, J. Wu, A. Chio, G. Restagno, G. Borghero, M. Sabatelli, D. Heckerman, E. Rogaeva, L. Zinman, J.D. Rothstein, M. Sendtner, C. Drepper, E.E. Eichler, C. Alkan, Z. Abdullaev, S.D. Pack, A. Dutra, E. Pak, J. Hardy, A. Singleton, N.M. Williams, P. Heutink, S. Pickering-Brown, H.R. Morris, P.J. Tienari, and B.J. Traynor. 2011. A hexanucleotide repeat expansion in C9ORF72 is the cause of chromosome 9p21-linked ALS-FTD. *Neuron*. 72:257-268.
- Robson, S.J., and R.D. Burgoyne. 1989. Differential localisation of tyrosinated, detyrosinated, and acetylated alpha-tubulins in neurites and growth cones of dorsal root ganglion neurons. *Cell Motil Cytoskeleton*. 12:273-282.
- Rohde, M., J. Puls, R. Buhrdorf, W. Fischer, and R. Haas. 2003. A novel sheathed surface organelle of the *Helicobacter pylori* cag type IV secretion system. *Mol Microbiol*. 49:219-234.
- Roos, J., T. Hummel, N. Ng, C. Klambt, and G.W. Davis. 2000. *Drosophila* Futsch regulates synaptic microtubule organization and is necessary for synaptic growth. *Neuron*. 26:371-382.
- Rosen, D.R. 1993. Mutations in Cu/Zn superoxide dismutase gene are associated with familial amyotrophic lateral sclerosis. *Nature*. 364:362.
- Rossoll, W., S. Jablonka, C. Andreassi, A.K. Kroning, K. Karle, U.R. Monani, and M. Sendtner. 2003. Smn, the spinal muscular atrophy-determining gene product, modulates axon growth and localization of beta-actin mRNA in growth cones of motoneurons. *J Cell Biol*. 163:801-812.
- Saadat, S., M. Sendtner, and H. Rohrer. 1989. Ciliary neurotrophic factor induces cholinergic differentiation of rat sympathetic neurons in culture. *J Cell Biol*. 108:1807-1816.
- Sagot, Y., M. Dubois-Dauphin, S.A. Tan, F. de Bilbao, P. Aebischer, J.C. Martinou, and A.C. Kato. 1995. Bcl-2 overexpression prevents motoneuron cell body loss but not axonal degeneration in a mouse model of a neurodegenerative disease. *J Neurosci*. 15:7727-7733.
- Sagot, Y., T. Rosse, R. Vejsada, D. Perrelet, and A.C. Kato. 1998. Differential effects of neurotrophic factors on motoneuron retrograde labeling in a murine model of motoneuron disease. *J Neurosci*. 18:1132-1141.
- Sagot, Y., S.A. Tan, J.P. Hammang, P. Aebischer, and A.C. Kato. 1996. GDNF slows loss of motoneurons but not axonal degeneration or premature death of pmn/pmn mice. *J Neurosci*. 16:2335-2341.

- Saumweber, T., A. Weyhersmuller, S. Hallermann, S. Diegelmann, B. Michels, D. Bucher, N. Funk, D. Reisch, G. Krohne, S. Wegener, E. Buchner, and B. Gerber. 2011. Behavioral and synaptic plasticity are impaired upon lack of the synaptic protein SAP47. *J Neurosci.* 31:3508-3518.
- Schaefer, M.K., H. Schmalbruch, E. Buhler, C. Lopez, N. Martin, J.L. Guenet, and G. Haase. 2007. Progressive motor neuronopathy: a critical role of the tubulin chaperone TBCE in axonal tubulin routing from the Golgi apparatus. *J Neurosci.* 27:8779-8789.
- Schmalbruch, H., H.J. Jensen, M. Bjaerg, Z. Kamieniecka, and L. Kurland. 1991. A new mouse mutant with progressive motor neuronopathy. *J Neuropathol Exp Neurol.* 50:192-204.
- Schmitt-John, T., C. Drepper, A. Mussmann, P. Hahn, M. Kuhlmann, C. Thiel, M. Hafner, A. Lengeling, P. Heimann, J.M. Jones, M.H. Meisler, and H. Jockusch. 2005. Mutation of Vps54 causes motor neuron disease and defective spermiogenesis in the wobbler mouse. *Nat Genet.* 37:1213-1215.
- Schweizer, U., J. Gunnarsen, C. Karch, S. Wiese, B. Holtmann, K. Takeda, S. Akira, and M. Sendtner. 2002. Conditional gene ablation of Stat3 reveals differential signaling requirements for survival of motoneurons during development and after nerve injury in the adult. *J Cell Biol.* 156:287-297.
- Sellin, M.E., P. Holmfeldt, S. Stenmark, and M. Gullberg. 2008. Op18/Stathmin counteracts the activity of overexpressed tubulin-disrupting proteins in a human leukemia cell line. *Exp Cell Res.* 314:1367-1377.
- Selvaraj, B.T., N. Frank, F.L. Bender, E. Asan, and M. Sendtner. 2012. Local axonal function of STAT3 rescues axon degeneration in the pmn model of motoneuron disease. *J Cell Biol.* 199:437-451.
- Sendtner, M., Y. Arakawa, K.A. Stockli, G.W. Kreutzberg, and H. Thoenen. 1991. Effect of ciliary neurotrophic factor (CNTF) on motoneuron survival. *J Cell Sci Suppl.* 15:103-109.
- Sendtner, M., R. Gotz, B. Holtmann, and H. Thoenen. 1997. Endogenous ciliary neurotrophic factor is a lesion factor for axotomized motoneurons in adult mice. *J Neurosci.* 17:6999-7006.
- Sendtner, M., B. Holtmann, and R.A. Hughes. 1996. The response of motoneurons to neurotrophins. *Neurochem Res.* 21:831-841.
- Sendtner, M., B. Holtmann, R. Kolbeck, H. Thoenen, and Y.A. Barde. 1992a. Brain-derived neurotrophic factor prevents the death of motoneurons in newborn rats after nerve section. *Nature.* 360:757-759.
- Sendtner, M., G.W. Kreutzberg, and H. Thoenen. 1990. Ciliary neurotrophic factor prevents the degeneration of motor neurons after axotomy. *Nature.* 345:440-441.

- Sendtner, M., H. Schmalbruch, K.A. Stockli, P. Carroll, G.W. Kreutzberg, and H. Thoenen. 1992b. Ciliary neurotrophic factor prevents degeneration of motor neurons in mouse mutant progressive motor neuronopathy. *Nature*. 358:502-504.
- Sendtner, M., K.A. Stockli, and H. Thoenen. 1992c. Synthesis and localization of ciliary neurotrophic factor in the sciatic nerve of the adult rat after lesion and during regeneration. *J Cell Biol*. 118:139-148.
- Shen, Y., K. Schlessinger, X. Zhu, E. Meffre, F. Quimby, D.E. Levy, and J.E. Darnell, Jr. 2004. Essential role of STAT3 in postnatal survival and growth revealed by mice lacking STAT3 serine 727 phosphorylation. *Mol Cell Biol*. 24:407-419.
- Sheu, J.Y., D.J. Kulhanek, and F.P. Eckenstein. 2000. Differential patterns of ERK and STAT3 phosphorylation after sciatic nerve transection in the rat. *Exp Neurol*. 166:392-402.
- Shi, W., M. Inoue, M. Minami, K. Takeda, M. Matsumoto, Y. Matsuda, T. Kishimoto, and S. Akira. 1996. The genomic structure and chromosomal localization of the mouse STAT3 gene. *Int Immunol*. 8:1205-1211.
- Shumyatsky, G.P., G. Malleret, R.M. Shin, S. Takizawa, K. Tully, E. Tsvetkov, S.S. Zakharenko, J. Joseph, S. Vronskaya, D. Yin, U.K. Schubart, E.R. Kandel, and V.Y. Bolshakov. 2005. stathmin, a gene enriched in the amygdala, controls both learned and innate fear. *Cell*. 123:697-709.
- Siddiquee, K., S. Zhang, W.C. Guida, M.A. Blaskovich, B. Greedy, H.R. Lawrence, M.L. Yip, R. Jove, M.M. McLaughlin, N.J. Lawrence, S.M. Sebti, and J. Turkson. 2007. Selective chemical probe inhibitor of Stat3, identified through structure-based virtual screening, induces antitumor activity. *Proc Natl Acad Sci U S A*. 104:7391-7396.
- Simon, C.M., S. Jablonka, R. Ruiz, L. Tabares, and M. Sendtner. 2010. Ciliary neurotrophic factor-induced sprouting preserves motor function in a mouse model of mild spinal muscular atrophy. *Hum Mol Genet*. 19:973-986.
- Simpson, E.P., Y.K. Henry, J.S. Henkel, R.G. Smith, and S.H. Appel. 2004. Increased lipid peroxidation in sera of ALS patients: a potential biomarker of disease burden. *Neurology*. 62:1758-1765.
- Skourti-Stathaki, K., N.J. Proudfoot, and N. Gromak. 2011. Human senataxin resolves RNA/DNA hybrids formed at transcriptional pause sites to promote Xrn2-dependent termination. *Mol Cell*. 42:794-805.
- Smith, R.G., Y.K. Henry, M.P. Mattson, and S.H. Appel. 1998. Presence of 4-hydroxynonenal in cerebrospinal fluid of patients with sporadic amyotrophic lateral sclerosis. *Ann Neurol*. 44:696-699.
- Soto, Y., H. Conde, R. Aroche, V. Brito, P. Luaces, A. Nasiff, A. Obregon, and A.M. Vazquez Lopez. 2009. Autoantibodies to oxidized low density lipoprotein in relation with coronary artery disease. *Hum Antibodies*. 18:109-117.

- Sreedharan, J., I.P. Blair, V.B. Tripathi, X. Hu, C. Vance, B. Rogelj, S. Ackerley, J.C. Durnall, K.L. Williams, E. Buratti, F. Baralle, J. de Belleruche, J.D. Mitchell, P.N. Leigh, A. Al-Chalabi, C.C. Miller, G. Nicholson, and C.E. Shaw. 2008. TDP-43 mutations in familial and sporadic amyotrophic lateral sclerosis. *Science*. 319:1668-1672.
- Stahl, N., T.G. Boulton, T. Farruggella, N.Y. Ip, S. Davis, B.A. Witthuhn, F.W. Quelle, O. Silvennoinen, G. Barbieri, S. Pellegrini, and et al. 1994. Association and activation of Jak-Tyk kinases by CNTF-LIF-OSM-IL-6 beta receptor components. *Science*. 263:92-95.
- Stahl, N., S. Davis, V. Wong, T. Taga, T. Kishimoto, N.Y. Ip, and G.D. Yancopoulos. 1993. Cross-linking identifies leukemia inhibitory factor-binding protein as a ciliary neurotrophic factor receptor component. *J Biol Chem*. 268:7628-7631.
- Stahl, N., T.J. Farruggella, T.G. Boulton, Z. Zhong, J.E. Darnell, Jr., and G.D. Yancopoulos. 1995. Choice of STATs and other substrates specified by modular tyrosine-based motifs in cytokine receptors. *Science*. 267:1349-1353.
- Stahl, N., and G.D. Yancopoulos. 1994. The tripartite CNTF receptor complex: activation and signaling involves components shared with other cytokines. *J Neurobiol*. 25:1454-1466.
- Stockli, K.A., L.E. Lillien, M. Naher-Noe, G. Breitfeld, R.A. Hughes, M.C. Raff, H. Thoenen, and M. Sendtner. 1991. Regional distribution, developmental changes, and cellular localization of CNTF-mRNA and protein in the rat brain. *J Cell Biol*. 115:447-459.
- Stockli, K.A., F. Lottspeich, M. Sendtner, P. Masiakowski, P. Carroll, R. Gotz, D. Lindholm, and H. Thoenen. 1989. Molecular cloning, expression and regional distribution of rat ciliary neurotrophic factor. *Nature*. 342:920-923.
- Subramaniam, J.R., W.E. Lyons, J. Liu, T.B. Bartnikas, J. Rothstein, D.L. Price, D.W. Cleveland, J.D. Gitlin, and P.C. Wong. 2002. Mutant SOD1 causes motor neuron disease independent of copper chaperone-mediated copper loading. *Nat Neurosci*. 5:301-307.
- Sun, F., K.K. Park, S. Belin, D. Wang, T. Lu, G. Chen, K. Zhang, C. Yeung, G. Feng, B.A. Yankner, and Z. He. 2011. Sustained axon regeneration induced by co-deletion of PTEN and SOCS3. *Nature*. 480:372-375.
- Szolajski, E., and J. Chroboczek. 2011. Faithful chaperones. *Cell Mol Life Sci*. 68:3307-3322.
- Takeda, K., T. Kaisho, N. Yoshida, J. Takeda, T. Kishimoto, and S. Akira. 1998. Stat3 activation is responsible for IL-6-dependent T cell proliferation through preventing apoptosis: generation and characterization of T cell-specific Stat3-deficient mice. *J Immunol*. 161:4652-4660.
- Takeda, K., K. Noguchi, W. Shi, T. Tanaka, M. Matsumoto, N. Yoshida, T. Kishimoto, and S. Akira. 1997. Targeted disruption of the mouse Stat3 gene leads to early embryonic lethality. *Proc Natl Acad Sci U S A*. 94:3801-3804.

- Tararuk, T., N. Ostman, W. Li, B. Bjorkblom, A. Padzik, J. Zdrojewska, V. Hongisto, T. Herdegen, W. Konopka, M.J. Courtney, and E.T. Coffey. 2006. JNK1 phosphorylation of SCG10 determines microtubule dynamics and axodendritic length. *J Cell Biol.* 173:265-277.
- Taylor, A.M., M. Blurton-Jones, S.W. Rhee, D.H. Cribbs, C.W. Cotman, and N.L. Jeon. 2005. A microfluidic culture platform for CNS axonal injury, regeneration and transport. *Nat Methods.* 2:599-605.
- Tian, G., Y. Huang, H. Rommelaere, J. Vandekerckhove, C. Ampe, and N.J. Cowan. 1996. Pathway leading to correctly folded beta-tubulin. *Cell.* 86:287-296.
- Tran, A.D., T.P. Marmo, A.A. Salam, S. Che, E. Finkelstein, R. Kabarriti, H.S. Xenias, R. Mazitschek, C. Hubbert, Y. Kawaguchi, M.P. Sheetz, T.P. Yao, and J.C. Bulinski. 2007. HDAC6 deacetylation of tubulin modulates dynamics of cellular adhesions. *J Cell Sci.* 120:1469-1479.
- Turkson, J., and R. Jove. 2000. STAT proteins: novel molecular targets for cancer drug discovery. *Oncogene.* 19:6613-6626.
- Vainberg, I.E., S.A. Lewis, H. Rommelaere, C. Ampe, J. Vandekerckhove, H.L. Klein, and N.J. Cowan. 1998. Prefoldin, a chaperone that delivers unfolded proteins to cytosolic chaperonin. *Cell.* 93:863-873.
- Vance, C., B. Rogelj, T. Hortobagyi, K.J. De Vos, A.L. Nishimura, J. Sreedharan, X. Hu, B. Smith, D. Ruddy, P. Wright, J. Ganesalingam, K.L. Williams, V. Tripathi, S. Al-Saraj, A. Al-Chalabi, P.N. Leigh, I.P. Blair, G. Nicholson, J. de Belleruche, J.M. Gallo, C.C. Miller, and C.E. Shaw. 2009. Mutations in FUS, an RNA processing protein, cause familial amyotrophic lateral sclerosis type 6. *Science.* 323:1208-1211.
- Vejsada, R., J.L. Tseng, R.M. Lindsay, A. Acheson, P. Aebischer, and A.C. Kato. 1998. Synergistic but transient rescue effects of BDNF and GDNF on axotomized neonatal motoneurons. *Neuroscience.* 84:129-139.
- Verma, N.K., J. Doulat, A.M. Davies, A. Long, W.Q. Liu, C. Garbay, D. Kelleher, and Y. Volkov. 2009. STAT3-stathmin interactions control microtubule dynamics in migrating T-cells. *J Biol Chem.* 284:12349-12362.
- Voloshin, O., Y. Gocheva, M. Gutnick, N. Movshovich, A. Bakhrat, K. Baranes-Bachar, D. Bar-Zvi, R. Parvari, L. Gheber, and D. Raveh. 2010. Tubulin chaperone E binds microtubules and proteasomes and protects against misfolded protein stress. *Cell Mol Life Sci.* 67:2025-2038.
- Watabe-Uchida, M., K.A. John, J.A. Janas, S.E. Newey, and L. Van Aelst. 2006. The Rac activator DOCK7 regulates neuronal polarity through local phosphorylation of stathmin/Op18. *Neuron.* 51:727-739.

- Watson, C.J., and W.R. Miller. 1995. Elevated levels of members of the STAT family of transcription factors in breast carcinoma nuclear extracts. *Br J Cancer*. 71:840-844.
- Weber-Nordt, R.M., C. Egen, J. Wehinger, W. Ludwig, V. Gouilleux-Gruart, R. Mertelsmann, and J. Finke. 1996. Constitutive activation of STAT proteins in primary lymphoid and myeloid leukemia cells and in Epstein-Barr virus (EBV)-related lymphoma cell lines. *Blood*. 88:809-816.
- Wegenka, U.M., J. Buschmann, C. Luttkicken, P.C. Heinrich, and F. Horn. 1993. Acute-phase response factor, a nuclear factor binding to acute-phase response elements, is rapidly activated by interleukin-6 at the posttranslational level. *Mol Cell Biol*. 13:276-288.
- Wegenka, U.M., C. Luttkicken, J. Buschmann, J. Yuan, F. Lottspeich, W. Muller-Esterl, C. Schindler, E. Roeb, P.C. Heinrich, and F. Horn. 1994. The interleukin-6-activated acute-phase response factor is antigenically and functionally related to members of the signal transducer and activator of transcription (STAT) family. *Mol Cell Biol*. 14:3186-3196.
- Wegrzyn, J., R. Potla, Y.J. Chwae, N.B. Sepuri, Q. Zhang, T. Koeck, M. Derecka, K. Szczepanek, M. Szelag, A. Gornicka, A. Moh, S. Moghaddas, Q. Chen, S. Bobbili, J. Cichy, J. Dulak, D.P. Baker, A. Wolfman, D. Stuehr, M.O. Hassan, X.Y. Fu, N. Avadhani, J.I. Drake, P. Fawcett, E.J. Lesnfsky, and A.C. Lerner. 2009. Function of mitochondrial Stat3 in cellular respiration. *Science*. 323:793-797.
- Wen, H.L., Y.T. Lin, C.H. Ting, S. Lin-Chao, H. Li, and H.M. Hsieh-Li. 2010. Stathmin, a microtubule-destabilizing protein, is dysregulated in spinal muscular atrophy. *Hum Mol Genet*. 19:1766-1778.
- Wen, Z., Z. Zhong, and J.E. Darnell, Jr. 1995. Maximal activation of transcription by Stat1 and Stat3 requires both tyrosine and serine phosphorylation. *Cell*. 82:241-250.
- Wiese, S., T. Herrmann, C. Drepper, S. Jablonka, N. Funk, A. Klausmeyer, M.L. Rogers, R. Rush, and M. Sendtner. 2010. Isolation and enrichment of embryonic mouse motoneurons from the lumbar spinal cord of individual mouse embryos. *Nat Protoc*. 5:31-38.
- Williamson, T.L., and D.W. Cleveland. 1999. Slowing of axonal transport is a very early event in the toxicity of ALS-linked SOD1 mutants to motor neurons. *Nat Neurosci*. 2:50-56.
- Wirth, B., L. Brichta, and E. Hahnen. 2006. Spinal muscular atrophy: from gene to therapy. *Semin Pediatr Neurol*. 13:121-131.
- Witte, H., and F. Bradke. 2008. The role of the cytoskeleton during neuronal polarization. *Curr Opin Neurobiol*. 18:479-487.
- Witte, H., D. Neukirchen, and F. Bradke. 2008. Microtubule stabilization specifies initial neuronal polarization. *J Cell Biol*. 180:619-632.

- Wong, P.C., C.A. Pardo, D.R. Borchelt, M.K. Lee, N.G. Copeland, N.A. Jenkins, S.S. Sisodia, D.W. Cleveland, and D.L. Price. 1995. An adverse property of a familial ALS-linked SOD1 mutation causes motor neuron disease characterized by vacuolar degeneration of mitochondria. *Neuron*. 14:1105-1116.
- Yao, Y., M. Suraokar, B.G. Darnay, B.G. Hollier, T.E. Shaiken, T. Asano, C.H. Chen, B.H. Chang, Y. Lu, G.B. Mills, D. Sarbassov, S.A. Mani, J.L. Abbruzzese, and S.A. Reddy. 2013. BSTA Promotes mTORC2-Mediated Phosphorylation of Akt1 to Suppress Expression of FoxC2 and Stimulate Adipocyte Differentiation. *Sci Signal*. 6:ra2.
- Yokogami, K., S. Wakisaka, J. Avruch, and S.A. Reeves. 2000. Serine phosphorylation and maximal activation of STAT3 during CNTF signaling is mediated by the rapamycin target mTOR. *Curr Biol*. 10:47-50.
- Zhao, C., J. Takita, Y. Tanaka, M. Setou, T. Nakagawa, S. Takeda, H.W. Yang, S. Terada, T. Nakata, Y. Takei, M. Saito, S. Tsuji, Y. Hayashi, and N. Hirokawa. 2001. Charcot-Marie-Tooth disease type 2A caused by mutation in a microtubule motor KIF1Bbeta. *Cell*. 105:587-597.
- Zhong, Z., Z. Wen, and J.E. Darnell, Jr. 1994. Stat3: a STAT family member activated by tyrosine phosphorylation in response to epidermal growth factor and interleukin-6. *Science*. 264:95-98.

8 APPENDIX

8.1 List of Figures

Figure 3.1	Various role of STAT3 in the cell	20
Figure 3.2	Microtubule biogenesis	22
Figure 4.1	Genotyping of <i>pmn</i> mouse line	42
Figure 4.2	Genotyping of STAT3 ^{fl} mouse line	43
Figure 4.3	Genotyping of STAT3 ^{KO} mouse line	44
Figure 5.1.1	Survival of motoneurons with various neurotrophic factors	56
Figure 5.1.2	CNTF rescues axon outgrowth in <i>pmn</i> mutant motoneurons	57
Figure 5.2.1	CNTF activated p-STAT3Y705 localized in cytoplasm of primary motoneurons	59
Figure 5.2.2	Specificity of p-STAT3Y705 antibody (cell signaling 9131)	60
Figure 5.2.3	Compartmentalized cultures to study the localization of activated STAT3	62
Figure 5.3.1	Expression of STAT3 ^{wt} EYFP, STAT3 ^{EE434-435AA} EYFP and STAT3 ^{Y705F} EYFP mutants in primary motoneurons	64
Figure 5.3.2	STAT3 ^{EE434-435AA} EYFP does not induce GFAP induction in neural stem cells	65
Figure 5.3.3	STAT3 phosphorylation but not its transcriptional activity is required for CNTF mediated axon growth in <i>pmn</i> mutant motoneurons	67
Figure 5.4.1	Co-localization of STAT3-EYFP and Stathmin in cultured motoneurons	69
Figure 5.4.2	Testing of Stathmin antibodies for immunoprecipitation	70
Figure 5.4.3	CNTF enhances STAT3 Stathmin interaction	72
Figure 5.4.4	STAT3 phosphorylation at Y705 is required for its interaction with Stathmin	73
Figure 5.5.1	Lentiviral knockdown of Stathmin in primary motoneurons	75
Figure 5.5.2	Stathmin knockdown rescues axonal pathology in <i>pmn</i> mutant motoneurons	76
Figure 5.5.3	Stathmin levels are not altered in <i>pmn</i> mutant motoneurons	77
Figure 5.6.1	Localization of different posttranslational	79

	modified forms of α -tubulin	
Figure 5.6.2	Levels of tyrosinated and acetylated tubulin in <i>pnn</i> mutant motoneurons	80
Figure 5.6.3	Microtubule fractionation in primary motoneurons	82
Figure 5.6.4	Stabilization of microtubules with taxol promotes axon growth in <i>pnn</i> mutant motoneurons	84
Figure 5.7.1	CNTF enhances microtubule regrowth in cultured motoneurons	87
Figure 5.7.2	CNTF enhances microtubule regrowth in cultured motoneurons	88
Figure 5.8.1	Tryptophan to Glycine (W-G) substitution in TBCE renders it unstable	91
Figure 5.8.2	CNTF does not increase the levels of TBCE	92
Figure 5.8.3	Localization of TBCE mRNA in primary motoneurons	94
Figure 5.8.4	CNTF does not alter expression of TBCE mRNA in primary motoneurons	95
Figure 5.9	pSTAT3 ^{Y705} is upregulated in sciatic nerves of <i>pnn</i> mutant mice	97
Figure 5.10.1	Characterization of antibodies against SYAP1	100
Figure 5.10.2	SYAP1 knockdown in primary motoneurons	101
Figure 5.10.3	Co-localization of TBCE and SYAP1 in primary motoneurons	102
Figure 5.10.4	SYAP1 interaction with TBCE	103
Figure 6.1	Scheme of CNTF mediated microtubules observed in <i>pnn</i> mutant motoneurons	112

8.2 List of Tables

Table 4.1	Composition of SDS polyacrylamide gel	31
Table 4.2	List of Antibodies	37
Table 4.3	List of Plasmids	38
Table 4.4	PCR components and cycling conditions for genotyping <i>pnn</i> mutant mice	41
Table 4.5	Expected product size for different genotypes of <i>pnn</i> after MnlI restriction digestion	42
Table 4.6	PCR components and cycling conditions for genotyping STAT3 ^{FL} mice	43
Table 4.7	PCR components and cycling conditions for genotyping STAT3 ^{KO} mice	44
Table 4.8	PCR components and cycling conditions for real time PCR analysis of <i>Tbce</i> mRNA level	45
Table 4.9	Number of motoneurons plated for different experiments	47
Table 4.10	PCR components and cycling conditions for site directed mutagenesis of STAT3Y705F-EYFP	54

8.3 List of Abbreviations

ALS	Amyotrophic lateral sclerosis
APRF	Acute phase response factor
ANOVA	Analysis of variance
BDNF	Brain derived neurotrophic factor
bFGF	Basic fibroblast growth factor
bp	base pair
CMV	Cyto megalovirus
CNS	Central nervous system
CNTF	Ciliary neurotrophic factor
CNTFR α	CNTF receptor α
DEPC	Diethyl pyro-carbonate
DIV	Days <i>in-vitro</i>
DNA	Deoxyribonucleic acid
DOCK7	Dedicator of cytokinesis 7
EGF	Epidermal growth factor
ERK1/2	Extracellular regulated signal kinase 1/2
FL	Floxed
GAPDH	Glyceraldehyde 3-phosphate dehydrogenase
GDNF	Glial derived neurotrophic factor
GFAP	Glial fibrillary acidic protein
GFP	Green fluorescent protein
GPI	Glycophosphatidylinositol
GP130	Glycoprotein 130
HBSS	Hank's balanced salt solution
HEK293	Human embryonic kidney cell line 293
HDAC6	Histone deacetylase 6
hnRNPR	heterogeneous ribonuclear protein R
IgG	Immunoglobulin G
IL6	Interleukin 6
JAK	Janus kinase
kDa	kilo Dalton
KIF	Kinesin super family

KO	Knock-out
LIF	Leukaemia inhibitory factor
LIFR β	LIF receptor β
LRR	Leucine rich repeat
LTD	Long term depression
MAPK	Mitogen activated protein kinase
MAP	microtubule associated protein
MT	Microtubule
MTOC	Microtubule organization center
mTOR	Mammalian target of rapamycin
NFL	Neurofilament light chain
NMJ	Neuro muscular junction
NMRI	Naval medical research institute
N2A	Neuro2A
PCR	Polymerase chain reaction
PI3K	Phosphoinositide 3 kinase
pmn	progressive motor neuronopathy
PTEN	Phosphatase and tensin homolog
RNA	Ribonucleic acid
SAP47	Synapse associated protein 47
SCG10	Superior cervical ganglion-10
SCLIP	SCG10-like protein
SDS-PAGE	Sodium-dodecyl sulfate polyacrylamide gel electrophoresis
SEM	Standard error of mean
siRNA	Small interference RNA
SH2	Src homology domain
SMA	Spinal muscular atrophy
SMN	Survival motor neuron
SOD1	Superoxide dismutase 1
SOCS3	Suppressor of cytokine signaling 3
snRNP's	Small nuclear ribonuclear proteins
STAT	Signal transducer and activator of transcription
SYAP1	Synapse associated protein 1
TBCE	Tubulin binding chaperone E

TBCE-L	TBCE like protein
TDP43	TAR DNA binding protein 43
TTL	Tubulin tyrosine ligase
VPS54	Vesicle sorting protein 54
WT	Wildtype

9 DECLARATION

I hereby declare that the work presented here was performed by me. All the materials and resources that have been utilized in this work are solely enclosed in this thesis. I also declare that the following dissertation entitled “Role of CNTF-STAT3 signaling in *progressive motor neuronopathy* mice, a model for motoneuron degenerative disease” has not been submitted earlier and has not been used for obtaining any other equivalent qualification in any other organization. Additionally, other than this degree I have not applied or will not attempt to apply for any other degree, title or qualification in relation to this work.

Bhuvaneish, Thangaraj Selvaraj.

10 ACKNOWLEDGEMENTS

Pursuing the Ph.D has been phenomenal and nothing short of overwhelming experience. Since the day I arrived in Würzburg its been a steep learning curve, both personally and professionally, and I have enjoyed every bit of variety that came along each day. I am highly indebted to many people whom I had met and interacted all through this exciting journey.

First and foremost, I place my sincere gratitude to my supervisor Prof. Dr. Michael Sendtner for giving me this great opportunity to pursue doctoral dissertation under his guidance. You have been a constant source of encouragement, giving valuable advice, guidance and undying support during the hard times. I am very thankful to you for keeping faith in me to perform such a challenging scientific project. I truly admire your dedication to science and your work ethics, which have been a great influence in shaping my career.

I have been privileged to get to know and interact with Prof. Dr. Erich Buchner and thankfully he has been my supervisor as well. You have been a vital cog to complete my dissertation in Würzburg. Without your help, I couldn't imagine being in this part of the world. I am very thankful to you for introducing me to this project and helping me out in various administrative hurdles. I would also like to appreciate the time and effort you had put in teaching me the basics during initial days of my Ph.D. Thank you very much.

I would like to share credit of my work with Nici, who over the years have become a great friend. It was always great fun to work with you. I will always cherish the time we spent in lab together discussing about the whole world. It was real joy learning German (although selective) and Skiing from you. Thanks a lot for your help.

I owe my sincere gratitude to Dr. Narayan Subramanian and Dr. Thomas Herrmann for teaching me the basic techniques and all the nitty gritty's of scientific experiments.

It gives me great pleasure in acknowledging Prof. Dr. Anna Maria Musti, Dr. Robert Blum & Dr. Carsten Drepper for their invaluable scientific inputs and advice, which has helped me immensely during the time I spent in Würzburg.

This thesis would not have been possible without the highly commendable work of Regine Sendtner, Joachim Horschig, Victor Buterus, Helga Brunner, Dr. Bettina Holtman for giving me the animals for my experiments day in and day out, especially during the time of our manuscript revision. Similarly, I would like to thank Elke Spirk for her overwhelming support in generating viruses for my experiments. It was just stupendous.

I am indebted to all my colleagues who have supported me with a lot of patience during all these years. Special thanks to Christian Simon, Lidia Albanito, Benjamin Dombert, Preeti Yadav, Reena Rathod, Michael Glinka, Christina Mais, Rajeev Sivadasan, Chandrakanth Reddy, Lena Saal, Dominique Schmitt, Steven Havlicek, Andrea Wetzel, Dr. Rudolf Götz, Dr. Sibylle Jablonka, Frank Kreiger, Dirk Püringer, Patrick Lüningschrör, Stefanie Rauskolb Michael Briese, Mehri Moradi, Samera Samleben, Beatriz Blanco, Erich Müller, Thomas Andreska. It was super fun to work with you guys.

I would like to thank all the technical and administrative assistance I received from Michaela Keßler, Judita Grimm, Zuzana Fouskova, Manuela Kohles, Nicole Elflein, Christian Mehling, Hildegard Troll, Urveen Oberoi-Lehrieder. I highly appreciate your efforts.

I cannot find words to express my gratitude to my parents, my wife Deepika and my brother Abi for their unconditional love and support. I would like to dedicate my doctoral dissertation to them.

This thesis would be a dream had it not been for the excellent funding from DFG-SFB 581. I would like to sincerely thank them for giving me this opportunity.

I had met many great friends in Würzburg and had many unforgettable moments because of them. I owe a great deal to all of them.

Bhuvaneish.T.S

11. CURRICULUM VITAE

Bhuvaneish, Thangaraj Selvaraj

DATE OF BIRTH: 05-06-1985

EDUCATION

Institute of Clinical Neurobiology, University of Würzburg
Ph.D., Molecular neurobiology, expected by December 2012

Government College of Technology, Anna University
B.Tech., Industrial Biotechnology, June 2002-2006, Aggregate-74.30%

D.A.V Higher Secondary School, Chennai, India
12th Grade Science major, June 2000-2006, Aggregate-92.34%

Asan Memorial Senior Secondary School, Chennai, India
10th Grade, May 2000, Aggregate-80%

RESEARCH EXPERIENCE

Ph.D Research (Integrated -*July 2007 onwards*) at Institute of Clinical Neurobiologie, University of Würzburg under the guidance of Prof. Michael Sendtner. Project involves understanding the pathomechanism of ciliary derived neurotrophic factor (CNTF) activated STAT3 signaling rescues axon degeneration in the *pnm* mouse model for motoneuron disease. A novel cytoplasmic function of STAT3 has been identified to play a role in microtubule dynamics thereby facilitating the rescue of *pnm* mouse.

Junior Research Fellow (*September 2006 - May 2007*) at National Center for Biological Sciences under Prof. Veronica Rodrigues. Involved in a project of generation of transgenic *Drosophila melanogaster* by microinjection technique using transposable elements such as P-elements, Piggy Bacs, and Mariner elements. Behavioural experiments in *Drosophila* Japanese *gal4* lines and studying the gustatory defects by silencing the gustatory receptors present in the proximity of the *gal4* insertion sites and thereby identifying novel genes.

Project student (*April 2005 - June 2005*) at Department of Genetics, Madras Medical Mission under the guidance of Ramakrishnan.M and Prof. Sivanandham. Analysis of chromosomal aberrations in patients having congenital heart disease using cytogenetic tools such as karyotyping and fluorescent *in-situ* hybridization (FISH)

Project student (*April 2004 - July 2004*) at Department of Cell and Molecular biology, Madras Diabetes Research Foundation under the guidance of Dr. Balasubramanyam.M. Studied the role of DNA damage in patients with type-2 diabetes using Comet assay.

PUBLICATION

“Local axonal function of STAT3 rescues axon degeneration in the *pmn* model of motoneuron disease” *J. Cell Biol.* 199:437-451. doi:10.1083/jcb.201203109
Bhuvaneish Thangaraj Selvaraj, Nicolas Frank, Florian L.P. Bender, Esther Asan and Michael Sendtner.

“CNTF, STAT3 and new therapies for axonal degeneration: what are they and what can they do?” Editorial review article currently in press in Expert Review of Neurotherapeutics
Bhuvaneish Thangaraj Selvaraj and Michael Sendtner

POSTER PRESENTATION

Poster presentation at NGF 2012 meeting in Würzburg
“CNTF -STAT3 signaling mediates axon maintenance in mouse model of Amyotrophic lateral sclerosis”
Nicolas Frank, Bhuvaneish Thangaraj Selvaraj, Florian Bender, Michael Sendtner

Poster presentation at Society for Neuroscience, November-2010 in San Diego
“Characterization of axon degeneration in *pmn* mice, a model of motoneuron disease”
Bhuvaneish Thangaraj Selvaraj, Nicolas Frank, Florian Bender, Michael Sendtner

Poster presentation at 3rd International workshop of molecular and cellular mechanisms of axon degeneration, Eibsee, Germany, October 3 - 6, 2010.
“Characterization of axon degeneration in *pmn* mice, a model of motoneuron disease”
Bhuvaneish Thangaraj Selvaraj, Nicolas Frank, Florian Bender, Michael Sendtner